Understanding Barriers to Efficient Nucleic Acid Delivery with Bioresponsive Block Copolymers

by

Daniel Kenneth Bonner

B.S. Materials Science and Engineering
Cornell University, 2006

Submitted to the Division of Health Sciences and Technology in Partial Fulfillment of the Requirements for the Degree of

Doctor of Philosophy in Medical Engineering

at the

Massachusetts Institute of Technology

February 2012

Signature of Author_____
Harvard-MIT Division of Health Sciences and Technology
December 13, 2011

Certified by: _____
Paula T. Hammond, Ph.D.
Bayer Professor of Chemical Engineering
Thesis Supervisor

Certified by: _____
Robert S. Langer, Sc.D.
Institute Professor
Thesis Supervisor

Accepted by: _____
Ram Sasisekharan, PhD
Edward Hood Taplin Professor of Health Sciences and Technology
and Biological Engineering
Director, Harvard-MIT Division of Health Sciences and Technology

Thesis Committee

Thesis Supervisor
Paula T. Hammond, Ph.D.
Bayer Professor of Chemical Engineering
Massachusetts Institute of Technology

Thesis Supervisor
Robert S. Langer, Sc.D.
Institute Professor
Massachusetts Institute of Technology

Thesis Committee Chair
Sangeeta N. Bhatia, M.D., Ph.D.
Professor of Health Sciences and Technology
Professor of Electrical Engineering and Computer Science
Massachusetts Institute of Technology

Thesis Committee Member
K. Dane Wittrup, Ph.D.
C.P. Dubbs Professor of Chemical Engineering and Biological Engineering
Massachusetts Institute of Technology

Table of Contents

Dedication

To my wife Joanna

Acknowledgements

I want to thank my thesis advisors, Professors Paula Hammond and Bob Langer, for being amazing mentors and role models for me. Paula, your infectious enthusiasm for science always kept me excited about the next set of experiments and new ideas. Bob, your ability to distill the most important aspects of any problem was truly remarkable and helped me maintain focus on what mattered most. I feel so fortunate to have been able to train under two incredibly bright and successful scientists who also display sincere humility and generosity.

I want to thank the other members of my thesis committee, Professors Dane Witt up and Sangeeta Bhatia, for their invaluable advice. I sincerely appreciated the discussions we've had and the scientific and professional guidance you have given me.

I want to thank those who collaborated with me for being generous with their time and materials to pursue findings that I could not have obtained on my own.

I want to thank the many members of the Hammond and Langer Labs for their support, scientific discussions, instrument and laboratory training, mentorship, and friendship.

I want to thank the dedicated undergraduate researchers who worked with me and are now well on their way to outstanding careers: Hilda Buss, Alan Leung, Jane Chen-Liang, Loice Chingozha, Amy Du, and Ted Cybulski.

I want to thank the core facilities staff at the Whitehead Institute and Koch Institute, particularly Nicki Watson, Wendy Salmon, Glenn Parades, Dick Cook, Natalia Schiller, Alla Leshinsky, and Sumeet Gupta.

I want to thank Dr. James Evans for training on the Cellomics automated microscopy system and helpful discussions.

I want to thank the many staff members who have helped me, supported me, and been wonderful friends, including members of the HST, ChemE, and KI staff. This experience would not have been as positive as it was without you.

I want to thank Kris Wood, Michael Goldberg, David Nguyen, and Eric Verploegen in particular for their scientific and professional mentorship.

I want to thank my previous research supervisors, Dr. Erik Herz, Professor Uli Wiesner, and Professor Frans Spaepen, for fostering a love of science and introducing me to the laboratory.

I want to thank the National Defense Science and Engineering Graduate Fellowship, the National Science Foundation Graduate Research Fellowship, the Martinos family, the Harvard-MIT Division of Health Sciences and Technology, the Koch Institute, the

National Institutes of Health, and the American Recovery and Reinvestment Act for funding various parts of this work.

I want to thank my fellow ChemE and HST classmates for everything from helping me when I got stuck on a homework set to cheering me up when an experiment went poorly.

I want to thank my family and friends for making each day of my life something to be treasured.

Finally, I want to thank my wife, Joanna, for being the truly amazing person that she is. Thank you for being everything to me. And also for helping with a couple of the captions that weren't cross-referencing properly.

List of Tables & Figures

Understanding Barriers to Efficient Nucleic Acid Delivery with Bioresponsive Block Copolymers

by

Daniel Kenneth Bonner

Submitted to the Division of Health Sciences and Technology on January 13, 2012 in Partial Fulfillment of the Requirements for the Degree of Doctor of Philosophy in Medical Engineering

Abstract

The delivery of nucleic acids has the potential to revolutionize medicine by allowing previously untreatable diseases to be clinically addressed. Viral delivery systems have been held back by immunogenicity and toxicity concerns, but synthetic vectors have lagged in transfection efficiency. This thesis describes the rational design and systematic study of three classes of bioresponsive polymers for nucleic acid delivery. A central theme of the study was understanding how the structure of the polymers impacted each of the intracellular steps of delivery, rather than solely the end result. A powerful tool for efficiently quantifying endosomal escape was developed and applied to each of the material systems described. First, a linear-dendritic poly(amido amine) -poly(ethylene glycol) (PAMAM-PEG) block copolymer system previously developed in our lab was evaluated and its ability to overcome the sequential barriers of uptake, endosomal escape, and nuclear import were characterized. Next, a class of crosslinked linear polyethyleimine (xLPEI) hyperbranched polymers, which can contain disulfide-responsive linkages, were synthesized and investigated. It was demonstrated that free polymer in solution, not the presence of a functional bioresponsive domain, was responsible for the highly efficient and relatively nontoxic DNA delivery of this promising class of crosslinked polyamines. Finally, this analysis was applied to siRNA delivery by a library of amine-functionalized synthetic polypeptides. The pH-responsive secondary structure, micelle formation, and ester hydrolysis were studied prior to the discrete barrier-oriented analysis of the siRNA delivery potential of this library. It is hoped that the tools, materials, and systemic analysis of structure-function relationships in this thesis will enhance the process of discovery and development of clinically relevant gene carriers.

Thesis Supervisor: Paula T. Hammond
Bayer Professor of Chemical Engineering

Thesis Supervisor: Robert S. Langer
Institute Professor

Chapter 1. Background

1.1 The Promise of Gene Therapy

Many diseases for which there is current unmet medical need could potentially be treated with nucleic acid therapies [1]. Gene expression introduced in target tissues could replace defective genes that result from inherited or acquired disease. Though revolutionary, gene therapy has not yet been successful clinically due to the difficulty of delivering DNA into nuclei of cells which require it [2].

1.2 Gene Delivery Vectors

The major classes of vectors capable of transfection are presented in this section, including modified viruses, cationic lipids, and cationic polymers.

1.2.1 Viruses

A successful gene delivery vehicle must evade the immune system and efficiently deliver its nucleic acid payload into the nuclei of target cells for transcription. Nature already has developed such a structure: the virus. It is possible to insert desired recombinant DNA into a viral construct and achieve transfection [3]. Currently, the most popular viral vectors are retroviruses and adenoviruses, due to their ability to infect a wide variety of cell types, efficient gene transfer, and relatively long research history [4-6]. However, viral vectors are unlikely to have long-term clinical impact due to concerns of genome insertion and immunotoxicity [7, 8]. The need for viable alternatives is underscored by the fact that viral vectors are still the overwhelming choice of vector in clinical trials [9].

1.2.2 Cationic Lipids

Cationic lipids were first demonstrated as highly effective transfection agents by Felger, et. al in 1987 using DOTMA (dioleyloxypropyltrimethylammonium) [10]. It is believed that the lipid-DNA complexes are taken into the cell via endocytosis and then released from the endosome due to the lipid's membrane disruption properties [11]. Though *Lipofectamine*™ was much more efficient than previous non-viral delivery vehicles, toxicity remains a concern, as membrane disruption can be harmful as well as helpful [12].

1.2.3 Cationic Polymers

Cationic polymers have the potential to be safe, effective DNA carriers [13-15]. Positive charge condenses and complexes with negatively-charged DNA [16]. Many polymers such as polyethyleneimine (PEI) have amine groups which can be protonated in order to achieve endosomal escape via the proton sponge effect (see 1.3.1). PEI is widely used and is considered one of the most efficient commercial polymers for transfection [16, 17]. It is synthesized in either linear or branched forms and transfection efficiency is quite sensitive both branching and molecular weight [18, 19]. Toxicity is one drawback to PEI if not modified with polyethylene glycol (PEG) [20, 21]. Furthermore, PEI is still far less efficient than viral vectors, limiting its clinical utility. Other cationic polymers used in gene delivery such as poly-L-lysine [22], chitosan [23], polyorthoesters [24], poly-β-aminoesters [25, 26], and dendritic polymers(discussed separately in the following section) also generally suffer from low transfection efficiency but remain relatively non-toxic.

1.2.4 Dendrimer-based Vectors

Dendrimers are branched polymers with a hierarchically ordered, tree-like structure [27]. Dendrimers are thus multivalent and can express functional groups or charges in great concentration at higher generations. Cationic dendrimers have found utility in gene delivery applications due to their high charge density and buffering potential of interior amines [28, 29]. In an initial success, Haensler and Szoka showed that negatively charged polyamidoamine (PAMAM) could be used to transfect a variety of cell lines [28]. Haensler and Szoka used so-called starburst, or cascade, dendrimers, which consist of a dense network of internal tertiary amine groups. These amine groups are helpful facilitating endosomal escape via the proton sponge effect (see 1.3.1). A counterintuitive result that followed indicated that partially degraded PAMAM dendrimers showed up to a fifty fold increase in transfection efficiency relative to intact PAMAM [30]. It is theorized that this is due to increased conformational flexibility, though the precise cell-vector interactions have not been thoroughly studied. PAMAM dendrimers were also used to effectively halt tumor growth in mice by delivering anti-angiogenesis genes [31]. Like other polycationic polymers, dendrimers complex with DNA by charge association. Transfection efficiency has been shown to be highly sensitive to small changes in the ratio of primary amines to DNA [32]. Additionally, dendrimer generation has also been shown to have a strong influence on both efficiency and toxicity [33]. Kukowska-Latallo et. al. report an increase over several orders of magnitude in transfection efficiency through 10 generations [33]. While certain modifications can greatly increase transfection efficiency, dendrimers are still inefficient in comparison with viral vectors [34]. Furthermore, cytotoxicity of dendrimers has been studied and is non-trivial [35].

Modification with hydrophilic coatings has been shown to decrease the cytotoxicity of the otherwise toxic cationic dendrimers, but at the expense of transfection efficiency [12, 35]. Our laboratory has previously conjugated PEG to PAMAM to reduce cytotoxicity and the binding of serum proteins in accordance with previously reported properties of PEG [36, 37]. With further functionalization and optimization, novel structures can be designed using PEG and PAMAM to create vectors that will be both relatively non-toxic and highly efficient.

1.3 Barriers to Effective Gene Delivery

Rational design of safe, effective gene delivery vectors hinges on a proper understanding of the physiological obstacles before the vector reaches the cell and the subcellular barriers encountered thereafter. The most important intracellular barriers to successful transfection are presented in Figure 1.1.

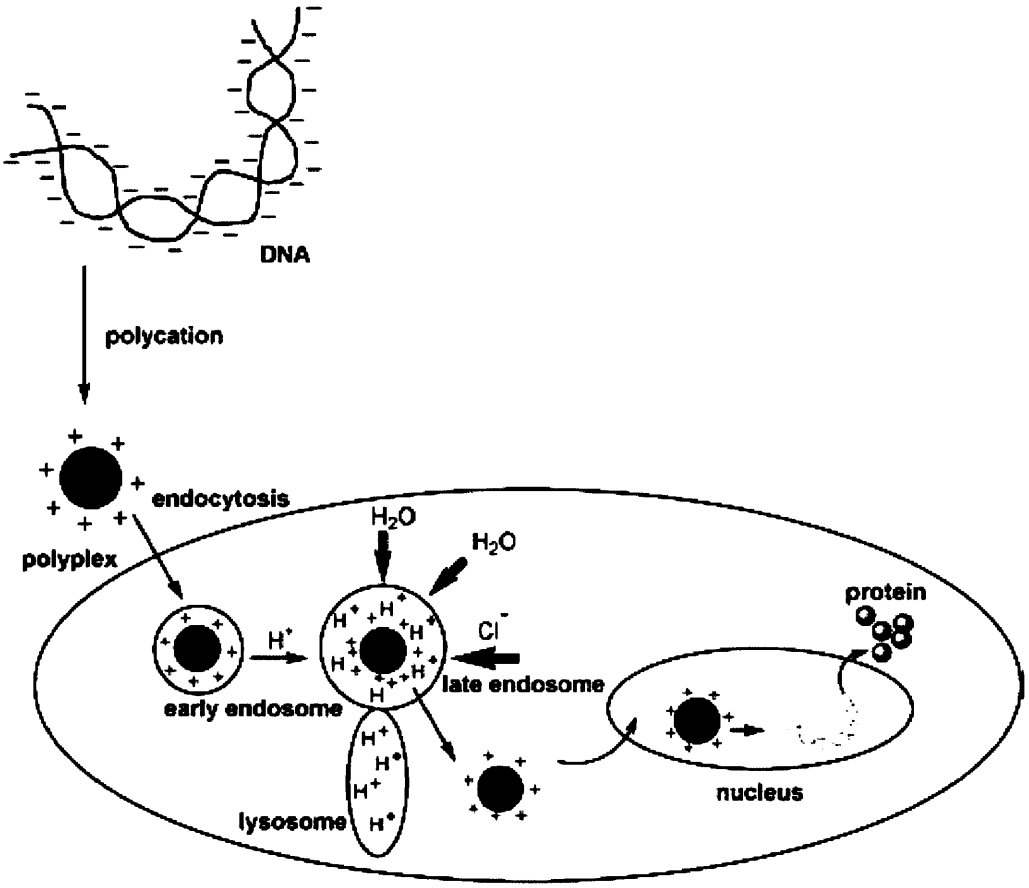

Figure 1.1 Barriers to Intracellular Gene Delivery
DNA is condensed with polycations into ordered structures such as spheroids. These condensates interact with the cell membrane and are endocytosed. Such polycations as PEI destabilize the endosome by the "proton sponge effect" resulting in escape of the polyplex from the endosome. The polyplex is subsequently translocated into the nucleus, followed by decondensation and separation of the DNA from the polycationic delivery vehicle, either outside or inside the nuclear membrane. The released DNA subsequently undergoes transcription and translation giving rise to the protein product [38].

1.3.1 Intracellular Barriers to Gene Delivery

Once the polyplex has reached the target cell of interest, it must be internalized. Internalization can happen via a variety of mechanisms, summarized in Figure 1.2 and well reviewed here [39]. Polymer-based gene delivery vehicles such as PEI and PAMAM make use of both the clathrin-mediated and caveolae-dependent pathways, though some dependence on cell type has been noted [40-42].

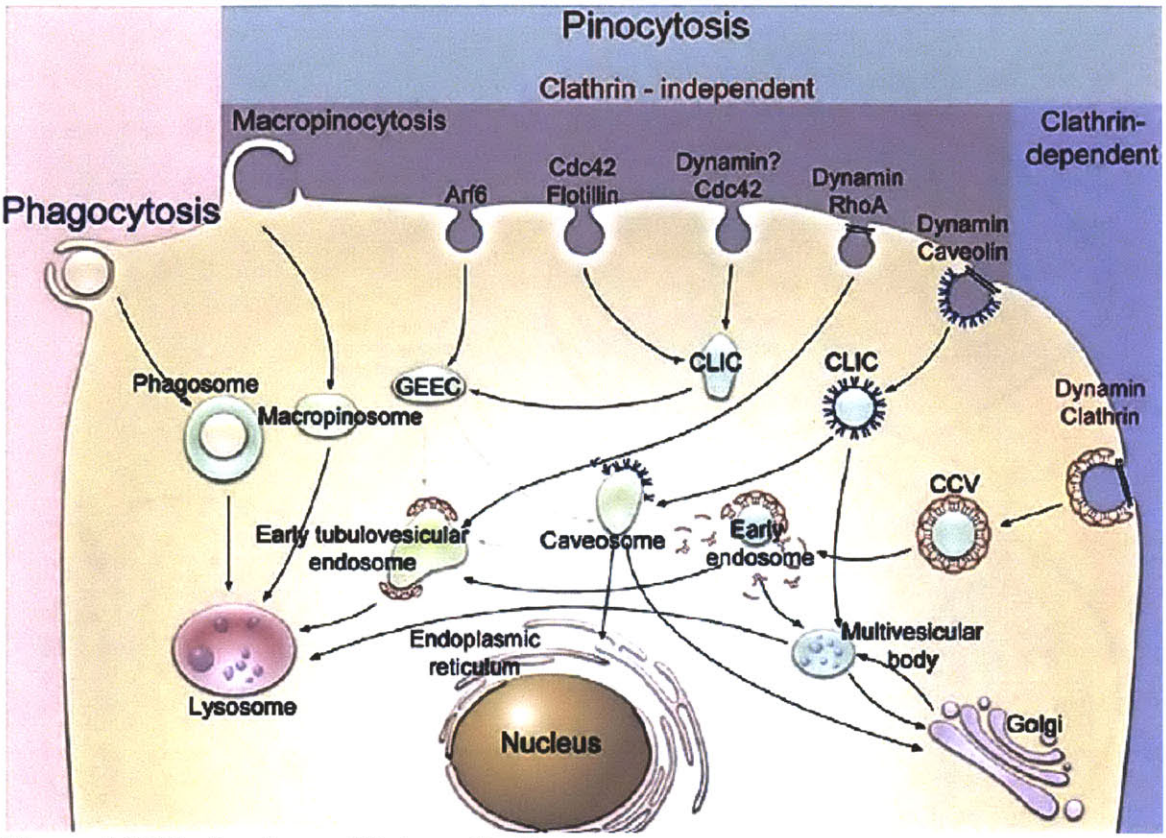

Figure 1.2 Mechanisms of Internalization
Polyplexes may internalized by a variety of pathways involving various aspects of cellular machinery. [39]

After internalization, the polyplex is enclosed in an endosome, from which it must escape to evade degradation. Endosomal escape can be achieved by membrane disrupting peptides [43, 44], small molecule agents such as chloroquine [45], the amphiphilic nature of lipid gene carriers, or the so-called proton sponge effect [46, 47]. The proton sponge effect describes the ability of amine groups on cationic polymers to buffer the endosomal environment by becoming protonated, and is described in Figure 1.3. Protons are continuously pumped into the endosome, leading to an excess of chloride counterions which causes membrane rupture due to osmotic flow of water into the endosome.

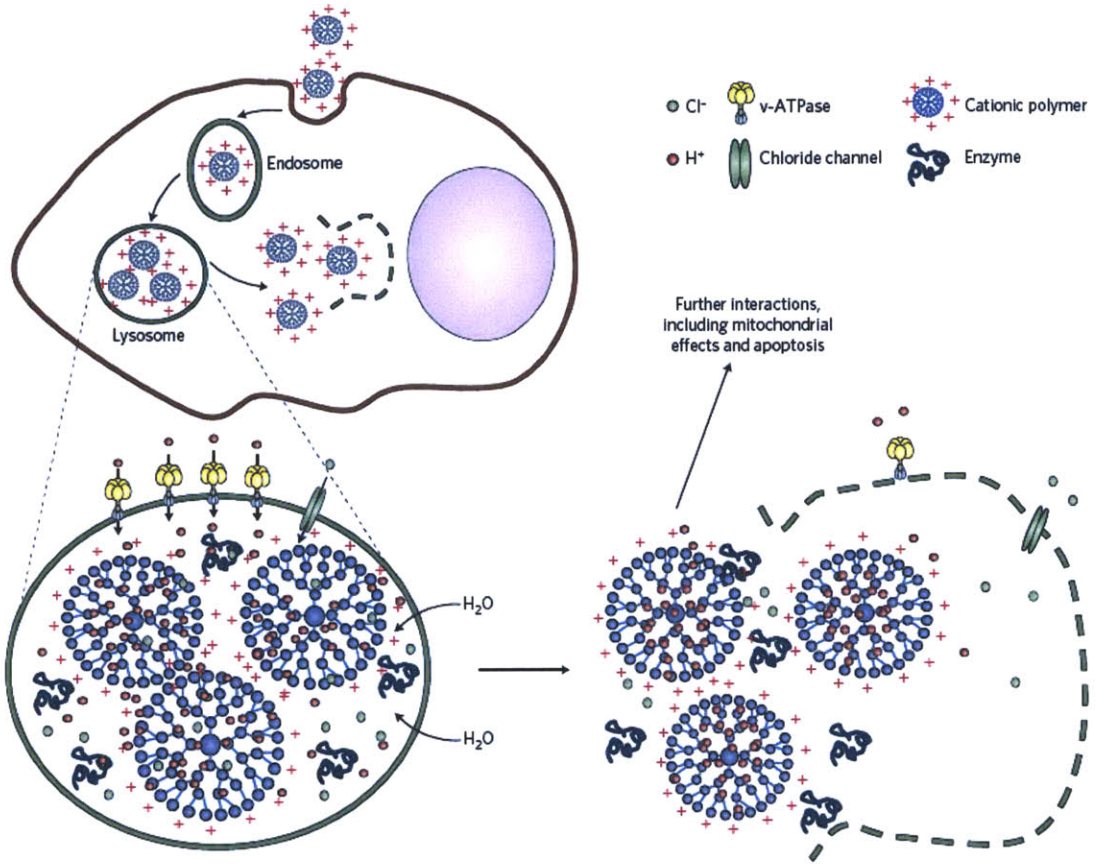

Figure 1.3 Endosomal Escape via the Proton Sponge Effect
Cationic polymers present in endosomes are protonated as the cell attempts to decrease endosomal pH for lysosomal fusion. The excess of protons needed to effect the needed pH change leads to an increase in chloride counter ions, resulting in osmotic swelling and burst of the vesicle [48].

Figure 1.4 shows the impact of secondary and tertiary amines capable of buffering endosomal pH and causing proton-sponge mediated rupture. Polymers capable of endosomal buffering (PAM, PEI in figure) are able to increase the endosomal chloride content and slow the drop in pH relative to poly-L-lysine (POL in figure), which has no buffering activity in this pH range. As shown in panel C, this leads to an increase in endosomal size which ultimately leads to rupture [49].

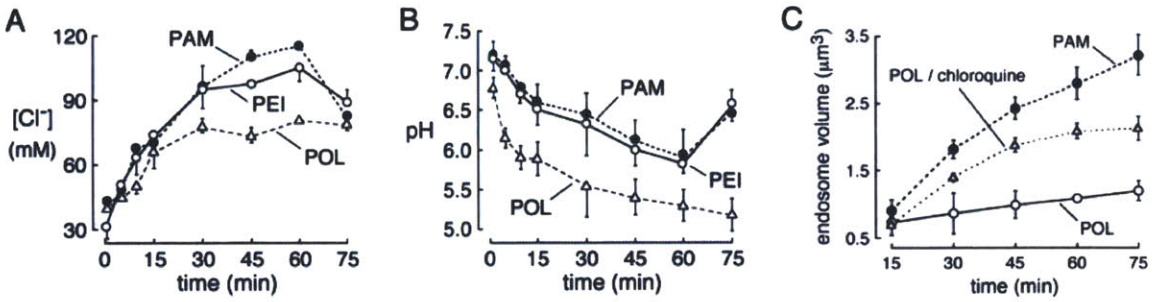

Figure 1.4 Effect of Polymer Buffering on Endosomal Escape
Polyamidoamine dendrimers (PAM), PEI, and Poly-L-Lysine (POL) polyplexes were added to cells along with probes allowing for the measurement of endosomal chloride content (A) and pH (B). Endosomal volume (C) was tracked via microscopy [49].

Once released from the endosome, the plasmid DNA must avoid degradation by nucleases present in the cytosol [50]. For many systems, it can be unclear when the DNA and polymer actually dissociate, but if unpacking has happened prior to the DNA reaching the nucleus, nuclease degradation is an issue. If DNA binding is too tight, transport through the cytosol to the nucleus can be quite difficult because the polyplex must translocate in a dense cellular protein environment [51]. In 1984, Kalderon et. al demonstrated that a sequence of amino acids served as a nuclear localization signal (NLS) that promoted entry into the nucleus for proteins too large to normally penetrate the nuclear pore complex (NPC) via a class of endogenous proteins known as importins [52]. Conjugation of an NLS to the polymer or plasmid DNA directly has been somewhat effective in increasing transfection activity [53-61]. Figure 1.5 outlines several strategies for attaching NLS sequences to polymers, including covalent attachment, attraction by a DNA-targeting sequence (DTS), attachment of an NLS using a peptide nucleic acid (PNA) clamp, and simple electrostatic association of the often cationic NLS [62]. Other strategies that have been employed involve small molecule glucocorticoids, such as dexamethasone, to bind receptors on the nuclear envelope [63].

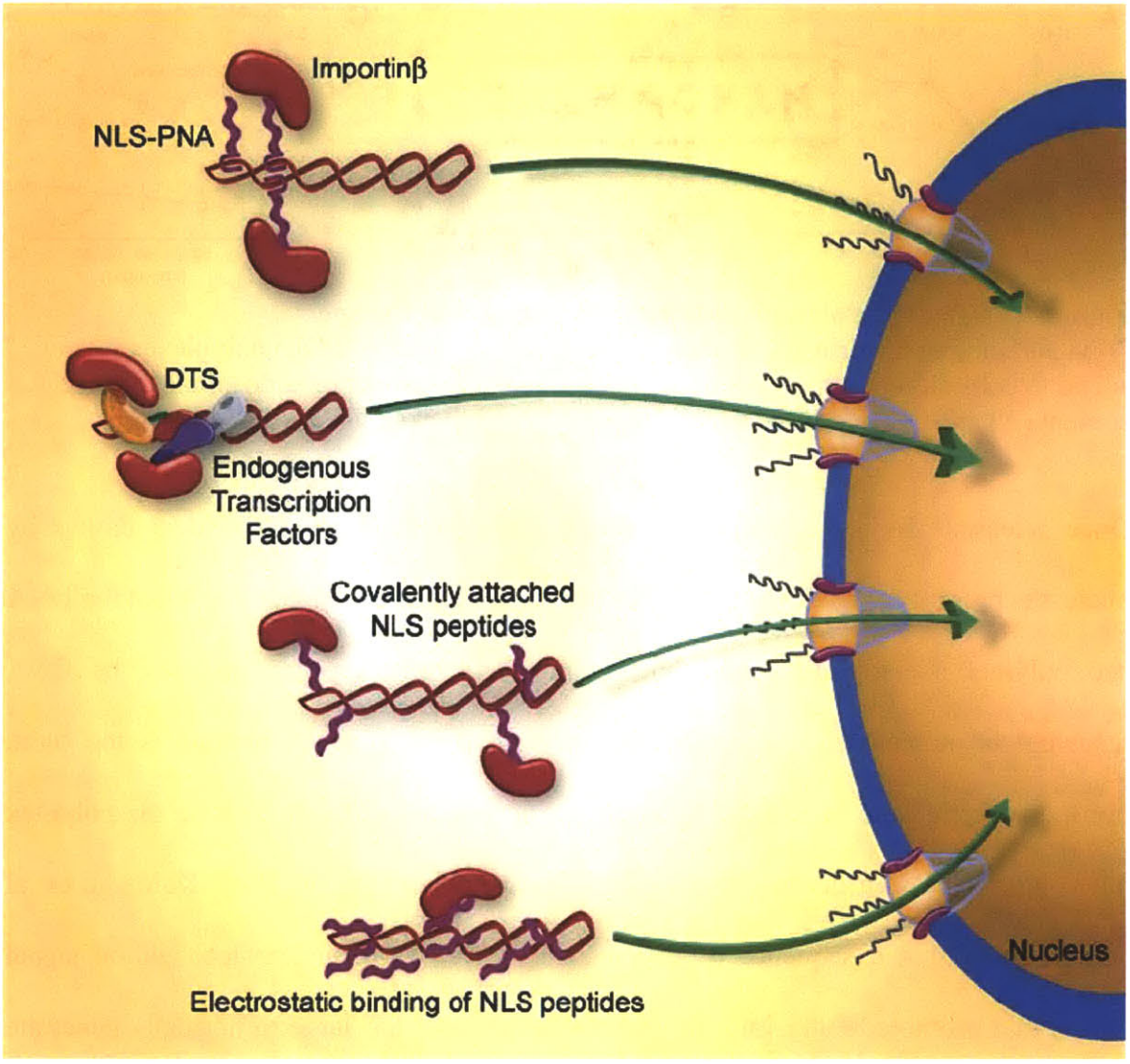

Figure 1.5 Strategies for Enhancing Nuclear Import of DNA
Several methods for attracting importins for active uptake of DNA through the nuclear pore complex are shown [62].

1.3.2 Extracellular Barriers to Gene Delivery

DNA will be degraded by serum nucleases unless shielded by some type of physical vector, such as a polymer [64]. Serum proteins can also non-specifically bind to polyplexes and cause particle aggregation, which will cause polyplexes to be cleared from the blood stream, or become trapped in fine capillary beds [65]. Additionally, the

immune system can bind opsonizing proteins to the vector surface, which leads to immune clearance [66]. However, it has been shown that coating a vector with PEG will significantly reduce binding of serum proteins, though at the expense of transfection efficiency [36]. Furthermore, cell membranes carry a negative surface charge, and as such, will non-specifically uptake positively charged polyplexes [67]. The approach many have taken to address both non-specific uptake and transfection loss with PEGylation is to attach a cell-specific targeting ligand to the surface of the polyplex such as an antibody or a small molecule (e.g. folate or mannose) for which the target cell has a receptor [68-71].

1.3.3 Analysis of Barrier Evasion Properties

Detailed analysis of the specific barriers which hinder gene delivery is crucial for the rational design of efficient carriers. Varga et. al. used quantitative PCR to compare the intracellular rate-limiting steps for the most popular commercial vectors in rapidly dividing hepatoblastoma cells (C3A) [19]. It is difficult however, to draw conclusions about the rate-limiting step in cells such as dendritic cells or macrophages which are not rapidly dividing as hepatoblastoma cells are, and thus would have more intact nuclear envelopes [34]. Subcellular DNA can also be tracked using confocal fluorescence microscopy, which can quantitate location of DNA in various locations as well as determine its complexation state [72-74]. These techniques have been used to compare the relative efficiencies of adenovirus and Lipofectamine, with the interesting result that the strength of the adenovirus was a four order-of-magnitude increase in protein generated by plasmids which had already made it inside the nucleus [75]. This type of mechanistic insight is critical and suggests a need for biodegradable vectors, improved

plasmid design, and an emphasis on understanding more about individual barriers to transfection.

1.3.4 Effects of Free Polymer

In addition to understanding how polyplexes are interacting with the various barriers to delivery, it is critical to understand the details of these interactions. The role of free polymer, excess polymer that is unbound to the polyplex, has been explored in very few studies, though its role has been shown to be critical for transfection [76-78]. Figure 1.6A shows the purification of free branched PEI 25k from a standard preparation of PEI polyplexes at an N/P ratio of 10. Multiple studies have estimated the fraction of PEI actually binding DNA to correspond to approximately an N/P of 3, indicating that 70% of the PEI is free in solution [76, 77]. As demonstrated in Figure 1.6B, when this free polymer is removed, transfection is reduced by over an order of magnitude. However, when this polymer is re-introduced, even several hours after initial treatment, transfection efficiency is recovered. Thus, it is clear that polymer gene delivery vehicles exist not as a homogenous solution but as two independent components – polyplexes and free polymer, each of which play an important role in transfection.

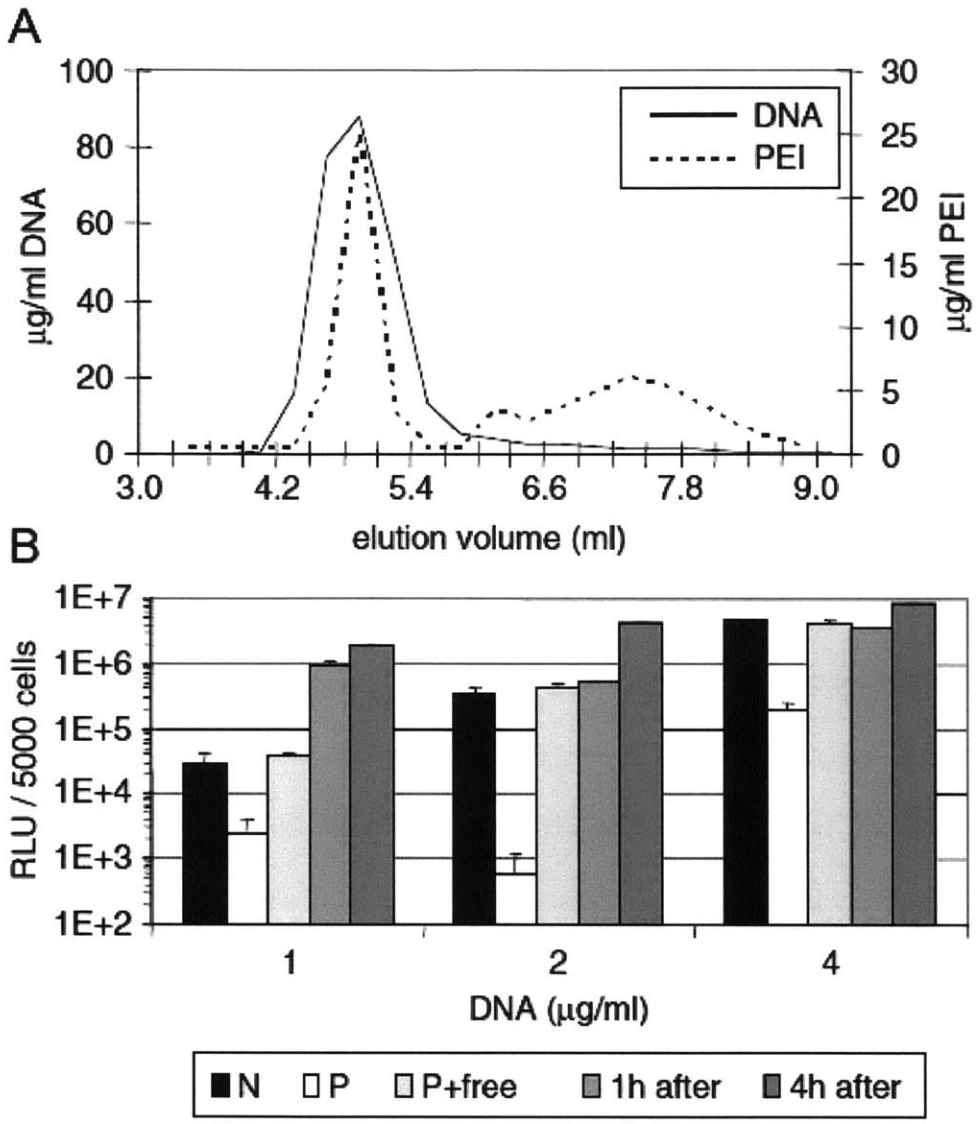

Figure 1.6 Effects of Free Polymer on Transfection
(A) Size exclusion chromatography (SEC) purification of a preparation of bPEI 25k polyplexes prepared at N/P = 10. (B) Transfection efficiency of N/P 10 bPEI polyplexes as assembled (N), after removal of free bPEI (P), purified polyplexes supplemented with an equal amount of free PEI which was added either immediately upon polyplex treatment (P+free), 1 hr after, or 4h after [76].

1.4 Thesis Overview

The complexity of the gene delivery problem necessitates a systematic and thorough approach to engineering solutions. In particular, consideration of structure-function relationships regarding not only overall transfection efficiency but also the discrete

barriers to delivery is crucial. In this work, we apply the concept of systematic barrier evaluation to nucleic acid delivery systems containing bioresponsive domains designed to effectively address multiple barriers. Chapter 2 describes the evaluation a linear-dendritic PAMAM-PEG block copolymer system previously developed in our lab. A method for quantifying endosomal escape in high-throughput is introduced and the merits of the system relative to uptake, endosomal escape, and nuclear import are discussed. Chapter 3 introduces a class of crosslinked linear PEI hyperbranched polymers which can contain disulfide-responsive linkages. The role of the disulfide bond in the efficiency and cytotoxicity of this class of polymers is studied and the role of unbound free polymer relative to internalization and endosomal escape is clarified. Chapter 4 demonstrates the applicability of this analysis to siRNA delivery, in this case to a library of amine-functionalized synthetic polypeptides. The pH-responsive secondary structure, micelle formation, and ester hydrolysis are discussed prior to the discrete barrier-oriented analysis of the siRNA delivery potential of this library.

1.5 References

1. Somia, N. and I.M. Verma, *Gene therapy: trials and tribulations.* Nat Rev Genet, 2000. **1**(2): p. 91-99.
2. Verma, L.M., et al., *Gene Therapy: Promises, Problems and Prospects*. 2000, Springer.
3. Walther, W. and U. Stein, *Viral vectors for gene transfer - A review of their use in the treatment of human diseases.* Drugs, 2000. **60**(2): p. 249-271.
4. Enders, J.F., et al., *Adenoviruses: group name proposed for new respiratory-tract viruses.* Science, 1956. **124**(3212): p. 119-20.
5. Dinh, A.-T., T. Theofanous, and S. Mitragotri, *A Model for Intracellular Trafficking of Adenoviral Vectors*. 2005. p. 1574-1588.
6. Rosenberg, S.A., et al., *Gene-Transfer into Humans - Immunotherapy of Patients with Advanced Melanoma, Using Tumor-Infiltrating Lymphocytes Modified by Retroviral Gene Transduction.* New England Journal of Medicine, 1990. **323**(9): p. 570-578.

7. Marshall, E., *Gene therapy: Second child in French trial is found to have leukemia.* Science, 2003. **299**(5605): p. 320-320.
8. Marshall, E., *Clinical trials - Gene therapy death prompts review of adenovirus vector.* Science, 1999. **286**(5448): p. 2244-2245.
9. *Gene Therapy Clinical Trials Worldwide.* 2007 [cited 2007 3/1/2007]; Available from: http://wiley.co.uk/genmed/clinical/.
10. Felgner, P.L., et al., *Lipofection - a Highly Efficient, Lipid-Mediated DNA-Transfection Procedure.* Proceedings of the National Academy of Sciences of the United States of America, 1987. **84**(21): p. 7413-7417.
11. Xu, Y. and F.C. Szoka, Jr., *Mechanism of DNA release from cationic liposome/DNA complexes used in cell transfection.* Biochemistry, 1996. **35**(18): p. 5616-23.
12. Lv, H.T., et al., *Toxicity of cationic lipids and cationic polymers in gene delivery.* Journal of Controlled Release, 2006. **114**(1): p. 100-109.
13. Little, S.R., et al., *From The Cover: Poly-p amino ester-containing microparticles enhance the activity of nonviral genetic vaccines.* 2004. p. 9534-9539.
14. Little, S.R. and R. Langer, *Nonviral delivery of cancer genetic vaccines.* Adv Biochem Eng Biotechnol, 2005. **99**: p. 93-118.
15. Glover, D.J., H.J. Lipps, and D.A. Jans, *TOWARDS SAFE, NON-VIRAL THERAPEUTIC GENE EXPRESSION IN HUMANS.* Nature Reviews Genetics, 2005. **6**(4): p. 299-310.
16. Kan, P.L., A.G. Schatzlein, and I.F. Uchegbu, *Polymers Used for the Delivery of Genes in Gene Therapy*, in *Polymers in Drug Delivery*, I.F. Uchegbu and A.G. Schatzlein, Editors. 2006, CRC Press: Boca Raton.
17. Abdallah, B., et al., *A powerful nonviral vector for in vivo gene transfer into the adult mammalian brain: Polyethylenimine.* Human Gene Therapy, 1996. **7**(16): p. 1947-1954.
18. Wightman, L., et al., *Different behavior of branched and linear polyethylenimine for gene delivery in vitro and in vivo.* Journal of Gene Medicine, 2001. **3**(4): p. 362-372.
19. Varga, C.M., et al., *Quantitative comparison of polyethylenimine formulations and adenoviral vectors in terms of intracellular gene delivery processes.* Gene Therapy, 2005. **12**(13): p. 1023-1032.
20. Boussif, O., M.A. Zanta, and J.P. Behr, *Optimized galenics improve in vitro gene transfer with cationic molecules up to 1000-fold.* Gene Therapy, 1996. **3**(12): p. 1074-1080.
21. Parhamifar, L., et al., *Polycation cytotoxicity: a delicate matter for nucleic acid therapy—focus on polyethylenimine.* Soft Matter, 2010. **6**: p. 4001.
22. Wu, G.Y. and C.H. Wu, *Receptor-mediated in vitro gene transformation by a soluble DNA carrier system [published erratum appears in J Biol Chem 1988 Jan 5;263(1):588].* 1987. p. 4429-4432.
23. Roy, K., et al., *Oral gene delivery with chitosan-DNA nanoparticles generates immunologic protection in a murine model of peanut allergy.* Nature Medicine, 1999. **5**(4): p. 387-391.
24. Heller, J., et al., *Poly(ortho esters): synthesis, characterization, properties and uses.* Advanced Drug Delivery Reviews, 2002. **54**(7): p. 1015-1039.

25. Akinc, A., et al., *Synthesis of poly(beta-amino ester)s optimized for highly effective gene delivery.* Bioconjug Chem, 2003. **14**(5): p. 979-88.
26. Anderson, D.G., et al., *Structure/property studies of polymeric gene delivery using a library of poly(beta-amino esters).* Mol Ther, 2005. **11**(3): p. 426-34.
27. Bosman, A.W., H.M. Janssen, and E.W. Meijer, *About Dendrimers: Structure, Physical Properties, and Applications.* 1999. p. 1665-1688.
28. Haensler, J. and F.C. Szoka, *Polyamidoamine Cascade Polymers Mediate Efficient Transfection of Cells in Culture.* Bioconjugate Chemistry, 1993. **4**(5): p. 372-379.
29. Paleos, C.M., D. Tsiourvas, and Z. Sideratou, *Molecular Engineering of Dendritic Polymers and Their Application as Drug and Gene Delivery Systems.* 2007.
30. Tang, M.X., C.T. Redemann, and F.C. Szoka, *In vitro gene delivery by degraded polyamidoamine dendrimers.* Bioconjugate Chemistry, 1996. **7**(6): p. 703-714.
31. Loïc Vincent, J.V.J.-Y.P.H.B.P.O.A.M.C.M.M.M.H.L.J.-P.V.C.S.H.L., *Efficacy of dendrimer-mediated angiostatin and TIMP-2 gene delivery on inhibition of tumor growth and angiogenesis: <I>In vitro</I> and <I>in vivo</I> studies.* 2003. p. 419-429.
32. Bielinska, A.U., et al., *DNA complexing with polyamidoamine dendrimers: Implications for transfection.* Bioconjugate Chemistry, 1999. **10**(5): p. 843-850.
33. Kukowska-Latallo, J.F., et al., *Efficient transfer of genetic material into mammalian cells using Starburst polyamidoamine dendrimers.* 1996. p. 4897-4902.
34. Brunner, S., et al., *Cell cycle dependence of gene transfer by lipoplex polyplex and recombinant adenovirus.* Gene Therapy, 2000. **7**(5): p. 401-407.
35. Malik, N., et al., *Dendrimers: Relationship between structure and biocompatibility in vitro, and preliminary studies on the biodistribution of I-125-labelled polyamidoamine dendrimers in vivo.* Journal of Controlled Release, 2000. **65**(1-2): p. 133-148.
36. Ogris, M., et al., *PEGylated DNA/transferrin-PEI complexes: reduced interaction with blood components, extended circulation in blood and potential for systemic gene delivery.* Gene Therapy, 1999. **6**(4): p. 595-605.
37. Kris C. Wood, S.R.L.R.L.P.T.H., *A Family of Hierarchically Self-Assembling Linear-Dendritic Hybrid Polymers for Highly Efficient Targeted Gene Delivery.* 2005. p. 6704-6708.
38. Thomas, M. and A.M. Klibanov, *Non-viral gene therapy: polycation-mediated DNA delivery.* Applied Microbiology and Biotechnology, 2003. **62**(1): p. 27-34.
39. Sahay, G., D.Y. Alakhova, and A.V. Kabanov, *Endocytosis of nanomedicines.* Journal of Controlled Release. **145**(3): p. 182-195.
40. Rejman, J., A. Bragonzi, and M. Conese, *Role of Clathrin- and Caveolae-Mediated Endocytosis in Gene Transfer Mediated by Lipo- and Polyplexes.* Mol Ther, 2005. **12**(3): p. 468-474.
41. Khalil, I.A., et al., *Uptake Pathways and Subsequent Intracellular Trafficking in Nonviral Gene Delivery.* Pharmacological Reviews, 2006. **58**(1): p. 32-45.
42. von Gersdorff, K., et al., *The Internalization Route Resulting in Successful Gene Expression Depends on both Cell Line and Polyethylenimine Polyplex Type.* Mol Ther, 2006. **14**(5): p. 745-753.

43. Murthy, N., et al., *The design and synthesis of polymers for eukaryotic membrane disruption.* Journal of Controlled Release, 1999. **61**(1-2): p. 137-143.
44. Wagner, E., et al., *Influenza-Virus Hemagglutinin-Ha-2 N-Terminal Fusogenic Peptides Augment Gene-Transfer by Transferrin Polylysine DNA Complexes - toward a Synthetic Virus-Like Gene-Transfer Vehicle.* Proceedings of the National Academy of Sciences of the United States of America, 1992. **89**(17): p. 7934-7938.
45. Read, M.L., et al., *Barriers to Gene Delivery Using Synthetic Vectors*, in *Advances in Genetics*. 2005, Academic Press. p. 19-46.
46. Behr, J.P., *The proton sponge: A trick to enter cells the viruses did not exploit.* Chimia, 1997. **51**(1-2): p. 34-36.
47. Akinc, A., et al., *Exploring polyethylenimine-mediated DNA transfection and the proton sponge hypothesis.* Journal of Gene Medicine, 2005. **7**(5): p. 657-663.
48. Nel, A.E., et al., *Understanding biophysicochemical interactions at the nano-bio interface.* Nature materials, 2009. **8**: p. 543-57.
49. Sonawane, N.D., F.C.S. Jr, and A.S. Verkman, *Chloride accumulation and swelling in endosomes enhances DNA transfer by polyamine-DNA polyplexes, J.* Biol. Chem., 2003. **278**: p. 44826-44831.
50. Lechardeur, D., et al., *Metabolic instability of plasmid DNA in the cytosol: a potential barrier to gene transfer.* Gene Therapy, 1999. **6**(4): p. 482-497.
51. Pouton, C.W., et al., *Targeted delivery to the nucleus.* Advanced Drug Delivery Reviews, 2007. **59**(8): p. 698-717.
52. Kalderon, D., et al., *A short amino acid sequence able to specify nuclear location.* Cell, 1984. **39**(3 Pt 2): p. 499-509.
53. Torchilin, V.P., *RECENT APPROACHES TO INTRACELLULAR DELIVERY OF DRUGS AND DNA AND ORGANELLE TARGETING.* 2006. p. 343-375.
54. Chan, C.-K. and D.A. Jans, *Using nuclear targeting signals to enhance non-viral gene transfer.* Immunol Cell Biol, 2002. **80**(2): p. 119-130.
55. Goldfarb, D.S., et al., *Synthetic Peptides as Nuclear-Localization Signals.* Nature, 1986. **322**(6080): p. 641-644.
56. Ludtke, J.J., et al., *A nuclear localization signal can enhance both the nuclear transport and expression of 1 kb DNA.* Journal of Cell Science, 1999. **112**(12): p. 2033-2041.
57. Nigg, E.A., *Nucleocytoplasmic transport: Signals, mechanisms and regulation.* Nature, 1997. **386**(6627): p. 779-787.
58. Ohno, M., M. Fornerod, and I.W. Mattaj, *Nucleocytoplasmic transport: The last 200 nanometers.* Cell, 1998. **92**(3): p. 327-336.
59. Dean, D.A., *Import of plasmid DNA into the nucleus is sequence specific.* Experimental Cell Research, 1997. **230**(2): p. 293-302.
60. Zanta, M.A., P. Belguise-Valladier, and J.P. Behr, *Gene delivery: A single nuclear localization signal peptide is sufficient to carry DNA to the cell nucleus.* Proceedings of the National Academy of Sciences of the United States of America, 1999. **96**(1): p. 91-96.
61. Robbins, J., et al., *2 Interdependent Basic Domains in Nucleoplasmin Nuclear Targeting Sequence - Identification of a Class of Bipartite Nuclear Targeting Sequence.* Cell, 1991. **64**(3): p. 615-623.

62. Lam, a.P. and D.A. Dean, *Progress and prospects: nuclear import of nonviral vectors.* Gene therapy, 2010: p. 1-9.
63. Choi, J.S., et al., *Dexamethasone conjugated poly(amidoamine) dendrimer as a gene carrier for efficient nuclear translocation.* International Journal of Pharmaceutics, 2006. **320**(1-2): p. 171-178.
64. Chiou, H.C., et al., *Enhanced Resistance to Nuclease Degradation of Nucleic-Acids Complexed to Asialoglycoprotein-Polylysine Carriers.* Nucleic Acids Research, 1994. **22**(24): p. 5439-5446.
65. Dash, P.R., et al., *Factors affecting blood clearance and in vivo distribution of polyelectrolyte complexes for gene delivery.* Gene Therapy, 1999. **6**(4): p. 643-650.
66. Patel, H.M., *Serum opsonins and liposomes: their interaction and opsonophagocytosis.* Crit Rev Ther Drug Carrier Syst, 1992. **9**(1): p. 39-90.
67. Mislick, K.A. and J.D. Baldeschwieler, *Evidence for the role of proteoglycans in cation-mediated gene transfer.* Proceedings of the National Academy of Sciences of the United States of America, 1996. **93**(22): p. 12349-12354.
68. Plank, C., et al., *Gene-Transfer into Hepatocytes Using Asialoglycoprotein Receptor Mediated Endocytosis of DNA Complexed with an Artificial Tetra-Antennary Galactose Ligand.* Bioconjugate Chemistry, 1992. **3**(6): p. 533-539.
69. Trubetskoy, V.S., et al., *Use of N-Terminal Modified Poly(L-Lysine) Antibody Conjugate as a Carrier for Targeted Gene Delivery in Mouse Lung Endothelial-Cells.* Bioconjugate Chemistry, 1992. **3**(4): p. 323-327.
70. Stahl, P.D., *The Mannose Receptor and Other Macrophage Lectins.* Current Opinion in Immunology, 1992. **4**(1): p. 49-52.
71. Wagner, E., et al., *Transferrin-Polycation Conjugates as Carriers for DNA Uptake into Cells.* Proceedings of the National Academy of Sciences of the United States of America, 1990. **87**(9): p. 3410-3414.
72. Keiji Itaka, A.H.Y.Y.K.N.H.K.K.K., *<I>In situ</I> single cell observation by fluorescence resonance energy transfer reveals fast intra-cytoplasmic delivery and easy release of plasmid DNA complexed with linear polyethylenimine*. 2004. p. 76-84.
73. Kong, H.J., et al., *Non-viral gene delivery regulated by stiffness of cell adhesion substrates.* Nat Mater, 2005. **4**(6): p. 460-464.
74. Akita, H., et al., *Quantitative Three-Dimensional Analysis of the Intracellular Trafficking of Plasmid DNA Transfected by a Nonviral Gene Delivery System Using Confocal Laser Scanning Microscopy.* Mol Ther, 2004. **9**(3): p. 443-451.
75. Hama, S., et al., *Quantitative comparison of intracellular trafficking and nuclear transcription between adenoviral and lipoplex systems.* Molecular Therapy, 2006. **13**: p. 786-94.
76. Boeckle, S., et al., *Purification of polyethylenimine polyplexes highlights the role of free polycations in gene transfer.* The journal of gene medicine, 2004. **6**: p. 1102-11.
77. Yue, Y., et al., *Revisit complexation between DNA and polyethylenimine - Effect of uncomplexed chains free in the solution mixture on gene transfection.* Journal of controlled release : official journal of the Controlled Release Society, 2010.

78. Yue, Y., et al., *Revisit complexation between DNA and polyethylenimine - effect of length of free polycationic chains on gene transfection.* Journal of controlled release : official journal of the Controlled Release Society, 2011.

Chapter 2. Intracellular Trafficking of Polyamidoamine – Polyethylene Glycol Block Copolymers in DNA Delivery

1.1 Abstract

The delivery of nucleic acids has the potential to revolutionize medicine by allowing previously untreatable diseases to be clinically addressed. Viral delivery systems have shown immunogenicity and toxicity dangers, but synthetic vectors have lagged in transfection efficiency. Previously, we have developed a modular, linear-dendritic block copolymer architecture with high gene transfection efficiency compared to commercial standards. This rationally designed system makes use of a cationic dendritic block to condense the anionic DNA and forms complexes with favorable endosomal escape properties. The linear block provides biocompatibility, protection from serum proteins, and can be functionalized with a targeting ligand. In this work, we quantitate performance of this system with respect to intracellular barriers to gene delivery using both high-throughput and traditional approaches. An image-based, high throughput assay for endosomal escape is described and applied to the block copolymer system. Nuclear entry is demonstrated to be the most significant barrier to more efficient delivery and will be addressed in future versions of the system.

1.2 Introduction

Nucleic acid therapies have unique potential as a transformative element in clinical medicine over the coming decades. The primary barrier to clinical application of gene therapy has been the lack of safe, efficient materials to deliver genes to appropriate tissues [1, 2]. A variety of viral vectors, including adenoviruses, adeno-associated viruses

(AAVs), and retroviruses have been studied as gene delivery agents [3]. While these materials can achieve high levels of protein expression, they have suffered from concerns of safety, immunogenicity, scale-up for manufacturing, and limited size of the delivered gene [1]. When viral vectors are used for transient gene expression, the increased immune response upon repeat injections becomes a limiting factor [4, 5].

Synthetic systems have been developed as a safer alternative to viral transfection, but have struggled to achieve efficiency (protein produced per plasmid) on the same order of magnitude as viral vectors. Synthetic delivery systems include cationic polymers [6, 7], liposomes [8-10], and dendrimers [11, 12], among other material classes. Polymeric systems developed include linear and branched polyethyleneimine (PEI) [13], linear and dendritic polyamidoamine (PAMAM) [11], poly-β-amino esters (PBAE) [14-16], as well as many other linear and branched polyamines [17]. The molecular design of such polymeric systems must overcome several extracellular and intracellular barriers to achieve therapeutic levels of protein expression. In the bloodstream, DNA complexes must avoid hepatic and renal clearance, detection and removal by the immune system, binding to charged serum proteins, inter-complex aggregation, degradation by plasma nucleases and uptake by non-targeted somatic cells [18-21]. Complexes then must be taken up efficiently by the cells of interest, and escape the endosomal compartment into which they are initially trafficked. Failure to do so results in degradation in the lysosome, recycling to the cell membrane, and lack of transfection. Once out of the endosome, the complex must translocate to the nucleus and cross the nuclear membrane . Unpackaging of the DNA from the complex is also necessary prior to expression of the delivered plasmid by the host cell. As synthetic vectors do not contain transcription factors as

viruses do, the final expression of uncomplexed plasmids in the nucleus has been shown to be a bottleneck as well [22].

In order to address these barriers to transfection, our lab has previously developed a linear-dendritic block-copolymer system, in which a generation 5.0 PAMAM dendron is conjugated to a polyethylene glycol (PEG) linear block, which itself is end-linked to a targeting moiety [23, 24]. This PAMAM-G5-PEG system performed well *in vitro*, with transfection efficiencies nearly ten-fold greater than commercially available branched PEI, and it displayed targeted, receptor-mediated uptake with cytotoxicities significantly lower than unmodified PAMAM or PEI. The targeting moiety on the targeted PAMAM-G5-PEG conjugates is a short peptide, WIFPWIQL, identified from *in vivo* phage display techniques by the Arap/Pasqualini lab [25]. WIFPWIQL binds GRP78/BiP/HSP70 – a glucose-response protein found intracellularly at the endoplasmic reticulum (ER) in benign cell types, but on the cell membrane of many solid tumor cell types [26, 27]. In our previous publication, we reported on the synthesis, DNA complexation, and overall *in vitro* transfection efficiency of these conjugates. In this work, we characterize the intracellular trafficking of this system in order to identify the bottlenecks to more efficient delivery with these synthetic vectors, and further elucidate the mechanisms which enable any enhanced efficiency of this system over other common polyamines. We also introduce a new method for high-throughput screening of the endosomal escape properties of various polyplex formulations.

1.3 Materials and Methods

1.3.1 Materials

Generation 5.0 cystamine core PAMAM dendrimers were obtained from Dendritic Nanotechnologies (Mount Pleasant, MI) and used without further purification. Heterobifunctional poly (ethylene glycol) (Maleimide-PEG5k- N-hydroxysuccinimide) was obtained from Laysan Bio (Arab,AL). WIFPWIQL peptide was synthesized and purified by the MIT Biopolymers lab in the Swanson Core facilities at the Koch Institute. Immobilized Tris(2-carboxyethyl)phosphine (TCEP) reducing gel was obtained from Pierce (Thermo Fisher Scientific, Rockford, IL). Branched 25,000 g/mol (M_w) polyethyleneimine (PEI) and other chemical reagents were purchased from Sigma Aldrich (St. Louis, MO). DU145 cells and cell culture media were obtained from ATCC (Manassas, VA). pCMV-EGFP-N1 plasmid DNA was obtained from Aldevron Inc.(Fargo, ND). All other cell culture reagents were obtained from Invitrogen (Carlsbad, CA).

1.3.2 Block Copolymer Synthesis

PAMAM-G5-PEG block copolymers were prepared in a three-step synthesis. In the first step, generation 5.0 cystamine core PAMAM dendrimer (60.0 mg, 2.05 μmol) was reduced using immobilized TCEP gel (1.5 mL) for 90 min. Confirmation of the reduction was done using (5,5'-dithiobis-(2-nitrobenzoic acid) (DTNB, Ellman's reagent) to quantify free thiols and fluorescamine to quantify primary amines. Reduction was greater than 80%. In parallel, targeting peptide WIFPWIQL (7.1 mg, 6.5 μmol) was dissolved in DMSO at 5 mg/mL and added to a solution of Mal-PEG5k-NHS (30 mg, 5.4

μmol) in DMSO at 5 mg/mL. 20 μL triethylamine (TEA) was added to facilitate the reaction. After 30 min, this reaction was twice precipitated in cold ether, dissolved in PBS and reacted with the reduced PAMAM dendrimer for 24 hours. Untargeted polymers were synthesized by substituting monofunctional MAL-mPEG5k for the WIFPWIQL-PEG-MAL. The synthesized polymers were dialyzed against 8000 MWCO SpectraPOR (Spectrum Labs, Rancho Dominguez, CA) and lyophilized. Structure was confirmed by ^{1}H-NMR (400MHz, D_2O) δ (ppm) = 3.69 (s, CH_2CH_2O), 3.48 (t, $CONHCH_2C\mathbf{H}_2NH_2$), 3.30 (t, $CONHC\mathbf{H}_2CH_2NR$), 3.11 (t, $CONHC\mathbf{H}_2CH_2NH_2$), 2.85 (m, $NC\mathbf{H}_2CH_2CONH$), 2.64 (t, $CONHCH_2C\mathbf{H}_2NR$), 2.45 (m, $NCH_2C\mathbf{H}_2CONH$)

1.3.3 Cell Culture

DU145 cells were cultured in Minimum Essential Media (MEM) supplemented with 10% heat-inactivated fetal bovine serum (FBS) and 1% penicillin-streptomycin in a humidified 37°C atmosphere at 5% CO_2.

1.3.4 Transfection

Cells were trypsinized prior to transfection and seeded in 96-well plates at 5,000 cells/well overnight in a humidified 37°C atmosphere at 5% CO_2. PAMAM-PEG block copolymers were diluted in 25 mM sodium acetate buffer (NaAc) (pH 5.5) at 1.5 mg/mL initially and then further diluted into 25 μL of the same buffer in a separate 96-well plate at varying concentrations. 25 μL of pDNA at 0.06 mg/mL in NaAc was then added to each well and mixed by gentle pipetting. After 10 min for complex formation, 30 μL of the complexes were added to 200 μL of Opti-MEM supplemented with 10% FBS. After further mixing, 150 μL of the complexes in Opti-MEM were added to the cells (after

growth media had been removed). After 4 hours, the complexes in Opti-MEM were removed and growth media was added. Cells were assayed at 48 hr for GFP production using flow cytometry. 4000 – 10000 live cells per sample were analyzed. GFP production was normalized to that from transfection with an optimized formulation of 25kDa branched PEI [28]. p-values were calculated using a two-way analysis of variation and Bonferroni post-tests were performed on all conditions shown.

1.3.5 Flow Cytometry

Flow cytometry was performed in U-bottom 96-well plates using an LSR II HTS Flow cytometer (Becton-Dickinson, Mountain View, CA). To prepare samples, media was removed from cells and replaced with 25 μL trypsin for 5 minutes. 50 μL of PBS supplemented with 2% FBS was then added to each well, mixed, and the entire 75 μL cell suspension transferred into a U-bottom 96-well plate.

1.3.6 Polyplex Uptake

Block copolymers and PEI were labeled with fluorescein isothiocyanate (FITC) at a molar ratio of 4:1 (dye:polymer). Using the labeled polymers, polyplexes were formed and cells treated as described in the above section. At the time indicated, cells were removed from the incubator and analyzed using flow cytometry. p-values were calculated using a two-way analysis of variation and Bonferroni post-tests were performed on all conditions shown.

1.3.7 High-Throughput Endosomal Escape

Complexes were assembled and transfection was conducted as described above, except that 25 μM calcein was added to the Opti-MEM and cells were seeded in black-

sided, clear-bottom 96-well plates. 4 hours after transfection, 5 μL of a solution of Hoechst 33342 diluted to 1:30 in PBS was added. After 20 minutes of staining, complexes and free dye were removed, and the cells were washed 3 times with PBS. 150 μL of phenol-free Opti-MEM with 10% serum was added to each well before the plate was covered with an opaque sticker, foiled, and analyzed. Imaging was done using a Cellomics ArrayScan VTI HCS Reader (Thermo Fisher, Waltham, MA) and analysis was done using the included software as described below. 300 – 3000 live cells per sample were analyzed. p-values were calculated using an unpaired t-test.

20 fields per well were imaged with a 20x objective, yielding 300 – 3000 cells. Autofocus was used for each field, based on the nuclear (Hoechst) channel with no Z-Offset. Exposure time was fixed at 0.15 s. Objects (nuclei) were identified using the Isodata thresholding method and considered single cell nuclei if the object area was between 40 and 400 square pixels. After the nuclei were identified, the cytoplasmic area was defined as being a ring a fixed distance outside the nucleus. After defining "escaped" and "non-escaped" cells, the most accurate combination of parameters for separating the two was based on the average calcein channel intensity in the central nuclear region. Since the majority of the cytoplasmic volume appeared to be present outside this region, calcein-filled endosomes rarely existed in this region. However, in escaped cells, the cytoplasmic region above & below the nucleus, even with relatively low volume, would always have some calcein signal. A threshold in this value was empirically set and could vary based on camera type, light source, and exposure time. Methods defining the number of cytoplasmic spots and their intensity relative to the rest of the cytoplasm were ultimately inferior to this method. Future iterations of this assay may determine degree of

escape or identify cells with both diffuse and punctuate calcein staining. Finally, note the images shown in Figure 3 are intensity normalized in order to better visualize the punctate staining pattern – all calculations are done with unstreched images (and thus the apparently different level of background in Figure 3 is not a problem).

1.3.8 Confocal Microscopy

8-well Lab-Tek chamber slides (Thermo Fisher, Waltham, MA) were treated for 20 minutes with human fibronectin in PBS at 0.01 mg/mL. The fibronectin was removed and DU145 cells were trypsinized and seeded in each well at a concentration of 1000 cells/well 24 h before transfection. Plasmid DNA was labeled with Rhodamine-CX using the Label-IT kit (Mirus Bio, Madison, WI). Polymers were FITC-labeled as described earlier. Polyplexes between labeled DNA and labeled polymers were formed in NaAc buffer as described earlier. 40 μL of complexes were added to 160 uL phenol-free Opti-MEM (supplemented with 10% serum) and added to each well. Complexes were removed after 4 h and replaced with growth media. At 24 h, cells were fixed with 3.7% formaldehyde in PBS, stained with Hoechst 33342, and were washed 3 times with PBS. Imaging was done on a PerkinElmer Ultraview spinning disc confocal (PerkinElmer, Waltham, MA).

1.4 Results and Discussion

1.4.1 Synthesis

Synthesis of the PAMAM-G5-PEG linear-dendritic block copolymers was similar to that reported previously by our group [24] and is shown in Scheme 2.1. Briefly, generation 5.0, cystamine core dendrimers were first reduced to expose dendrons with a single thiol

moiety (yielding two dendron-thiols per dendrimer) . In parallel, the N-hydroxysuccinimide (NHS) group of a heterobifunctional PEG was first reacted with the terminal lysine on the WIFPWIQL peptide, leaving the maleimide group of the PEG block free for subsequent conjugation to the exposed thiol on the reduced PAMAM dendrimer. This synthetic approach is managed easily in aqueous solutions and can be generally applied to most targeting ligands.

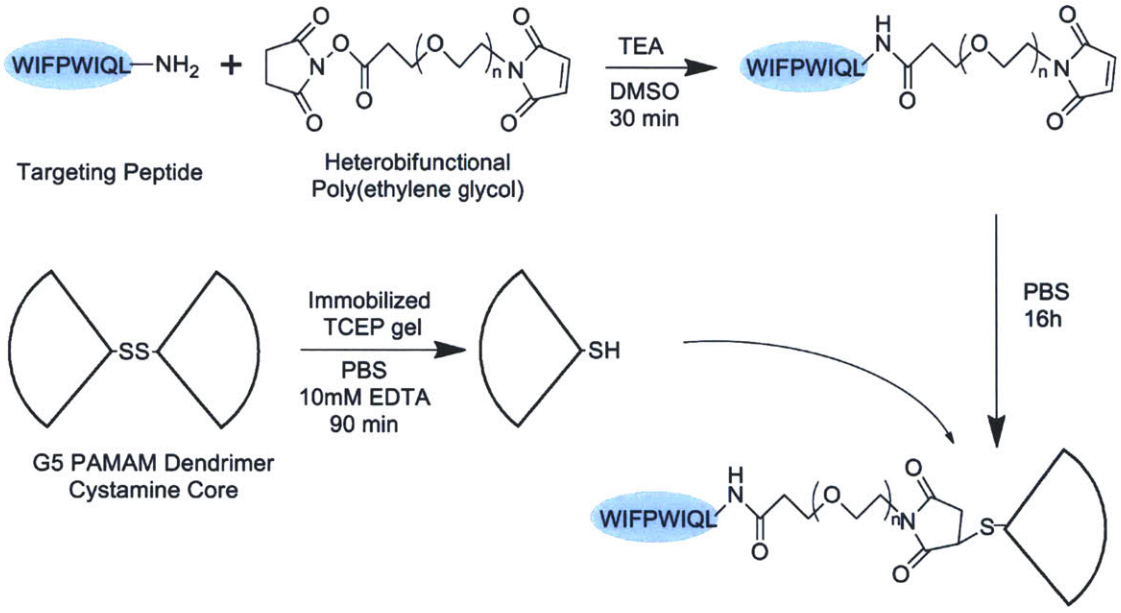

Scheme 2.1 Synthesis of PAMAM-G5-PEG-WIFP conjugates.
The targeting peptide is first reacted with a bifunctional linker before being precipitated and added to reduced G5 PAMAM dendrimer.

1.4.2 Overall Transfection

While the overall transfection efficiency of a gene carrier is a critical parameter to characterize, it is ultimately necessary to determine the bottlenecks – quantitatively if possible – in order to better design future iterations of the system. As shown in Figure 2.1A, the targeted block copolymers transfected DU145 cells nearly 8-fold better than

25kDa bPEI and nearly 4-fold better than an untargeted control block copolymer, which is consistent with our previously published studies using this system [24]. Figure 2.1B show that the presence of serum in the system limited the absolute percentage of cells transfected to a less than 3% and the fold increase of targeted block copolymer was 3-fold over both the untargeted control and PEI. While PEI is an efficient gene carrier in serum-free media, in more biologically relevant conditions (i.e. 10% or more serum), the advantage of the PEGylation in the block copolymer system becomes apparent [29].

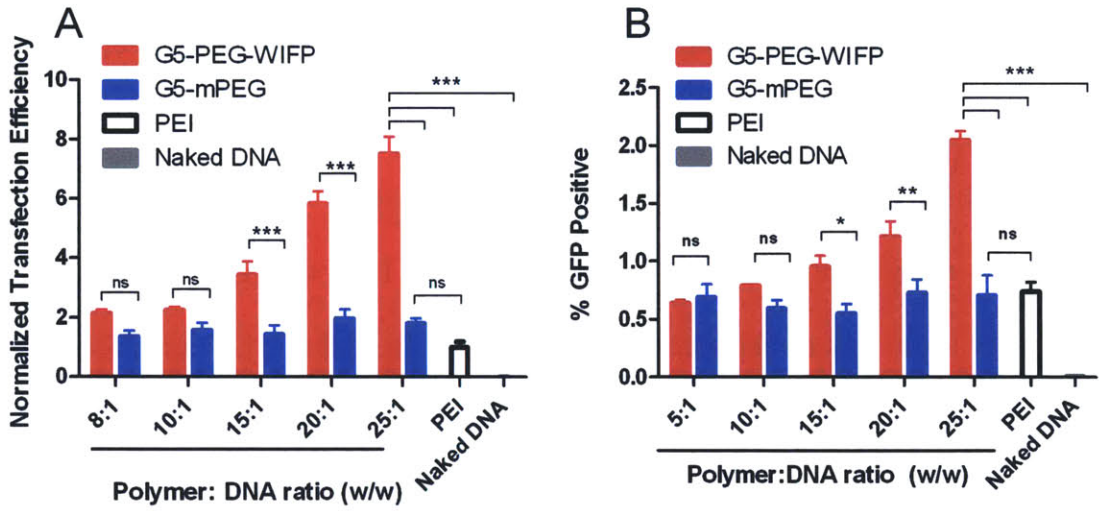

Figure 2.1 Normalized transfection efficiency (A) and percentage of cells transfected (B) of targeted and untargeted block copolymer formulations at various polymer:DNA ratios.
Transfections of EGFP were performed in 10% serum and analyzed 48 hrs later using flow cytometry. An optimized formulation of PEI at a polymer:DNA ratio of 2:1 was used and data is reported as mean fluorescence intensity normalized to that of the PEI transfected cells. Error bars represent SEM of 5 replicate experiments (*** = $p < 0.001$, ** = $p < 0.01$, * = $p < 0.05$, ns = not significant). These results are in agreement with

previously published reports of transfection efficiency of this block copolymer system (*26*).

1.4.3 Uptake

Once in the immediate vicinity of the target cell, the polyplex must first undergo binding and internalization. While it is possible to characterize many aspects of the binding and internalization process [30], at this time we chose to simply focus on the degree of polyplex association with the target cells. In this study, each polymer system was labeled with a fluorophore (FITC) and the labeled polyplexes were added to DU145 cells. Figure 2.2 shows the median cell associated fluorescence achieved by the various delivery vehicles after 1-4 hrs of incubation, as measured by flow cytometry. Intracellular uptake of the PAMAM-G5-PEG WIFP block copolymer complexes exhibit a 12-fold increased cellular uptake over PEI; the untargeted PAMAM-G5-PEG also yielded a 5-fold gain versus the PEI control. This is consistent with other reports that the PEG exterior shell generated in the block copolymer polyplexes gives a significant advantage in shielding them from adsorption of proteins [31]. The presence of serum proteins (particularly albumin) can abrogate the uptake of PEI by binding PEI complexes prior to cell uptake [29]. Of note is that the general relationship between the uptake efficiencies and overall transfection efficiencies of these polymers is similar, implying that at least one principal difference between their effectiveness is their differential uptake ability. However, the fold increases in the percentage of transfected cells of the block copolymers over PEI are much less than the fold increases in uptake, suggesting that PEI may be more effective at mediating downstream events. Another difference could lie in the endosomal trafficking of polyplexes internalized via GRP78 binding [32] versus those internalized via non-receptor mediated endocytosis, as increased uptake resulted in

increased transfection efficiency for the targeted polymer, but not for the untargeted control. This effect could also be due to potential downstream effects of the peptide in mediating endosomal escape or nuclear translocation. For each of the polymers, even though significant uptake is achieved, further evaluation is necessary to understand the subsequent barriers to transfection that result in relatively low transgene expression in comparison to viral vectors. A block copolymer with a scrambled peptide may have been a more ideal targeting control; however the polyplex size, charge and loading are unchanged by the presence of the peptide, indicating that the PEG control should be a good control of a non-targeted system. Additionally, our earlier communication [24], shows that the addition of competing ligand suppresses overall transfection efficiency, indicating that the uptake of these particles is receptor-mediated.

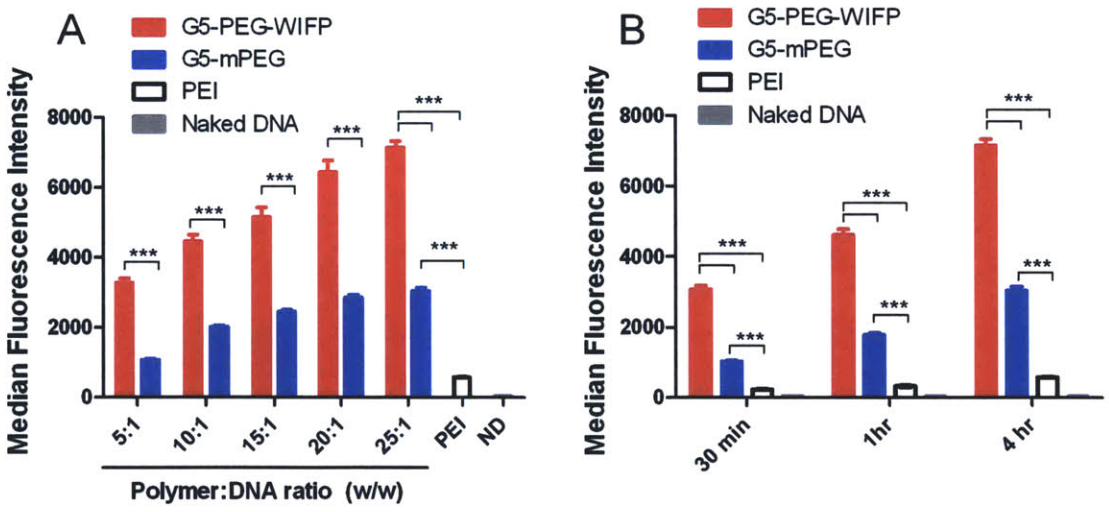

Figure 2.2 Uptake of polyplexes formed by targeted and untargeted block copolymers against PEI.
FITC-labeled polymers were complexed with EGFP plasmids and added to DU145 cells in 10% serum. Median cell associated fluorescence was measured at 30 min, 1h, and 4h as indicated in panel A (w/w = 25:1 for block copolymers). Panel B shows the effect of varying the polymer:DNA ratio of the block copolymers. Fluorescence was measured at 4 h in panel B. PEI was used at an optimized w/w ratio of 2:1. Error bars represent SEM of 5 replicate experiments (*** = $p < 0.001$, ** = $p < 0.01$, * = $p < 0.05$, ns = not

significant).

1.4.4 Endosomal Escape

Endosomal escape is a critical barrier to overcome in the delivery of nucleic acids. Measurement of endosomal escape is done frequently using fluorescence microscopy [33]. Commonly, a fluorescent marker for the endosomes (transferrin, fluorophore-modified dextrans, endosome/lysosome tracking dye) is employed, and escape is considered achieved if there is no co-localization between the polyplex and the endosomal marker [34]. However, this is difficult to measure and quantify in high throughput, thus screening a large library of materials or formulations for differences in endosomal escape performance is complex. Akinc et al. [35] describe a novel method for measuring the pH of the polyplex environment via high-throughput flow cytometry, but here we describe a direct method for quantifying the disruption of the endosome using an image-based high-throughput screening approach.

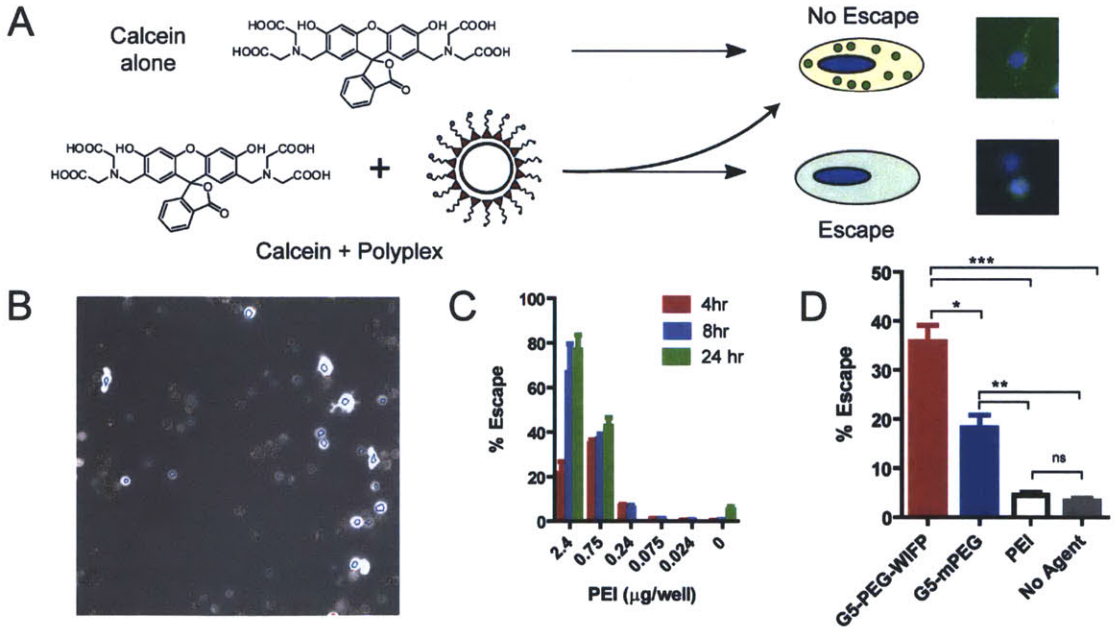

Figure 2.3 High Throughput Endosomal Escape.

Panel A is a schematic of the high-throughput calcein assay used to quantify endosomal escape. When calcein alone is taken up by cells, it remains in the endosomal compartments and thus a punctuate pattern of fluorescence in the cytoplasm is visible. With the addition of an endosomal escape agent, e.g. a polymer or polyplex, the calcein is released into the cytosol yielding a uniform pattern of fluorescence. The images in panel A are representative of these morphologies and taken at 20x. The images have been intensity normalized for this figure in order to more easily visualize the punctuate vs diffuse pattern of fluorescence. Nuclei are shown in blue, calcein as green. Panel B is a grayscale image of the calcein channel of DU145 cells treated with G5-PEG-WIFP polyplexes. The Cellomics algorithm has differentiated cells with endosomal escape (blue circle overlay) vs. those without (orange circle overlay). In panel C, the concentration of PEI is increased as is the time in which the cells were exposed to the calcein/escape agent. Panel D shows the percentage of escaped cells from treatments with various polyplex formulations in OPTI-MEM with 10% serum. PAMAM based polyplexes were used at a 25:1 w/w ratio. PEI was used at 2:1 w/w ratio. Error bars are SEM of 3 replicates (*** = $p < 0.001$, ** = $p < 0.01$, * = $p < 0.05$, ns = not significant).

The high-throughput approach uses the fact that calcein is a membrane-impermeable fluorophore that can be taken up by cells and trafficked through endosomes to lysosomes, but cannot achieve endosomal/lysosomal escape [36, 37]. In the presence of an escape agent, calcein will be released and is seen throughout the cell. (Fig. 2.3A). Using an automated fluorescent microscope, the two phenotypes can be differentiated in real-time by algorithms using spatial fluorescence information. Figure 2.3B shows a representative image (20x magnification) in which the algorithm has identified cells which have undergone endosomal escape vs. those that have not. Figure 2.3C is an example of an assay validation experiment in which increasing amounts of PEI were added and the escape measured at different time points. As expected, escape percentage increased with increasing concentrations of PEI and increasing incubation time. When applied to the block copolymer systems studied, a similar pattern to that of the uptake and overall transfection efficiency was observed. The observed escape percentage relationship between targeted and untargeted PAMAM block copolymers was similar to that of the uptake, suggesting the endosomal escape properties were relatively unchanged

between the two polymers. This is consistent with the fact that these two polymer differ only in the presence of a targeting ligand, and thus the pH-responsive PAMAM structure remains the same. The low escape percentage of the PEI is likely due to its poorer uptake relative to the block copolymers as its escape percentage is greatly enhanced in the absence of serum (data not shown).

1.4.5 Nuclear Uptake and DNA Unpackaging

While endosomal escape could be visualized and quantitated using a high-throughput approach, dissociation of the polyplex and nuclear uptake were followed using traditional confocal microscopy techniques. In this case, both the plasmid DNA and polymers were labeled in order to track polyplex dissociation. Figure 2.4 shows representative images of a 24-hour incubation of dual-labeled polyplexes. There is substantially more plasmid DNA delivered by the targeted block copolymer in comparison with the untargeted polymer or PEI. Again, this is due primarily to the differential uptake between the three systems. Additionally, it is apparent that the PAMAM-PEG micelles are not completely dissociated, as there is significant co-localization between the polymer and DNA channels. In the case of the targeted PAMAM-PEG, it is possible to visualize a yellow core at the center of areas of red fluorescence, indicating that there is still polymer associated with most polyplexes. Finally, it is evident that the polyplexes are localized to an area near the nucleus, but not inside, such as a microtubule organization center (MTOC) [38]. Uptake into the nucleus should be readily seen 24 hours after initial application, but the fact that it is not observed with these materials indicates nuclear localization to be a significant barrier to delivery. The observed gene expression can likely be attributed to either the small percentage of

decomplexed DNA that is non-specifically chaperoned into the nucleus or to cells in which the nuclear membrane was not intact (e.g. in the process of dividing) [39]. In this case, some polyplexes accessing the nucleus may still be fully or partially condensed, but even partially complexed polyplexes could participate in gene transcription [40]. The lack of efficient nuclear uptake and polyplex decondensation represents a significant barrier to further transfection efficiency and represents an area in which these polymers can be improved, possibly by the incorporation of a nuclear localization sequence.

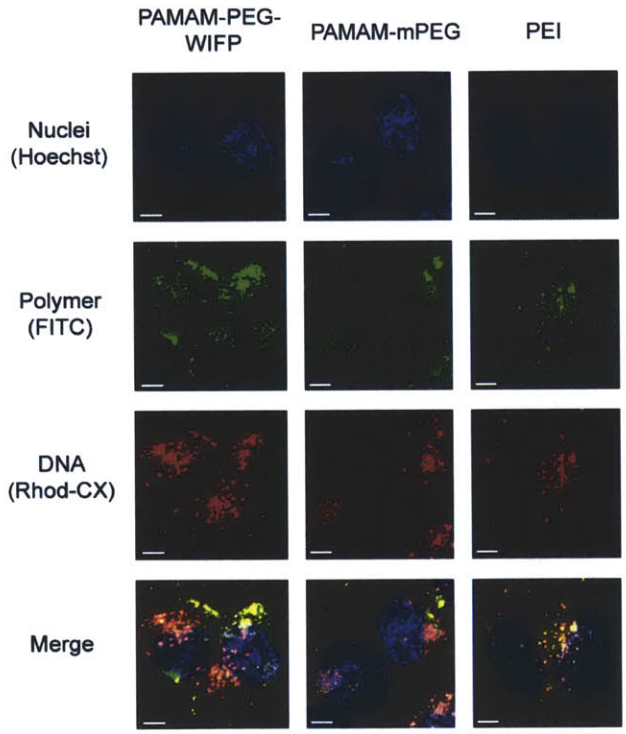

Figure 2.4 Confocal fluorescence micrographs of cells transfected with targeted/untargeted block copolymers as well as PEI.
Transfection took place in 10% serum and micrographs were taken on fixed cells 24h after polyplexes were added. Scale bars are 5 microns. In the merged channel, yellow indicates colocalization of polymer (green) and DNA (red).

For the targeted block copolymers, nearly 100% of cells took up complexes (see Supporting Information) , 36% achieved endosomal escape, but only 2% were ultimately transfected. Less than 6% of cells which experienced escape were transfected by either

targeted or untargeted block copolymer, while over 15% of escaped cells were transfected by PEI. This underscores that while the escape of these block copolymers polymers is efficient, downstream events after endosomal escape represent the most important challenges going forward. Addressing these challenges will be important because even as currently designed, these promising targeted block copolymers are capable of superior transfection relative to PEI in the presence of serum.

1.5 Summary

PAMAM-PEG block copolymers have shown promise as gene delivery agents. Here we have shown this system to be nearly an order of magnitude more potent than PEI *in vitro* and have examined the bottlenecks the system faces. While targeted uptake remains efficient, even in the presence of serum, endosomal escape and unpackaging of DNA polyplexes afterward could be further improved. To that end, we have demonstrated a tool to screen libraries of compounds to rapidly determine the best structures and formulations for endosomal escape. Finally, we have shown that nuclear translocation appears to be the primary obstacle to more efficient transfection in this system – further engineering of the system to promote active delivery of polyplexes into the nucleus could greatly enhance transfection.

1.6 References

1. Somia, N. and I.M. Verma, *Gene therapy: trials and tribulations.* Nat Rev Genet, 2000. **1**(2): p. 91-99.
2. Schaffert, D. and E. Wagner, *Gene therapy progress and prospects: synthetic polymer-based systems.* Gene therapy, 2008. **15**: p. 1131-8.
3. Walther, W. and U. Stein, *Viral vectors for gene transfer - A review of their use in the treatment of human diseases.* Drugs, 2000. **60**(2): p. 249-271.

4. Zaiss, A.K. and D.A. Muruve, *Immunity to adeno-associated virus vectors in animals and humans: a continued challenge.* Gene Ther, 2008. **15**(11): p. 808-816.
5. Nayak, S. and R.W. Herzog, *Progress and prospects: immune responses to viral vectors.* Gene Therapy, 2010. **17**(3): p. 295-304.
6. Glover, D.J., H.J. Lipps, and D.A. Jans, *Towards Safe, Nonviral Therapeutic Gene Expression in Humans.* Nature Reviews Genetics, 2005. **6**(4): p. 299-310.
7. Kan, P.L., A.G. Schatzlein, and I.F. Uchegbu, *Polymers Used for the Delivery of Genes in Gene Therapy*, in *Polymers in Drug Delivery*, I.F. Uchegbu and A.G. Schatzlein, Editors. 2006, CRC Press: Boca Raton.
8. Felgner, P.L., et al., *Lipofection - a Highly Efficient, Lipid-Mediated DNA-Transfection Procedure.* Proceedings of the National Academy of Sciences of the United States of America, 1987. **84**(21): p. 7413-7417.
9. Kogure, K., et al., *Multifunctional envelope-type nano device (MEND) as a non-viral gene delivery system.* Advanced Drug Delivery Reviews, 2008. **60**(4-5): p. 559-571.
10. Legendre, J.-Y. and F.C. Szoka Jr, *Delivery of Plasmid DNA into Mammalian Cell Lines Using pH-Sensitive Liposomes: Comparison with Cationic Liposomes.* Pharmaceutical Research, 1992. **9**(10): p. 1235-1242.
11. Haensler, J. and F.C. Szoka, *Polyamidoamine Cascade Polymers Mediate Efficient Transfection of Cells in Culture.* Bioconjugate Chemistry, 1993. **4**(5): p. 372-379.
12. Tang, M.X., C.T. Redemann, and F.C. Szoka, *In vitro gene delivery by degraded polyamidoamine dendrimers.* Bioconjugate Chemistry, 1996. **7**(6): p. 703-714.
13. Abdallah, B., et al., *A powerful nonviral vector for in vivo gene transfer into the adult mammalian brain: Polyethylenimine.* Human Gene Therapy, 1996. **7**(16): p. 1947-1954.
14. Anderson, D.G., et al., *Structure/property studies of polymeric gene delivery using a library of poly(beta-amino esters).* Mol Ther, 2005. **11**(3): p. 426-34.
15. Anderson, D.G., D.M. Lynn, and R. Langer, *Semi-automated synthesis and screening of a large library of degradable cationic polymers for gene delivery.* Angew Chem Int Ed Engl, 2003. **42**(27): p. 3153-8.
16. Lynn, D.M., et al., *Accelerated discovery of synthetic transfection vectors: parallel synthesis and screening of a degradable polymer library.* J Am Chem Soc, 2001. **123**(33): p. 8155-6.
17. Fukushima, S., et al., *PEGylated Polyplex Micelles from Triblock Catiomers with Spatially Ordered Layering of Condensed pDNA and Buffering Units for Enhanced Intracellular Gene Delivery.* Journal of the American Chemical Society, 2005. **127**: p. 2810-2811.
18. Chiou, H.C., et al., *Enhanced Resistance to Nuclease Degradation of Nucleic-Acids Complexed to Asialoglycoprotein-Polylysine Carriers.* Nucleic Acids Research, 1994. **22**(24): p. 5439-5446.
19. Dash, P.R., et al., *Factors affecting blood clearance and in vivo distribution of polyelectrolyte complexes for gene delivery.* Gene Therapy, 1999. **6**(4): p. 643-650.

20. Patel, H.M., *Serum opsonins and liposomes: their interaction and opsonophagocytosis.* Crit Rev Ther Drug Carrier Syst, 1992. **9**(1): p. 39-90.
21. Mislick, K.A. and J.D. Baldeschwieler, *Evidence for the role of proteoglycans in cation-mediated gene transfer.* Proceedings of the National Academy of Sciences of the United States of America, 1996. **93**(22): p. 12349-12354.
22. Hama, S., et al., *Quantitative and mechanism-based investigation of post-nuclear delivery events between adenovirus and lipoplex.* Nucleic acids research, 2007. **35**: p. 1533-43.
23. Wood, K.C., et al., *A family of hierarchically self-assembling linear-dendritic hybrid polymers for highly efficient targeted gene delivery.* Angewandte Chemie (International ed. in English), 2005. **44**: p. 6704-8.
24. Wood, K.C., et al., *Tumor-targeted gene delivery using molecularly engineered hybrid polymers functionalized with a tumor-homing peptide.* Bioconjugate chemistry, 2008. **19**: p. 403-5.
25. Arap, M.A., et al., *Cell surface expression of the stress response chaperone GRP78 enables tumor targeting by circulating ligands ´.* Cancer Cell, 2004. **6**: p. 275-284.
26. Lee, A.S., *GRP78 Induction in Cancer: Therapeutic and Prognostic Implications.* Cancer Research, 2007. **67**: p. 3496-3499.
27. Li, J. and A.S. Lee, *Stress Induction of GRP78/BiP and Its Role in Cancer.* Current, 2006: p. 45-54.
28. Gabrielson, N.P. and D.W. Pack, *Acetylation of Polyethylenimine Enhances Gene Delivery via Weakened Polymer/DNA Interactions.* Biomacromolecules, 2006. **7**(8): p. 2427-2435.
29. Forrest, M.L., et al., *Partial Acetylation of Polyethylenimine Enhances In Vitro Gene Delivery.* Pharmaceutical Research, 2004. **21**(2): p. 365-371.
30. Sahay, G., D.Y. Alakhova, and A.V. Kabanov, *Endocytosis of nanomedicines.* Journal of Controlled Release. **145**(3): p. 182-195.
31. Giri, J., et al., *Interactions of Poly(amidoamine) Dendrimers with Human Serum Albumin: Binding Constants and Mechanisms.* ACS Nano: p. Article ASAP.
32. Ni, M., Y. Zhang, and A.S. Lee, *Beyond the endoplasmic reticulum: atypical GRP78 in cell viability, signalling and therapeutic targeting.* Biochem J, 2011. **434**(2): p. 181-8.
33. Payne, C.K., *Imaging gene delivery with fluorescence microscopy.* Nanomedicine, 2007. **2**: p. 847-60.
34. Akita, H., et al., *Quantitative Three-Dimensional Analysis of the Intracellular Trafficking of Plasmid DNA Transfected by a Nonviral Gene Delivery System Using Confocal Laser Scanning Microscopy.* Mol Ther, 2004. **9**(3): p. 443-451.
35. Akinc, A., et al., *Exploring polyethylenimine-mediated DNA transfection and the proton sponge hypothesis.* The journal of gene medicine, 2005. **7**: p. 657-63.
36. Hu, Y., et al., *Cytosolic Delivery of Membrane-Impermeable Molecules in Dendritic Cells Using pH-Responsive Core-Shell Nanoparticles.* Nano Letters, 2007. **7**(10): p. 3056-3064.
37. Jones, R.A., et al., *Poly(2-alkylacrylic acid) polymers deliver molecules to the cytosol by pH-sensitive disruption of endosomal vesicles.* Biochemical Journal, 2003. **372**: p. 65-75.

38. Barua, S. and K. Rege, *The influence of mediators of intracellular trafficking on transgene expression efficacy of polymer-plasmid DNA complexes.* Biomaterials. **31**(22): p. 5894-5902.
39. Pouton, C.W., et al., *Targeted delivery to the nucleus.* Advanced Drug Delivery Reviews, 2007. **59**(8): p. 698-717.
40. Bielinska, A.U., J.F. Kukowska-Latallo, and J.R. Baker, *The interaction of plasmid DNA with polyamidoamine dendrimers: mechanism of complex formation and analysis of alterations induced in nuclease sensitivity and transcriptional activity of the complexed DNA.* Biochimica et Biophysica Acta (BBA) - Gene Structure and Expression, 1997. **1353**(2): p. 180-190.

Chapter 3. Crosslinked Linear Polyethyleneimine Enhances Delivery of DNA to the Cytoplasm

3.1 Abstract

Crosslinked polyethylenimines (PEIs) have been frequently examined over the past decade since they can maintain the transfection efficiency of commercially available, 25k branched PEI, but exhibit less cytotoxicity. The argument is often made that the of such polymers, generally synthesized with either disulfide or hydrolytically degradable crosslinkers, is critical to the high efficiency and low toxicity of the system. In this work, we present a crosslinked linear PEI (xLPEI) system in which either disulfide-responsive or non-degradable linkages are incorporated. As with previous systems, strong transfection efficiency in comparison with commercial standards was achieved with low cytotoxicity. However, these properties were shown to be present whether the degradable or non-degradable crosslinker was used. Free polymer was demonstrated to be the critical factor determining transfection efficiency for these polymers, mediating efficient endosomal escape without signs of cell membrane damage. While several crosslinked PEI systems in the literature have demonstrated the effect of the disulfide moiety, this work demonstrates that disulfide-mediated unpackaging may not be as important as conventionally thought for some PEI systems.

3.2 Introduction

Clinical translation of gene therapy requires safe, efficient vectors. While viral vectors are efficient, remaining concerns regarding safety and immunogenicity have created a need for efficient synthetic vectors. One of the most studied polymers for DNA

delivery is polyethylenimine (PEI), a polycation with high charge density capable of pH buffering in physiologically beneficial ranges [1]. PEI, available in either linear or branched forms, is among the most efficient commercially available polymers, but also one of the most toxic [2]. It causes an acute cytotoxicity due to cell membrane disruption followed by induction of apoptosis by destabilization of mitochondrial membranes [3, 4]. Though PEI has frequently been used in both animals and humans for gene delivery, it has also been shown to aggregate red blood cells, bind complement, and cannot easily be broken down and excreted [5, 6].

Crosslinked low molecular weight PEIs have emerged as a strategy for overcoming cytotoxicity while maintaining relatively high transfection efficiency [7, 8]. Of particular interest are crosslinkers that are bioresponsive and can specifically degrade within the cytoplasm of the target cell [9-12]. Disulfide reduction and hydrolytic degradation are the strategies primarily employed to trigger intracellular release of DNA from crosslinked PEIs. PEI crosslinked with hydrolytically degradable crosslinkers has been shown to have efficiency equal or greater to bPEI 25k, as well as reduced toxicity [13-17]. Disulfide crosslinked polymers have been designed to take advantage of the intracellular reducing environment to effect release of the DNA in the cytoplasm [10]. Breunig et. al have shown transfection efficiencies of over 60% with over 90% cell viability in several cell lines transfected with disulfide crosslinked LPEI [18, 19]. Several other disulfide crosslinked PEI studies have reported efficiencies near or exceeding that of commercial standards with reduced cytotoxicity [20-22]. While intracellular disulfide reduction is frequently cited as being an important feature for excellent transfection and low toxicity, very few studies directly compare disulfide-linked

PEIs with PEIs crosslinked with a non-degradable crosslinker [23]. Some studies have modulated the intracellular reducing potential with either buthionine sulfoximine (BSO) or glutathione monomethyl ester (GSHMEE) [24-26], however these methods perturb normal cell physiology. In this work, we synthesize a series of crosslinked LPEIs containing either disulfide or non-degradable crosslinkers and evaluate the mechanism of high transfection efficiency and low cytotoxicity.

3.3 Materials and Methods

3.3.1 Materials

Linear Polyethylenimine (M_w of 2500 g/mol and 25000 g/mol) was purchased from Polysciences (Warrington, PA). Branched 25,000 g/mol (M_w) polyethylenimine (PEI) and other chemical reagents were purchased from Sigma Aldrich (St. Louis, MO). KB cells were obtained from ATCC (Manassas, VA). pCMV-EGFP-N1 plasmid DNA was obtained from Aldevron Inc.(Fargo, ND). All other cell culture reagents were obtained from Invitrogen (Carlsbad, CA).

3.3.2 Polymer Synthesis

One hundred (100) mg of linear polyethylenimine (LPEI, M_w = 2500 g/mol) was dissolved in a 2:1 mixture of methanol:dimethylsulfoxide (MeOH:DMSO) at a concentration of 0.33 g/mL. Succinic acid (SA) or dithiodipropionic acid (DTDP) was dissolved in 2:1 MeOH:DMSO at 0.3 g/mL and added to achieve crosslinker ratios of 0.02 – 0.1 mol crosslinker/mol lPEI monomer (M_w = 43 g/mol). N-hydroxysuccinimide (NHS) was dissolved in 2:1 MeOH:DMSO at 0.4 g/mL and 1.4 equivalents per carboxylic acid added. After all components were well mixed, 1.4 equivalents of 1-ethyl-

3-(3-dimethylaminopropyl) carbodiimide (EDC) dissolved in 2:1 MeOH:DMSO was added while the mixture was stirred vigorously. This reaction proceeded overnight and was then dialyzed against Milli-Q water for 2 days using a 12000-14000 MWCO SpectraPOR membrane. Nondegradable, SA crosslinked xLPEIs are labeled xL-*Y*, where Y is the mol % crosslinker (relative to LPEI monomer). Degradable, DTDP crosslinked polymers are labeled xL-SS-*Y*. **xL-*Y*** ^{1}H-NMR (400MHz, D_2O) δ=2.6 (t, -NCO-C**H$_2$**-C**H$_2$**-CON-), 3.0 (m, -C**H$_2$**-NH-C**H$_2$ -**), 3.45 (t, -C**H$_2$**-NCO-C**H$_2$**-). **xLSS-*Y*** ^{1}H-NMR (400MHz, H_2O) δ=2.6 (t, -NCO-C**H$_2$**- CH_2-S-S-), δ=2.95 (t, -NCO-CH_2- C**H$_2$**-S-S-), 3.0 (m, -C**H$_2$**-NH-C**H$_2$** -), 3.45 (t, -C**H$_2$**-NCO-C**H$_2$**-).

3.3.3 Cell Culture

KB cells were cultured in folate-free RPMI 1640 basal media supplemented with 10% heat-inactivated fetal bovine serum (FBS) and 1% penicillin-streptomycin in a humidified 37°C atmosphere at 5% CO_2.

3.3.4 Polyplex Formation

Fifty (50) μL xLPEI was aliquoted into wells of 96-well plate at concentrations ranging from 0.333 mg/mL to 0.0033 mg/mL. Twenty-five (25) μL of plasmid DNA at 0.05 mg/mL in PBS was added to each well and mixed well via pipette. Complexes were allowed to stand for 10 minutes. One hundred (100) μL of a 1:200 (v/v) solution of Quant-It Picogreen reagent in PBS was added to the wells of an opaque 96-well plate. Twenty (20) μL of polyplexes were added to the Picogreen plate and mixed well. After 5 minutes, fluorescence measurements were made (ex. 490/em. 525) on a Tecan Infinite

200 Pro. Measurements were normalized to that of free DNA (100% uncomplexed DNA) and background Picogreen (0% uncomplexed DNA).

3.3.5 Transfection

Cells were trypsinized prior to transfection and seeded in 96-well plates at 4,000 cells/well overnight in a humidified 37°C atmosphere at 5% CO_2 to be 60% confluent at the time of treatment. xLPEIs were diluted in PBS at 0.1 mg/mL initially and then further diluted into 25 μL of the same buffer in a separate 96-well plate at varying concentrations. Twenty-five (25) μL of pDNA at 0.05 mg/mL in PBS was then added to each well and mixed by gentle pipetting. After 10 min for complex formation, 30 μL of the complexes were added to 200 μL of Opti-MEM. After further mixing, 150 μL of the complexes in Opti-MEM were added to the cells (after growth media had been removed). Additional polymer was added either immediately or after 4 hours. After 8 hours, the complexes in Opti-MEM were removed and growth media was added. Cells were assayed at 48 hr for GFP production using flow cytometry. 4000 – 10000 live cells per sample were analyzed.

3.3.6 Flow Cytometry

Flow cytometry was performed in U-bottom 96-well plates using an LSR II HTS Flow cytometer (Becton-Dickinson, Mountain View, CA). To prepare samples, media was removed from cells and replaced with 25 μL trypsin for 5 minutes. One hundred (100) μL of PBS supplemented with 2% FBS and 0.005 mg/mL propidium iodide was then added to each well, mixed, and the entire 125 μL cell suspension transferred into a U-bottom 96-well plate.

3.3.7 Polyplex Uptake

Cells were trypsinized prior to transfection and seeded in 96-well plates at 8,000 cells/well overnight in a humidified 37°C atmosphere at 5% CO_2 to be 80% confluent at the time of treatment. Plasmid DNA was labeled with Rhodamine-CX using a Label-IT kit from Promega (Madison, WI). Polyplexes were formed and cells treated as described in the Transfection section, with labeled DNA mixed 1:1 with unlabeled DNA. At the time indicated, cells were washed twice with PBS and analyzed using flow cytometry. No propidium iodide was used due to spectral overlap with Rhodamine-CX.

3.3.8 Endosomal Escape

Cells were trypsinized prior to treatment and seeded in black-sided, clear-bottom 96-well plates at 8,000 cells/well overnight in a humidified 37°C atmosphere at 5% CO_2 to be 80% confluent at the time of treatment. Cells were treated with 100 μL of Opti-MEM containing 0.15 mg/mL calcein and varying concentrations of polymer. After 2 hours, the Opti-MEM was removed and cells were washed once with Opti-MEM and then incubated in Opti-MEM containing 0.1% (v/v) Hoechst 33342 for 20 minutes. After the cells were washed twice, 150 μL of phenol-free Opti-MEM was added to each well before the plate was covered with an opaque sticker, foiled, and analyzed. Imaging was done using a Cellomics ArrayScan VTI HCS Reader (Thermo Fisher, Waltham, MA) and analysis was done using the included software[27]. 300 – 3000 live cells per sample were analyzed.

3.3.9 LDH Release

The protocol used was adapted from the manufacturer's instructions of the Cyto-Tox ONE Assay kit. Cells were trypsinized prior to transfection and seeded in 96-well plates at 8,000 cells/well overnight in a humidified 37°C atmosphere at 5% CO_2 to be 80% confluent at the time of treatment. Cells were treated with 100 μL of Opti-MEM containing varying concentrations of polymer. After 2 hours, lysis buffer was added to untreated cells. After 4 hours, 50 μL of supernatant was removed and added to an opaque 96-well plate.50 μL of Cyto-Tox ONE reagent was added and mixed with gentle pipetting. After 10 min, 25 μL STOP solution was added and fluorescence was read on a Tecan Infinite 200 Pro plate reader (ex. 560 nm/ em. 590 nm).

3.3.10 Cell Viability

Cells were trypsinized prior to transfection and seeded in 96-well plates at 4,000 cells/well overnight in a humidified 37°C atmosphere at 5% CO_2 to be 60% confluent at the time of treatment. Cells were treated with 100 μL of Opti-MEM containing varying concentrations of polymer. After 4 hours, polymers were aspirated and wells replenished with growth media. After 48 hours, 10 μL of a 5 mg/mL solution of MTT reagent (3-(4,5-Dimethylthiazol-2-yl)-2,5-diphenyltetrazolium bromide) was added. After 4 hours, media was aspirated and replaced with DMF to dissolve formazan crystals. Absorbance at 570 nm was read on a Tecan Infinite 200 Pro plate reader.

3.4 Results

3.4.1 Synthesis

Low molecular weight LPEIs were crosslinked using EDC and NHS to form higher molecular weight structures more suitable for gene transfection (Scheme 3.1). Methanol/DMSO was chosen as the solvent system to enable high concentrations of reactants that could not be achieved in DMSO or water alone. NMR spectra showed that the incorporation of the crosslinker was nearly quantitative, however GPC analysis did not reveal a correlation between crosslinker ratio and molecular weight. Molecular weights (M_w) generally ranged from 30,000 - 50,000 g/mol. The lack of increase in molecular weight with greater crosslinker feed ratios is likely due to crosslinker reactions with methanol to form methyl esters on one of the two functional groups of the crosslinker (these subsequently hydrolyze to form acid groups during dialysis), thus decreasing the actual crosslinking while still incorporating a large amount of crosslinker. The presence of carboxylic acid groups in the xLPEIs with high crosslinker ratios was confirmed by FTIR. The ratio of the peak intensity of the carboxylic acid group to the tertiary amide group was much smaller for the 4% crosslinked polymers compared to the 8% crosslinked polymers.

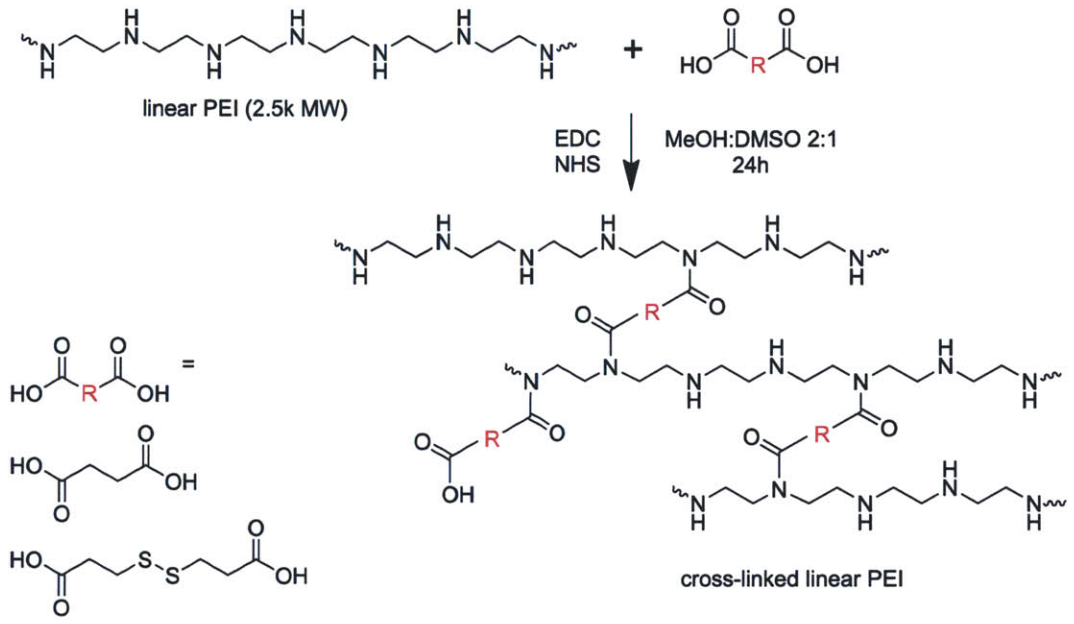

Scheme 3.1 Synthesis of crosslinked linear polyethylenimine.

3.4.2 Polyplex Formation

Complexation of plasmid DNA was measured by exclusion of Picogreen (Figure 3.2). Polyplexes were completely complexed at an N/P ratio of 5 – 10 for xLPEI , commercial lPEIs, and bPEI 1.8k. bPEI 25k completely complexed DNA at an N/P ratio of 3, consistent with reports from Wu et. al. [28]. The total amount of protection of DNA decreased with increasing crosslinker ratio. This is likely due to the introduction of carboxylic acids at high crosslink ratio that neutralize the charge of the amines as mentioned above. When completely complexed, DNA is still more available to Picogreen in the xLPEI polyplexes (33%) versus lPEI polyplexes (10%) and bPEI 25k polyplexes (<5 %). Polyplexes formed by xLPEIs in PBS had zeta potentials that were on average between 20 and 40 mV, with averaged diameters of approximately 350 – 500 nm.

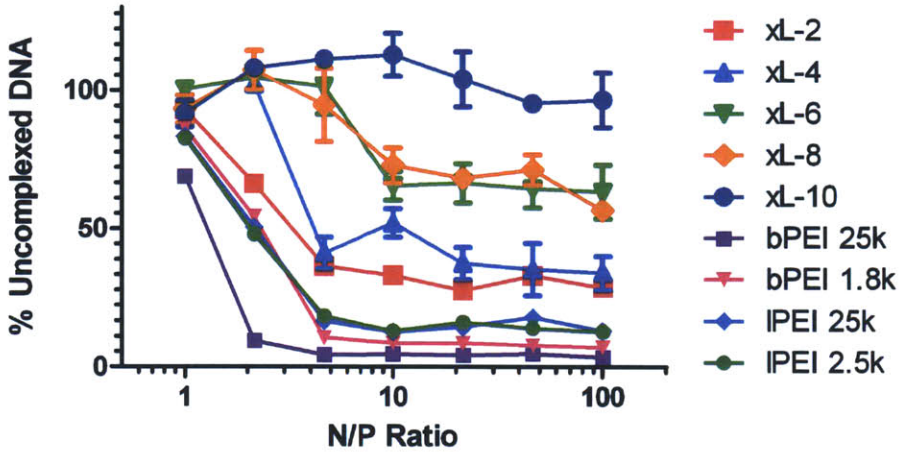

Figure 3.2 Complexation of plasmid DNA by crosslinked lPEI as a function of the percentage of crosslinker incorporated.

3.4.3 Transfection

Transfection of KB cells demonstrated that efficiency was optimal at a crosslinker ratio of 4% (Figure 3.3). At an N/P ratio of 40:1, 40% efficiency was achieved with over 90% viability, results consistent with those reported for similar materials [18]. This efficiency was slightly higher than that of bPEI 25k, lPEI 25k, and nearly as strong as Lipofectamine 2000. As expected, cell viability was much higher with xLPEI, though not for the xL-2, which contained the lowest feed ratio of crosslinker. Viability increased monotonically with crosslinking percentage rather than achieving a maximum, as seen with transfection efficiency. xLPEIs require relatively high N/P ratios in comparison to bPEI 25k and lPEI, though xL-2 does show some transfection at N/P 10. Figure 3.4 demonstrates that the transfection efficiency of xLPEIs is independent of the degradability of the crosslinker. Both transfection efficiency and cell viability are unchanged by the degradation of the crosslinker, suggesting that disulfide degradation may not be the primary means of DNA release for efficient transfection by these xLPEIs.

Given the relatively weak binding of the xLPEIs, release could be mediated electrostatically by exposure of the polyplex to the high concentrations of polyionic species in the intracellular environment. The xLPEIs are readily degraded by DTT as is consistent with similar systems, thus the similarity in release characteristics is not due to lack of disulfide degradation as a result of our particular synthetic scheme.

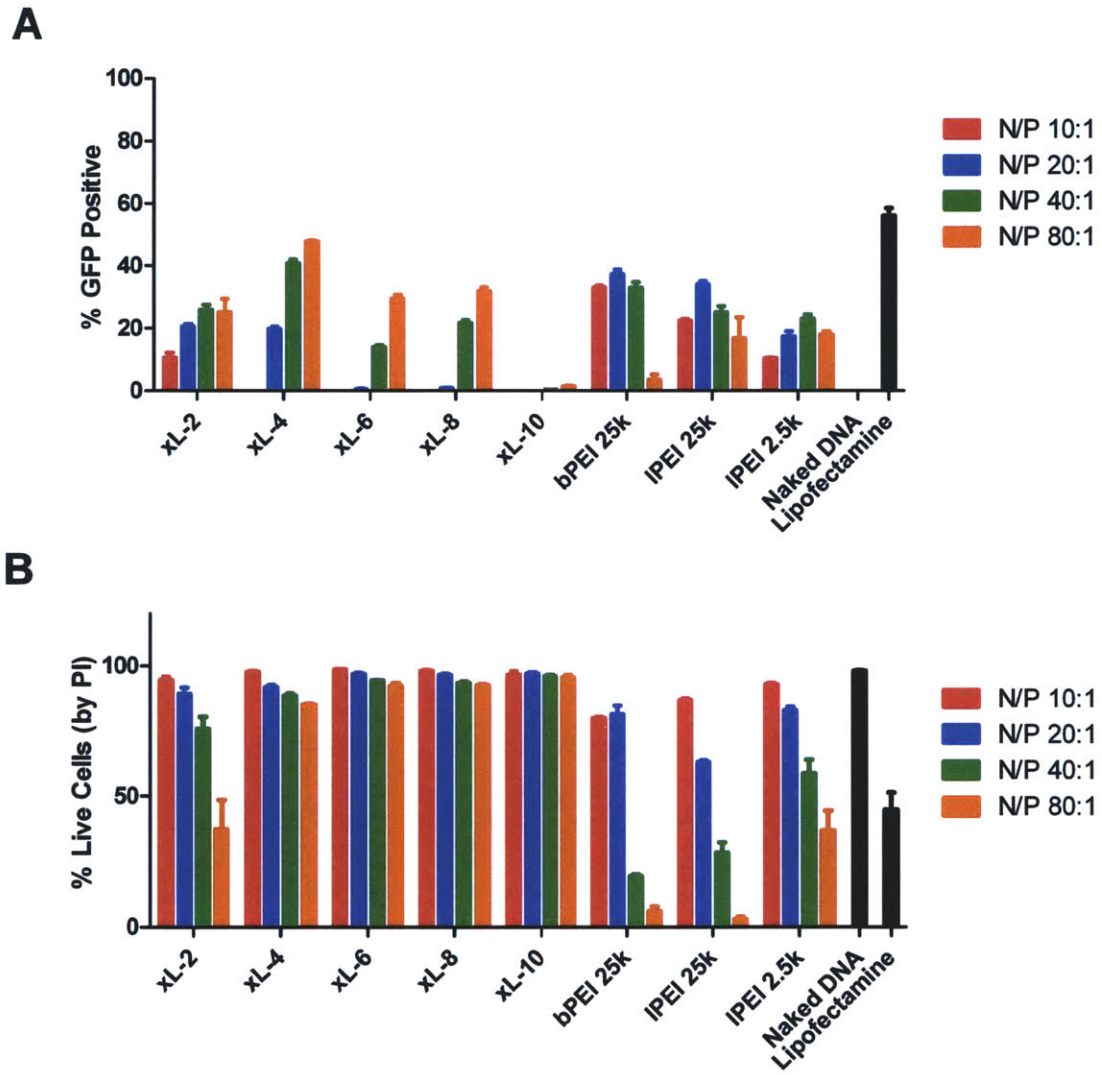

Figure 3.3 (A) Transfection efficiency of cells transfected with crosslinked lPEI as a function of crosslinking percentage and N/P ratio. (B) Relative viability of KB cells transfected in (A).

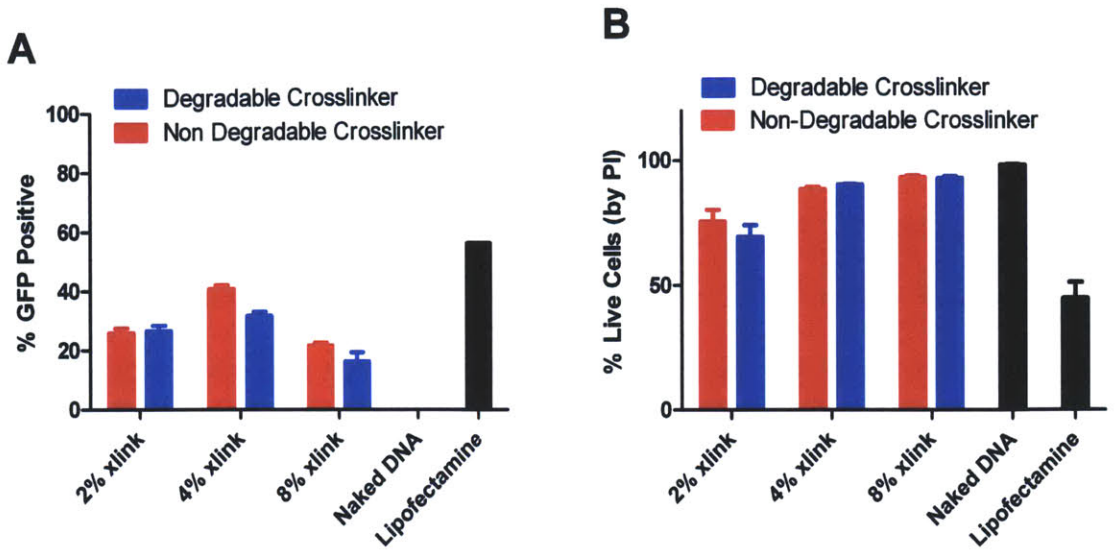

Figure 3.4 (A) Transfection efficiency of cells transfected with crosslinked lPEI as a function of cross-linker degradability. Polyplexes were formed at an N/P ratio of 40:1. (B) Relative viability of KB cells transfected in (A).

3.4.4 Free Polymer Effects

The relatively high N/P ratios at which maximal transfection efficiency was observed (Figure 3.3A) suggest that a relatively large amount of free polymer is present in solution during transfection, which has been previously shown to increase transfection efficiency [28, 29]. To further determine whether disulfide degradation or free xLPEI polymer was contributing to the higher transfection efficiency of the xLPEIs, the relative contributions of free polymer versus polyplex-bound polymer were investigated. Previously, Wu et al. examined the effect of free versus bound polymer by forming polyplexes at N:P ratios that were below that necessary for optimal transfection but still able to efficiently condense DNA [28, 30, 31]. Here, uptake, transfection, and cytotoxicity were measured in two sets of experiments. First, the condensing, or polyplex-bound, polymer was kept constant as the nondegradable bPEI and the free

polymer was varied (Figure 3.5). Subsequently, the free polymer was held constant (xL-4 used in all cases) while the condensing polymer was varied (Figure 3.6). In both cases, polyplexes were formed at N/P 10 (for xLPEI) or N/P 5 (for bPEI). These N/P ratios represent the lowest N/P ratio at which the final, maximum degree of complexation was reached for each system based on Figure 3.2. No method of separation was used to remove free polymer as that would result in complexes that were thermodynamically unstable in media with physiological salt concentrations [29]. The remaining fraction of free polymer was added either immediately following transfection or 4 hours afterward, after which the majority of the uptake is expected to have taken place.

Interestingly, it was seen that when bPEI was used as the condensing polymer, the addition of free xLPEI polymer led to similar ~30% transfection efficiency for both degradable and nondegradable xLPEI (Figure 3.5C). In either case, the polyplexes formed using bPEI as the condensing polymer would need to undergo unpackaging without the assistance of degradable linkers, indicating that disulfide degradation is not responsible for an efficiency boost in this particular system. In fact, under the majority of conditions studied, there was no significant difference between degradable and non-degradable xLPEIs. Figure 3.5B shows that cell uptake is high for bPEI 25k, with or without added polymer; in fact the immediate addition of free polymer, regardless of composition, had a negative effect on bPEI 25k uptake, agreeing with data from Boeckle, et. al. [29], who hypothesized that this was a result of competition by free polymer. On the other hand, when free polymer is added 4 hours later, the original high cell uptake is recovered. Most importantly, there is no difference in uptake of bPEI 25k polyplexes

when the type of free polymer is varied. Therefore uptake effects cannot explain the superior transfection of free xLPEI/bPEI25k polyplexes over free bPEI25k/bPEI25k polyplexes, indicating that the efficiency of xLPEI is likely also due to downstream events such as endosomal escape. Toxicity was actually increased when xLPEIs were used as free polymer instead of bPEI 25k, opposite of what may be expected based on standard transfection with homogenous polyplexes (Figure 3.3B). This may be due to xLPEI-mediated increased cytosolic delivery of bPEI, increasing the opportunity for bPEI to interact with mitochondria and cause apoptosis.

In Figure 3.6, different condensing polymers were employed while the free polymer was kept constant. Here, it can be seen that bPEI is more efficient than xLPEI as a condensing polymer and does not suffer a drop in transfection efficiency when free polymer is added at 4 hours instead of immediately (Figure 3.6C). There was also a clear decrease in transfection efficiency from the xLPEI complexed at the full 40:1 N/P ratio (Figure 3.6C, "high N/P" bars) to the 10:1 N/P ratio xLPEI polyplex to which the remaining 30 parts free xLPEI was added immediately (Figure 3.6C, "0 hr" bars). As was seen in earlier transfections, xLPEI was nearly non-toxic, while bPEI 25k showed significant toxicity when used as the condensing polymer (Figure 3.6D).

The xLPEI samples xL-4 and xL-SS-4 behave similarly despite differences in degradability, as noted above. For these systems, the addition of free polymer is necessary to observe any uptake at all by cells (Figure 3.6B). In the presence of immediately added xLPEI, there is a significant boost in cell uptake (60%); when free

polymer is added after 4 hours; however, the delay leads to a decrease in uptake by cells to 30 - 35% (Figure 3.6B). This fact, combined with the fact that uptake not seen at all when no additional polymer is added, suggests that uptake is decreased when the DNA polyplexes are incubated in the cell culture media for extended periods, perhaps due to gradual aggregation or the destabilization of the complexes in culture conditions over time. Cellular uptake for the xLPEI complexes thus appears to be dependent on the presence of additional polymer; this additional polymer may interact with the cell membrane or further condense particles to facilitate entry of the polyplexes to the cell. However, the size of polyplexes formed in Opti-MEM is not significantly reduced when free polymer is added. While further complexation by free polymer may play some role in increasing uptake for the loosely binding xLPEI as Fig 3.6B suggests, Figures 3.5B and 3.5C show that it is clearly impacting the transfection process downstream of uptake as well, likely by enhancing endosomal escape.

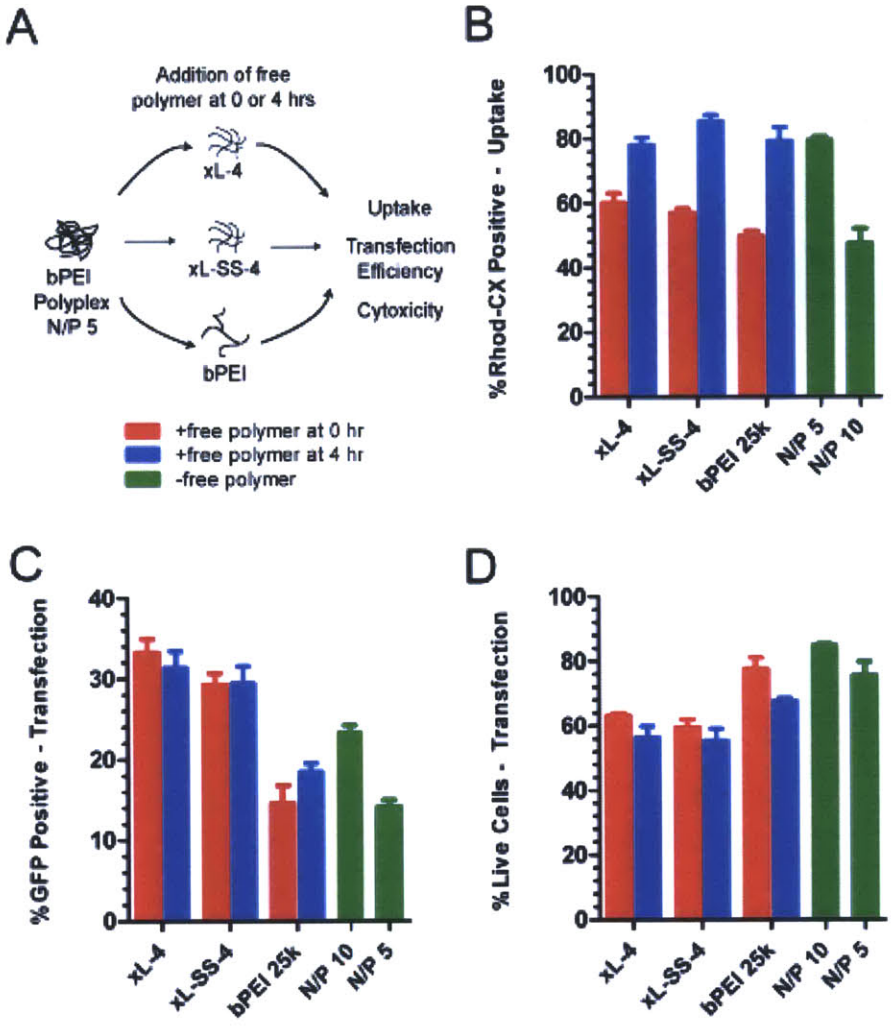

Figure 3.5 xLPEI Function as Free Polymer
(A) Experimental schematic. KB cells were treated with bPEI polyplexes formed at an N/P ratio of 5 and supplemented with free polymer at either 0 or 4 hours. Cells treated with polyplexes formed at N/P 10 or N/P 5 and unsupplemented with free polymer were present as controls. Free xLPEI (xL-4 – succinic acid crosslinked, non-degradable, xL-SS-4 – disulfide linked, degradable) was added to form a total N/P ratio of 40. Free bPEI was added to form a total N/P ratio of 10. (B) Percentage of cells taking up Rhodamine-CX labeled DNA polyplexes as measured by flow cytometry 6 hours after initial treatment. (C) Percentage of GFP positive cells 48 hours after initial treatment. (D) Percentage of live cells 48 hours after live treatment as measured by propidium iodide staining.

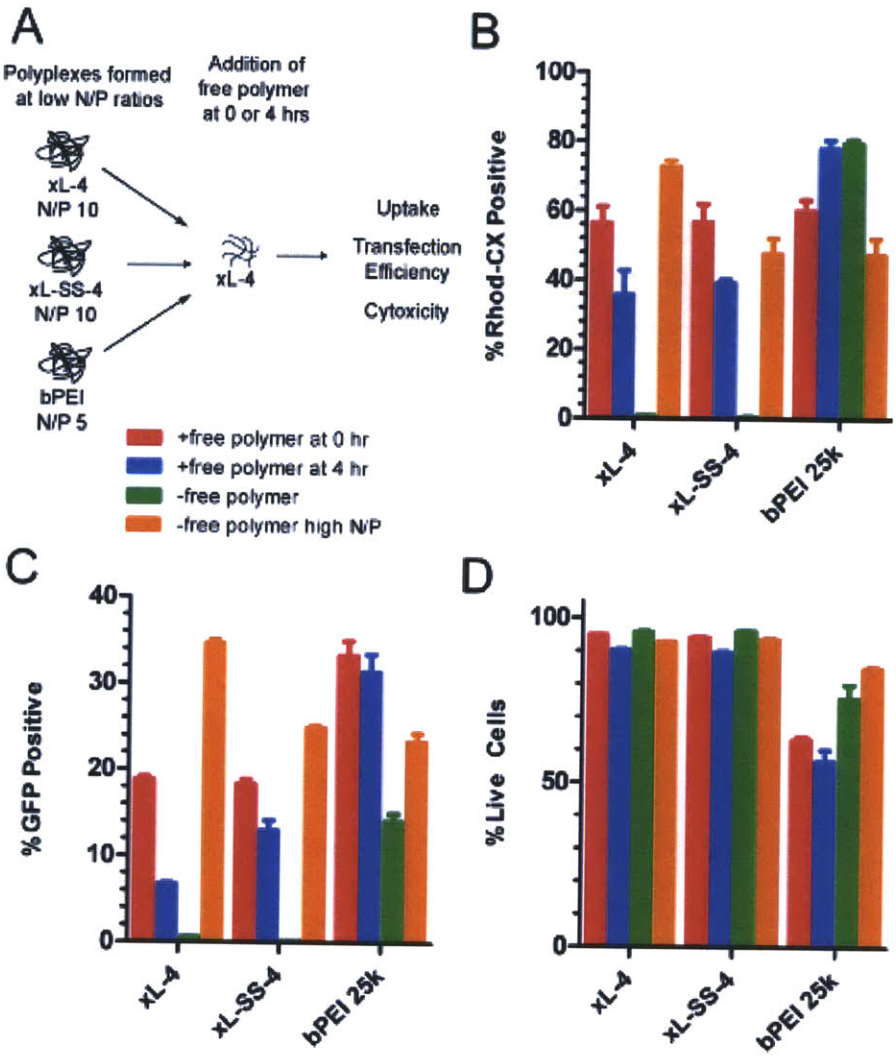

Figure 3.6 xLPEI Function as Condensing Polymer
(A) Experimental schematic. KB cells were treated with polyplexes formed at an N/P ratio of 5 (bPEI) or 10 (xLPEI) and either supplemented with free xL-4 polymer at 0 or 4 hours, or not supplemented at all. Cells treated with polyplexes formed at optimal high N/P ratios (xLPEI – N/P = 40, bPEI – N/P = 10) and unsupplemented with free polymer were also present as controls. Free xL-4 was added to form a total N/P ratio of 40. (B) Percentage of cells taking up Rhodamine-CX labeled DNA polyplexes as measured by flow cytometry 6 hours after initial treatment. (C) Percentage of GFP positive cells 48 hours after initial treatment. (D) Percentage of live cells 48 hours after live treatment as measured by propidium iodide staining.

3.4.5 Endosomal Escape

To determine the efficiency of free polymer in facilitating endosomal escape, a high-throughput calcein assay was used as previously described [27]; results of the assay are shown in Figure 3.7A for each of several PEI polymer systems. xLPEIs proved to be able to cause significant endosomal escape at concentrations between 3 and 10 μg/mL, with a steep increase in efficiency above a critical concentration, up to over 80%. In contrast, commercial LPEI's showed a more gradual increase in escape, facilitating calcein escape in over 50% of cells at 10 μg/mL. bPEI 25k was also able to cause calcein release at 10 μg/mL, while bPEI 1.8k was not able to effect any release up to 30 μg/mL. Interestingly, the commercial PEIs showed a decrease in escape with concentrations above 10 μg/mL, possibly due to calcein leaking out of the cells entirely as a result of membrane damage. In order to determine the extent of membrane destabilization by the xLPEIs, LDH leakage was measured as a function of free polymer concentration (Figure 3.7B). 25k bPEI and lPEI showed significant membrane damage above 3 μg/mL, as did lPEI 2.5k. Both xLPEI species did not show any membrane damage at concentrations up to 30 μg/mL, despite facilitating escape in over 75% of cells at this concentration. xLPEIs also demonstrate a ~ 1.5 log increase in LD50, with no toxicity effects at 10 μg/mL, the concentration at which escape becomes highly efficient (Figure 3.7C).

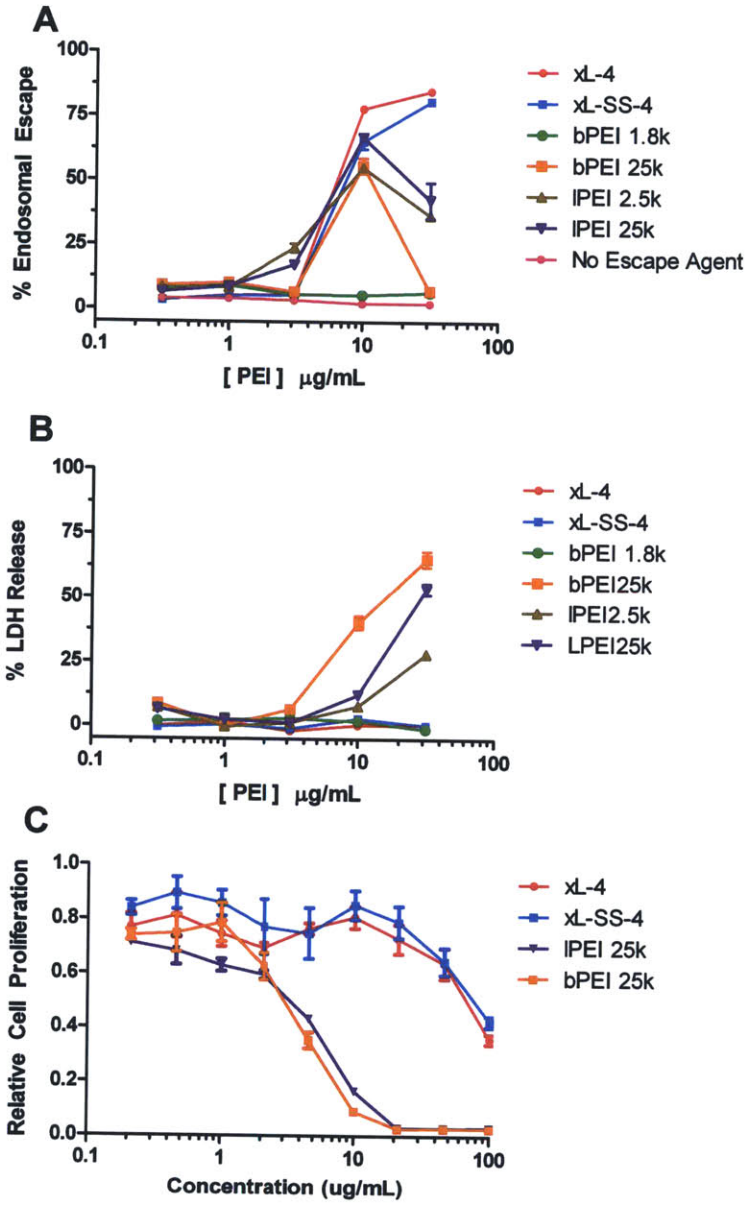

Figure 3.7 Toxicity and Endosomal Escape of free PEI
(A) Activity of lactate dehydrogenase (LDH) in the supernatant of cells treated with crosslinked and commercial PEIs. (B) Percentage of cells exhibiting endosomal escape in high-throughput calcein assay (see methods) when treated with crosslinked and commercial PEIs. (C) Relatively viability of cells as measured by an MTT assay

3.5 Discussion

As mentioned in the introduction, different PEI crosslinking techniques have been reported, generally utilizing either a bifunctional crosslinker or derivitizing primary

amines into thiols for subsequent disulfide formation. We opted to use EDC coupling, as it requires only dicarboxylic acid functionality from the crosslinker, which can be designed to be responsive to various stimuli; furthermore, the crosslinking can be achieved in a one-pot approach in various solvents depending on the solubility of the crosslinker. The choice of polycation may also be varied, as only primary or secondary amines are required for crosslinking – here lPEI was chosen due to favorable efficiency and toxicity reports from previous work [18]. This synthetic approach is potentially amenable to a combinatorial development with a library of polycations and linkers responsive to different stimuli. For this study, a reducible and non-reducible crosslinker were chosen for incorporation. While crosslinker functionality was the critical feature for this design, the lengths were slightly different and thus a future study on the impact of crosslinker length could be of interest. The approach taken here resulted in crosslinked polymers with nearly quantitative integration of crosslinker. However, as noted in the results section, the presence of methanol in the solvent system resulted in free carboxylic acid formation at higher crosslinker ratios, decreasing the positive charge and limiting the molecular weight. Wu et al demonstrates the effect of controlled addition and an oxygen-free environment on the crosslinking of bPEI [32], however we wanted to keep the synthesis simple and scalable for future combinatorial implementation.

xLPEI was able to form polyplexes, though xLPEI polyplexes were looser than those formed with commercial bPEI 25k. DNA was more accessible, even at very high N/P ratios, than the 25k standards, likely a result of reduced net charge and thus efficacy of DNA condensation. Gosselin et. al demonstrated how different crosslinker chemistry could be used to avoid this charge neutralization [7]. Transfection efficiencies achieved

by xLPEIs agree well with those previously reported for KB cells [18]. The decrease in efficiency at higher crosslinking ratios is likely explained by the high amount of charge neutralization and poor complexation efficiency. Cell viability increases monotonically with crosslinker ratio, and hence charge neutralization, which may be the primary mechanism for decreased toxicity at the higher crosslink densities. At high N/P ratios, toxicity is likely dominated by free polymer effects, thus changes in polyplex size or charge should not have an impact on toxicity. Of great interest was the fact that both transfection efficiency and cell viability varied independently of crosslinker choice. This indicates that disulfide degradation may not be critical for either transfection or reduced toxicity in this xLPEI system.

The high transfection efficiencies shown in Figure 3.3 were achieved at high N/P ratios, indicating that free polymer likely plays an important role in transfection. Wu, et. al found that in a typical N/P 10 formulation of bPEI 25k, approximately 70% of the bPEI is free in solution. This agreed well with results from Wagner in which size exclusion chromatography was used to separate free polymer from polyplexes [29]. In both studies, it was found that transfection efficiency in the absence of free polymer was two orders of magnitude less efficient, but could be restored by the addition of free polymer, either immediately or several hours after initial polyplex addition. To investigate whether the high transfection efficiency was due to superior properties of xLPEI as free polymer, as a DNA condensation agent, or some combination of the two, a series of experiments was carried out in which bPEI 25k was substituted for xLPEI for the above functions. The increase in transfection efficiency when xLPEI is used as free polymer along with bPEI 25k polyplexes indicates free xLPEI plays an important role in

the increased transfection efficiency. To determine if the free polymer was functioning primarily to stimulate uptake of polyplexes, polyplex uptake was measured using labeled DNA. When bEI 25k was used to form polyplexes, uptake was relatively independent of free polymer addition, indicating the primary role of free xLPEI was downstream of uptake. Cell viability was dependent on both the choice of condensation polymer and free polymer, as systems with bPEI 25k included in either capacity experienced significant cytotoxicity. Differences in either efficiency or viability between degradable and non-degradable xLPEI were absent in most cases. This is consistent with xLPEI free polymer being the dominant factor in generating high transfection levels, as cytosolic polyplex unpackaging, a property improved by disulfide degradation, would not depend on free polymer.

In experiments in which xLPEI was kept constant as the free polymer, uptake was greater when bPEI 25k was used as the condensing polymer versus xLPEI. xLPEI was shown to be inefficient at both uptake and transfection in the absence of free polymer, suggesting that free polymer may be necessary for additional complexation prior to uptake. Additional polyplex condensation by free polymer was not seen in sizing experiments, but Figure 3.6 still suggests some role for this process. The role of free xLPEI in this system thus depends on the identity of the polyplex used; for loose polyplexes it serves to additionally complex polyplexes after addition and for all polyplexes it enhances transfection processes downstream of uptake, such as endosomal escape.

Endosomal escape was probed rapidly using a high-throughput implementation of a calcein release assay reported previously by our group [27, 33]. xLPEIs were able to mediate escape in over 60% of cells at 10 □g/mL, the approximate concentration of free polymer in a 40:1 N/P formulation. In comparison, bPEI 25k caused escape in less than 10% of cells at 3 □g/mL, approximately the concentration at which free polymer exists at the optimized bPEI 25k formulation of N/P 10:1 [28]. bPEI 25k was effective in causing escape at 10 □g/mL, but at slightly lower efficiencies than xLPEI, and causing significant membrane damage. This membrane damage also manifested itself as a loss of calcein at 30 □g/mL. However, xLPEI showed no evidence of membrane damage at 30 □g/mL, a concentration at which escape was seen in over 75% of cells. Overall cell viability was also shown to be substantially better for xLPEI and no loss of viability was seen at 10 □g/mL, the concentration which achieved escape in over 60% of cells. Taken together, this shows that free xLPEI is able to effectively mediate endosomal escape without the membrane toxicity observed in commercially available PEIs.

In summary, we have shown that polycations crosslinked with a disulfide linkage are not necessarily highly efficient and less toxic as a result of the disulfide linkage itself. In the case of the xLPEIs synthesized in this work, free polymer was shown to be primarily responsible for the high efficiency and decreased toxicity of this system. Free xLPEI was shown to be effective in mediating endosomal escape with no observed membrane toxicity. More investigation into the role of free polymer in delivery of DNA will increase the understanding of how polymer structure and delivery function are related.

3.6 Summary

In summary, we have shown that polycations crosslinked with a disulfide linkage are not necessarily highly efficient and less toxic as a result of the disulfide linkage itself. In the case of the xLPEIs synthesized in this work, free polymer was shown to be primarily responsible for the high efficiency and decreased toxicity of this system. Free xLPEI was shown to be effective in mediating endosomal escape with no observed membrane toxicity.

3.7 References

1. Boussif, O., et al., *A versatile vector for gene and oligonucleotide transfer into cells in culture and in vivo: polyethylenimine.* Proceedings of the National Academy of Sciences, 1995. **92**: p. 7297-301.
2. Kawakami, S., et al., *Evaluation of Proinflammatory Cytokine Production Induced by Linear and Branched Polyethylenimine / Plasmid DNA Complexes in Mice.* Pharmacology, 2006. **317**: p. 1382-1390.
3. Moghimi, M., et al., *A two-stage poly(ethylenimine)-mediated cytotoxicity: implications for gene transfer/therapy.* Molecular Therapy, 2005. **11**: p. 990-5.
4. Parhamifar, L., et al., *Polycation cytotoxicity: a delicate matter for nucleic acid therapy—focus on polyethylenimine.* Soft Matter, 2010. **6**: p. 4001.
5. Merkel, O.M., et al., *In vitro and in vivo complement activation and related anaphylactic effects associated with polyethylenimine and polyethylenimine-graft-poly(ethylene glycol) block copolymers.* Biomaterials, 2011: p. 1-7.
6. Fischer, D., et al., *A Novel Non-Viral Vector for DNA Delivery Based on Low Molecular Weight, Branched Polyethylenimine: Effect of Molecular Weight on Transfection Efficiency and Cytotoxicity.* Pharmaceutical Research, 1999. **16**(8): p. 1273-1279.
7. Gosselin, M., W. Guo, and R. Lee, *Efficient gene transfer using reversibly cross-linked low molecular weight polyethylenimine.* Bioconjugate Chemistry, 2001. **12**: p. 989-94.
8. Neu, M., D. Fischer, and T. Kissel, *Recent advances in rational gene transfer vector design based on poly(ethylene imine) and its derivatives.* Journal of Gene Medicine, 2005. **7**: p. 992-1009.
9. Meng, F., W.E. Hennink, and Z. Zhong, *Reduction-sensitive polymers and bioconjugates for biomedical applications.* Biomaterials, 2009. **30**: p. 2180-98.
10. Bauhuber, S., et al., *Delivery of nucleic acids via disulfide-based carrier systems.* Advanced Materials, 2009. **21**: p. 3286-306.
11. Salcher, E.E. and E. Wagner, *Chemically Programmed Polymers for Targeted DNA and siRNA Transfection.* Anion Sensing, 2010: p. 227-249.

12. Du, F.-S., et al., *Intelligent nucleic acid delivery systems based on stimuli-responsive polymers.* Soft Matter, 2010. **6**: p. 835.
13. Knorr, V., M. Ogris, and E. Wagner, *An acid sensitive ketal-based polyethylene glycol-oligoethylenimine copolymer mediates improved transfection efficiency at reduced toxicity.* Pharmaceutical Research, 2008. **25**: p. 2937-45.
14. Kloeckner, J., et al., *Gene carriers based on hexanediol diacrylate linked oligoethylenimine: effect of chemical structure of polymer on biological properties.* Bioconjugate Chemistry, 2006. **17**: p. 1339-45.
15. Thomas, M., et al., *Cross-linked Small Polyethylenimines : While Still Nontoxic , Deliver DNA Efficiently to Mammalian Cells in Vitro and in Vivo.* Small, 2005. **22**: p. 20-22.
16. Forrest, M.L., J.T. Koerber, and D.W. Pack, *A degradable polyethylenimine derivative with low toxicity for highly efficient gene delivery.* Bioconjugate Chemistry, 2003. **14**: p. 934-40.
17. Lin, C. and J.F.J. Engbersen, *The role of the disulfide group in disulfide-based polymeric gene carriers.* Expert Opinion on Drug Delivery, 2009. **6**(4): p. 421-439.
18. Breunig, M., et al., *Breaking up the correlation between efficacy and toxicity for nonviral gene delivery.* Proceedings of the National Academy of Sciences, 2007. **104**: p. 14454-9.
19. Breunig, M., et al., *Fluorescence resonance energy transfer: evaluation of the intracellular stability of polyplexes.* European Journal of Pharmaceutics and Biopharmaceutics, 2006. **63**: p. 156-65.
20. Lee, Y., et al., *Visualization of the Degradation of a Disulfide Polymer, Linear Poly(ethylenimine sulfide), for Gene Delivery.* Synthesis, 2007: p. 13-18.
21. Deng, R., et al., *Dynamic and structural scalings of the complexation between pDNA and bPEI in semidilute and low-salt solutions.* Biopolymers, 2010. **93**: p. 571-7.
22. Peng, Q., Z. Zhong, and R. Zhuo, *Disulfide Cross-Linked Polyethylenimines (PEI) Prepared via Thiolation of Low Molecular Weight PEI as Highly Efficient Gene Vectors.* Bioconjugate Chemistry, 2008. **19**(2): p. 499-506.
23. Lin, C., et al., *Linear poly(amido amine)s with secondary and tertiary amino groups and variable amounts of disulfide linkages: Synthesis and in vitro gene transfer properties.* Journal of Controlled Release, 2006. **116**(2): p. 130-137.
24. Read, M.L., et al., *A versatile reducible polycation-based system for efficient delivery of a broad range of nucleic acids.* Nucleic Acids Research, 2005. **33**: p. e86.
25. Carlisle, R.C., et al., *Polymer-coated polyethylenimine/DNA complexes designed for triggered activation by intracellular reduction.* Journal of Gene Medicine, 2004. **6**: p. 337-44.
26. Son, S., K. Singha, and W.J. Kim, *Bioreducible BPEI-SS-PEG-cNGR polymer as a tumor targeted nonviral gene carrier.* Biomaterials, 2010. **31**: p. 6344-54.
27. Bonner, D.K., et al., *Intracellular Trafficking of Polyamidoamine - Poly(ethylene glycol) Block Copolymers in DNA Delivery.* Bioconjugate Chemistry, 2011. **22**(8): p. 1519-1525.

28. Yue, Y., et al., *Revisit complexation between DNA and polyethylenimine - Effect of uncomplexed chains free in the solution mixture on gene transfection.* Journal of Controlled Release, 2010.
29. Boeckle, S., et al., *Purification of polyethylenimine polyplexes highlights the role of free polycations in gene transfer.* Journal of Gene Medicine, 2004. **6**: p. 1102-11.
30. Yue, Y., et al., *Revisit complexation between DNA and polyethylenimine - effect of length of free polycationic chains on gene transfection.* Journal of Controlled Release, 2011. **152**(1): p. 143-151.
31. Dai, Z., et al., *Elucidating the interplay between DNA-condensing and free polycations in gene transfection through a mechanistic study of linear and branched PEI.* Biomaterials, 2011. **32**(33): p. 8626-8634.
32. Deng, R., et al., *Revisit the complexation of PEI and DNA — How to make low cytotoxic and highly efficient PEI gene transfection non-viral vectors with a controllable chain length and structure?* Journal of Controlled Release, 2009. **140**(1): p. 40-46.
33. Jones, R.A., et al., *Poly(2-alkylacrylic acid) polymers deliver molecules to the cytosol by pH-sensitive disruption of endosomal vesicles.* Biochemical Journal, 2003. **372**: p. 65-75.

Chapter 4. Evaluation of siRNA Delivery with Clickable pH Responsive Cationic Polypeptides and Block Copolymers

4.1 Abstract

A series of pH responsive synthetic polypeptides has been developed based on an N-carboxyanhydride ring opening polymerization combined with a facile and versatile click chemistry. Poly(γ-propargyl L-glutamate) (PPLG) homopolymers and poly(ethylene glycol-b-γ-propargyl L-glutamate) (PEG-b-PPLG) block copolymers were functionalized with various amine moieties that range in pKa and hydrophobicity, providing the basis for a library of new synthetic structures that can be tuned for specific interactions and responsive behaviors. Here we evaluate the pH responsive behavior of the new polypeptides and the hydrolysis of the ester containing amine side chains. We examine the reversible micellization with block copolymers of the polypeptides and evaluate the siRNA delivery potential of this library. While this PPLG library was able to efficiently complex siRNA, gene-specific knockdown could not be achieved. Analysis of barriers to transfection demonstrated that adequate uptake was followed by an inability to escape the endosome, most likely due to low charge density.

4.2 Introduction

Synthetic polypeptides have received attention because of their unique structural properties and biocompatibility [1-4]. Like their naturally occurring analogs, these molecules have a poly(amino acid) backbone and possess the ability to fold into stable secondary structures. Helical structures, in particular, allow for proteins to optimally

display surface moieties that dictate cell signaling and molecular docking [5]. This property gives synthetic polypeptides an advantage over most traditional polymers that can only adopt a random coil structure. A considerable amount of research has been performed on synthetic polypeptides to better understand the complex features of proteins and to gain insight into their secondary structures [6-10]. Synthetic polypeptides can be synthesized on a large scale by the ring opening polymerization (ROP) of N-carboxyanhydrides (NCA) formed from naturally occurring amino acids. These simple homopolypeptides are able to arrange into or change their secondary structure based on solution conditions [7-10]. Although these macromolecules' secondary structure can be controlled to some extent, we are limited by the given side chain, which dictates polymer function, structure, and responsive behavior to temperature or pH among many other properties.

Recently, we reported a new approach to the manipulation of synthetic polypeptide composition and function through the introduction of a new NCA polymer, poly(γ-propargyl L-glutamate) (PPLG) [11], which contains a pendant alkyne group that can be reacted with an azide by the alkyne-azide cycloaddition click reaction [11, 12]. This synthetic strategy allows for the convenient and efficient functionalization of a polypeptide without the need for protection and deprotection steps. To demonstrate the efficiency of polymer modification, we used a model PPLG-g-PEG system, for which we were able to attain a "grafting onto" efficiency of over 96% [11]. Since our initial report, other research groups have extended this platform methodology of combining NCA polymerization and click chemistry side chain modification. Chen et al. used PPLG to click on several different azide functionalized monosaccharides to form

glycopolypeptides [13]. Tang and Zhang reported the synthesis of poly(γ-azidopropyl-L-glutamate), which was functionalized with alkyne containing mannose moieties via the alkyne-azide cycloaddition click reaction [14]. Sun and Schlaad developed thiol-ene clickable polypeptides, where they synthesized poly(D,L-allylglycine) and clicked on thiol functionalized sugars [15]. Huang et al. synthesized poly(D,L-propargylglycine) and clicked on azide containing protected galactose, using alkyne-azide cycloaddition click chemistry [16].

By employing our PPLG platform for the click chemistry of amino-functional groups, we have developed several new pH responsive macromolecules. A unique aspect of these new amine-functionalized polypeptides is the ability to buffer and in some cases, undergo a solubility phase transition with degree of ionization, while adopting an α-helical structure over biologically relevant pHs. These polymers include both poly(γ-propargyl L-glutamate) (PPLG) based homopolymers and poly(ethylene glycol-b-γ-propargyl L-glutamate) (PEG-b-PPLG) block copolymers substituted with various amine moieties that range in pKa and hydrophobicity, providing the basis for a library of new synthetic structures that can be tuned for specific interactions and responsive behaviors.

The new PPLG based cationic polypeptides have the potential to be used for many different applications. Polypeptides have been investigated as smart molecules in lipid membranes [17-19], liquid crystals used in optical storage and display devices [4], vehicles for drug and gene delivery [3, 20-29] , anti-fouling coatings [30], components for tissue engineering and biosensors, and synthetic mimics of naturally occurring molecules [1, 3, 31-34]. We have characterized the pH responsive behavior of the new polypeptides, the pH-dependent hydrolysis rate of the ester containing amine side chains,

and have performed preliminary experiments that demonstrate the potential use of these new materials for systemic drug and gene delivery. More specifically, for pH responsive drug delivery, one could design a micellar system that forms stable micelle drug carriers in the blood stream and normal tissue at extracellular conditions (pH 7.00-7.45) [35] but destabilizes in the endosome (early endosome pH 5.5-6.3 and late endosome pH < 5.5) [36] or in hypoxic regions of tumors (pH approaching 6.0) [35], to release the drug. To achieve this behavior, a pH responsive polypeptide is needed that is fully soluble at endosomal or tumor pH and insoluble at extracellular pH. We have determined the solubility behavior of the amine functionalized PPLG and the self-assembly behavior of the amine functionalized PEG-b-PPLG as a function of pH. For gene delivery, it is critical that the polymers complex with siRNA or DNA to form protective polymer-gene complexes (polyplexes); these polyplexes must escape the endosomal compartments into which they are initially trafficked upon internalization [37, 38]. One such mode of endosomal escape is through the so-called "proton sponge effect", in which the basic polymer buffers the endosome during acidification, leading to osmotic swelling and rupture [37, 39]. The buffering capacity of the new polypeptides has been explored using titrations to determine the pH range at which these polymers buffer. In addition, siRNA delivery studies have been performed to determine if these polymers can efficiently deliver siRNA and achieve knockdown. We are interested in using the PPLG system for siRNA delivery because it is particularly amenable to modification with different ratios of primary, secondary, or tertiary amines. This allows for the precise tuning of the functions of DNA binding and release (primary and secondary) versus endosomal escape (secondary and tertiary).

An additional unique aspect of these new polypeptides is that there is an ester linkage between the amine and the polymer backbone. These ester side chains can be hydrolyzed, leaving behind a carboxylic acid moiety, thus creating a charge shifting polymer (shifting with hydrolysis from positive to negative net charge). We have examined the rate of hydrolysis of the ester side chain at various pH conditions and the role the shift in overall polymer charge plays on disrupting the secondary structure. This hydrolysis and overall shift in charge from positive to negative could play a role in improving the safety and biodegradability of these substituted poly(γ-glutamic acid) based polymers [40-42], and may also aid in the delivery and subsequent unpackaging and release of nucleic acid based cargos that are delivered using these systems.

4.3 Materials and Methods

4.3.1 Materials

L-(+)-glutamic acid, 99% minimum was purchased from EMD Chemicals. 3-dimethylaminopropylchloride hydrochloride, 99% was purchased from Arcos Organics. Sunbright® amine terminated poly(ethylene glycol) was purchased from NOF Corporation. siRNA was purchased from Dharmacon RNAi Technologies and QuantiT Ribogreen RNA Reagent was purchased from Invitrogen. All other chemicals were purchased from Sigma Aldrich. HeLa cells stabling expressing both firefly and *Renilla* luciferease were generously provided by Alnylam (Cambridge, MA) [43]. All materials were used as received. Dual-Glo Luciferase Assay System was purchased from Promega. All other cell culture reagents were obtained from Invitrogen (Carlsbad, CA).

4.3.2 General Methods

^{1}H-NMR and ^{13}C NMR were recorded on Bruker 400 MHz FT-NMR spectrophotometer. Gel permeation chromatography measurements were carried out using a Water Breeze 1525 HPLC systems equipped with two Polypore columns operated at 75°C, series 2414 refractive index detector, series 1525 binary HPLC pump, and 717 plus autosampler. Waters' Breeze Chromatography Software Version 3.30 was used for data collection as well as data processing. DMF with 0.01M LiBr was the eluent for analysis, and samples were dissolved at 4-6mg/mL in DMF. The average molecular weight of the sample was calibrated against narrow molecular weight poly(methyl methacrylate) standards.

Acid-base titrations were performed on all amine functionalized PPLG. 3mL of 10mM amine in 125mM NaCl was adjusted to a pH of 3 using 1 M HCl. The solution was titrated with 10 μL aliquots of 0.1 M NaOH, measuring the pH with each addition. For polymers where precipitation was observed, UV/Vis measurements were obtained at 600nm to monitor the solution turbidity. UV/Visible measurements were carried out on an Agilent Technologies G3172A spectrometer.

4.3.3 Synthesis of γ-propargyl L-glutamate hydrochloride

L-glutamic acid (15g, 102mmol) was suspended in propargyl alcohol (550 mL) under argon. Chlorotrimethylsilane (28.5mL, 224mmol) was added dropwise to the suspension over 1 hour. The resulting solution was stirred at room temperature for two days until there was no undissolved L-glutamic acid. The reaction solution was precipitated into diethyl ether giving a white solid. The crude product was removed by filtration, dissolved in boiling isopropanol, and precipitated into diethyl ether. The product was filtered, washed with diethyl ether, and dried under vacuum to yield 19.13g (84.5%). ^{1}H-

NMR (400MHz, D_2O) δ=2.20 (m, 2H, CH_2), 2.63 (dt, 2H, CH-CO), 2.86 (t, 1H, C≡CH), 4.05 (t, 1H, CH), 4.69 (d, 2H, CH_2CO).

4.3.4 Synthesis of N-carboxyanhydride of γ-propargyl L-glutamate (PLG-NCA)

γ-propargyl L-glutamate hydrochloride (6g, 27mmol) was suspended in dry ethyl acetate (190mL). The solution was heated to reflux and triphosgene (2.67g, 9mmol) was added. The reaction solution was refluxed for 6 hours under nitrogen. The reaction solution was cooled to room temperature and any unreacted γ-propargyl L-glutamate hydrochloride was removed by filtration. The reaction solution was then cooled to 5°C and washed with 190 mL of water, 190 mL of saturated sodium bicarbonate, and 190 mL of brine all at 5°C. The solution was then dried with magnesium sulfate, filtered, and concentrated down to viscous oil (4.53g, 79.2% yield). ^{1}H-NMR (400MHz, $CDCl_3$) δ=2.20 (dm, 2H, CH_2), 2.49 (t, 1H, C≡CH), 2.58 (t, 2H, CH-CO), 4.39 (t, 1H, CH), 4.68 (d, 2H, CH_2CO), 6.5 (s, 1H, NH).

4.3.5 Synthesis of Poly(γ-propargyl L-glutamate) initiated by heptylamine

A typical procedure for the polymerization is as follows. To a flame dried Schlenk flask, heptylamine (14.5μL, 0.0980 mmol) and DMF (8mL) were combined under Ar. In a separate vial, PLG-NCA (1.552, 7.35 mmol) was dissolved in DMF (8mL) and added to the reaction flask. The reaction mixture was stirred for three days at room temperature. The polymer was precipitated into diethyl ether and removed by centrifugation (0.823g, 67.0% recovered, by ^{1}H-NMR n=75, by DMF GPC M_w=14,100, PDI=1.09). ^{1}H-NMR

(400MHz, [D_6] DMF) δ=2.28 (br m, 2H, CH_2), 2.55 (br m, 2H, CH-CO), 3.38 (br m, 1H, C≡CH), 4.09 (br m, 1H, CH), 4.76 (br m, 2H, CH_2CO), 8.5 (br m, 1H, NH).

4.3.6 Synthesis of Poly(ethylene glycol)-b-Poly(γ-propargyl L-glutamate)

A typical procedure for the polymerization is as follows. A round bottom flask was rinsed with acetone and oven dried. In a glove box, PEG-NH_2 (0.900g, 0.180mmol) was dissolved in DMF (9mL) in a round bottom flask. PLG-NCA (0.950g, 4.50mmol) was dissolved in dry DMF (9mL) added to the reaction flask. The reaction mixture was stirred for three days at room temperature. The reaction solution was concentrated with a rotary evaporator and dried under high vacuum to remove the DMF. To remove any residual PLG-NCA and DMF, the polymer was redissolved in dichloromethane precipitated into diethyl ether and removed by centrifugation (1.45g, 87.9% recovered, by ^{1}H-NMR n=23, by GPC PDI=1.09). ^{1}H-NMR (400MHz, [D_6] DMF) δ=2.28 (dm, 2H, CH_2 PPLG), 2.55 (dm, 2H, CH-CO PPLG), 3.38 (m, 1H, C≡CH PPLG), 3.59 (s, 4H, CH_2CH_2 PEG), 4.09 (m, 1H, CH PPLG), 4.76 (m, 2H, CH_2CO PPLG), 8.5 (m, 1H, NH PPLG).

4.3.7 Synthesis of 2-bromo-N-methylethanamine hydrobromide

2-bromo-N-methylethanamine hydrobromide was synthesized following the protocol presented by Shutte et al [44]. Briefly, in a round bottom flask, 48% w/w HBr (30mL) was cooled in an ice bath to 4°C and 2-(methylamino)ethanol (10 mL, 125mmol) was added dropwise. H_2O and HBr were distilled off and the crude product solution was cooled to 60°C. The solution was slowly added to a solution of cold acetone, where it precipitated out to form a white solid. The precipitant was removed, washed with cold

acetone, and dried under high vacuum (16.46g, 60.4% yield). ^{1}H-NMR δ (400MHz, D_2O) 3.69 (t, 2H, $BrCH_2$), 3.50 (t, 2H, CH_2N), 2.75 (s, 3H, CH_3).

4.3.8 General synthesis of amino azides

Organic azides can be EXPLOSIVE! A guide to safe handling and storage of organic azides can be found in "Click Chemistry: Diverse chemical function from a few good reactions" by Kolb et al [12]. The shorthand notation for each side group used in this article is provided in parentheses after the specific chemical name. Amino azides were synthesized using the protocol presented by Carboni et al [45]. A representative example, 3-dimethylamino-1-propylchloride hydrochloride (10g, 63 mmol) and sodium azide (8.22g, 126 mmol) were dissolved in water (1mL/mmol) and heated at 75°C for 15 h. The reaction mixture was cooled in an ice bath and NaOH (4g) was added. The solution phase separated and the organic phase was removed. The aqueous phase was extracted with diethyl ether twice. The organic layers were combined, dried with $MgSO_4$, and concentrated down to an oil (6.60g, 80.8% yield). 3-Azido-N,N-dimethylpropan-1-amine (dimethylpropanamine) ^{1}H-NMR (400MHz, $CDCl_3$) δ (ppm) = 3.30 (t, 2H, N_3CH_2), 2.30 (t, 2H, CH_2N), 2.17 (s, 6H, $N(CH_3)_2$), 1.71 (m, 2H, $N_3CH_2CH_2$). 2-Azidoethanamine (primary amine) ^{1}H-NMR (400MHz, $CDCl_3$) δ (ppm) = 3.32 (t, 2H, N_3CH_2), 2.83 (t, 2H, CH_2NH_2), 1.45 (s, 2H, NH_2). 2-Azido-N-methylethanamine (Secondary amine) ^{1}H-NMR (400MHz, $CDCl_3$) δ (ppm) = 3.45 (t, 2H, N_3CH_2), 2.72 (t, 2H, CH_2NH), 2.39 (s, 3H, CH_3), 1.28 (s, 1H, NH). 2-Azido-N,N-dimethylethanamine (Dimethylethanamine) ^{1}H-NMR (400MHz, $CDCl_3$) δ (ppm) = 3.32 (t, 2H, N_3CH_2), 2.47 (t, 2H, CH_2N), 2.24 (s, 6H, $N(CH_3)_2$). 2-Azido-N,N-diethylethanamine (diethylamine) ^{1}H-NMR (400MHz, $CDCl_3$) δ (ppm) = 3.25 (t, 2H,

N_3CH_2), 2.62 (t, 2H, CH_2CH_2N), 2.52 (q, 2.54, $N(CH_2CH_3)_2$), 1.00 (s, 6H, $(CH_2CH_3)_2$). N-(2-azidoethyl)-N-isopropylpropan-2-amine (diisopropylamine) ^{1}H-NMR (400MHz, $CDCl_3$) δ (ppm) = 3.01 (t, 2H, N_3CH_2), 2.98 (m, 2H, $N(CH(CH_3)_2)_2$), 2.62 (t, 2.54, CH_2N), 0.99 (d, 12H, $(CH_2(CH_3)_2)_2$).

4.3.9 General synthesis of substituted PPLG

A typical procedure started with a feed ratio of alkyne/azide/CuBr/PMDETA equal to 1/1.2/0.1/0.1. The PPLG (0.0750g, 0.45mmol alkyne repeat units), amino azide (0.069g, 0.54mmol 3-azido-N,N-dimethylpropan-1-amine), and PMDETA (9.4 μL, 0.045mmol) were all dissolved in DMF (3mL). The solution was degassed by bubbling argon through the solution for 20 minutes. CuBr catalyst (0.0064g, 0.045mmol) was added, and the reaction solution was stirred at room temperature, under argon. Once the reaction was complete, the reaction solution was purified by dialysis against water acidified by HCl (pH<4) for 2-3 days, followed by dialysis with Milli-Q water to remove acid before freeze drying. The final polymer was a white solid.

4.3.10 Circular Dichroism

Circular dichroism (CD) spectroscopy of polymer solutions was carried out using an Aviv model 202 CD spectrometer. Measurements were performed at 25 ± 0.1°C, sampling ever nm with a 3-5 s average time over the range of 195-260 nm (bandwidth = 1.0 nm). Measurements were taken using a cell with a 1mm path length. Samples were prepared at a concentration of 0.5-1 mg/mL in either buffer solutions or Mille-Q water with pH adjusted using 0.1M NaOH and 0.1M HCl solutions.

4.3.11 Critical Micelle Concentration

Critical micelle concentration measurements of the diblock polymers in aqueous solutions at different pH values were performed by fluorescence spectroscopy using a pyrene probe. Fluorescence peak intensity emissions ratios (*373* nm/ *384* nm) were plotted against the logarithm of polymer concentrations to determine CMC as the onset of micellization [46]. Fluorescence spectroscopy was carried out on a Horiba FluoroLog®-3 spectrofluorometer at 25 °C. A stock solution of pyrene at 5.00×10^{-7} M in water was prepared. Polymer samples were dissolved in the stock pyrene solution and diluted to specific concentrations.

Tapping-mode atomic force microscopy (AFM) measurements were conducted in air with a Dimension 3100 system (Digital Instruments, Santa Barbara, CA) operated under ambient conditions. The samples were prepared for AFM analysis by spin coating a silicon wafer with a polymer solution at a concentration of 1 mg/mL in Milli-Q water with the pH adjusted using 0.1M NaOH.

4.3.12 Ester Hydrolysis

Ester hydrolysis samples were prepared by dissolving polymer in a stock solution at 10 mg/mL for homopolymer and 20 mg/mL for diblock copolymer. The stock solutions were then diluted with pH buffer to a concentration of 0.5 mg/mL for homopolymer and 1 mg/mL for diblock copolymer. At various time points, samples were analyzed by CD. Samples were also freeze dried, reconcentrated in D_2O to 2.5 mg/mL for homopolymers and 3.75 mg/mL for diblock copolymers, acidified with trifluoroacetic acid to stop hydrolysis, and analyzed by ^{1}H-NMR.

4.3.13 siRNA Complexation and Dissociation

Ribogreen assays (QuantiT Ribogreen RNA Quantification Reagent, Invitrogen) were performed to determine the complexation efficiency of the polymers with siRNA. Ribogreen is a cyanine dye that is nearly non-fluorescent when unbound to RNA, but exhibits a >1000 fold enhancement in fluorescence when bound to RNA. When siRNA is complexed (e.g. by a polymer), it is unavailable to bind to Ribogreen and thus the fluorescence signal decreases relative to uncomplexed siRNA. 25 μL of siRNA at 0.006 μg/mL was aliquoted into wells of a 96 well plate and the appropriate amount of polymer was added to attain the desired polymer:siRNA ratio (w/w) in a total volume of 50 μL. After allowing 10 minutes for complexation, 20 μL of the complex solution was added to a black, flat-bottomed, polypropylene 96-well plate containing 100 μL of Ribogreen (diluted 1:200 per manufacturer instructions). The fluorescence of each well was measured on a Perkin Elmer Plate 1420 Multilabel Counter plate reader and the fraction of uncomplexed siRNA was determined by comparing the fluorescence of the polymer complexes with the fluorescence of a free siRNA control. For the heparin destabilization titrations, heparin (167 IU/mg) was dissolved in a stock solution at 0.5 IU/mL and added to polyplex/ribogreen solutions.

4.3.14 siRNA Knockdown

Transfection studies were performed in quadruplicate. HeLa cells were grown in 96-well plates at an initial seeding density of 2000 cells/well cell growth media comprised of Dulbecco's Modified Eagle Media (DMEM) supplemented with 10% fetal bovine serum (FBS) and 1% Pennicilin-Streptomycin. Cells were allowed to attach and proliferate for 24 hours in a humidified incubator at 37°C and 5% CO_2. 25 μL of siRNA

at 6 μg/mL in 25mM sodium acetate buffer was aliquoted into wells of a 96 well plate and the appropriate amount of polymer was added to attain the desired polymer:siRNA ratio (w/w) in a total volume of 50 μL/well. After mixing the polymer/siRNA solutions, the polyplexes were allowed to sit 10 minutes for complexation. 30 μL aliquots of the polyplex solution was then added to each well of a 96-well plate containing 200 μL/well Opti-Mem and the solution was mix. Growth media was removed from the cells and 150 μL/well of complex/Opti-Mem solution was added. Lipofectamine at a 4:1 ratio was used as a positive control. Naked siRNA was used as a negative control and as an internal standard. In all cases, the each well contained 50 ng or 150 ng siRNA. The cells were incubated for 4 hours, the media was removed and replaced with 10% serum-containing growth medium. A Luciferase assay was performed as using the Dual-Glo Luciferase Assay System (Promega, Madison, WI).

4.3.15 Cell viability

HeLa cells were seeded in a 96-well clear, flat-bottomed plate and transfected according to the above protocol. After 24 hrs, cell metabolic activity was assayed using the MTT cell proliferation assay (ATCC, Manassas, VA).

4.3.16 Polyplex Uptake

Block copolymers and PEI were labeled with fluorescein isothiocyante (FITC) at a molar ratio of 4:1 (dye:polymer). Using the labeled polymers, polyplexes were formed and cells treated as described in the above section. At the time indicated, cells were removed from the incubator and analyzed using flow cytometery. Flow cytometry was performed in U-bottom 96-well plates using a HTS LSR II Flow cytometer (Becton-Dickinson,

Mountain View, CA). To prepare samples, media was removed from cells and replaced with 25 μL trypsin for 5 minutes. 50 μL of PBS supplemented with 2% FBS was then added to each well, mixed, and the entire 75 μL cell suspension transferred into a U-bottom 96-well plate.

4.3.17 High-Throughput Endosomal Escape

Complexes were assembled and transfection was conducted as described above, except that 25 μM Calcein was added to the Opti-MEM and cells were seeded in black, clear-bottom 96-well plates. 4 hours after transfection, 5 μL of a solution of Hoechst 33342 diluted to 1:30 in PBS was added. After 20 min of staining, complexes and free dye were removed, and the cells were washed 3 times with PBS. 150 μL of phenol-free Opti-MEM with 10% serum was added to each well before the plate was covered with an opaque sticker, foiled, and analyzed. Imaging was done using a Cellomics ArrayScan VTI HCS Reader (Thermo Fisher, Waltham, MA) and analysis was done using the included software.

4.4 Results and Discussion

4.4.1 Polymer Synthesis

The PPLG polymers were prepared as previously described [11]. Briefly, γ-propargyl L-glutamate was reacted with triphosgene to form the NCA. PPLG and PEG-b-PPLG were prepared by ring opening polymerization in dimethylformamide (DMF) at room temperature by initiation with heptylamine and PEG-NH_2 (MW=5000), respectively. Table 4.1 summarizes the stoichiometric feed ratio of each polymerization, the degree of polymerization characterized by ^{1}H-NMR, and the molecular weight and molecular

weight distribution characterized by gel permeation chromatography (GPC) with DMF as the carrier solvent. The narrow polydispersities (1.09-1.25) and reaction feed ratio compared to the degree of polymerization by ^{1}H-NMR indicate that the polymerization is well controlled. Furthermore, this polymerization route allows for high molecular weight polymers with a degree of polymerization as high as 140. As indicated by Poché et al., a high degree of polymerization can be obtained if the NCA monomer purity is high; the washing strategy employed in this NCA monomer preparation does significantly improve the monomer purity by removing residual HCl [47].

			DMF GPC with PMMA		
Polymer	Feed ratio	DP by NMR	Mn	Mw	PDI
PPLG	25	30	6100	7600	1.25
PPLG	50	56	12700	14100	1.11
PPLG	75	75	17900	19400	1.09
PPLG	150	140	42900	50000	1.17
PEG-NH_2	--	--	10000	11500	1.14
PEG-b-PPLG	25	23	14600	15800	1.08

Table 4.1 Summary of PPLG Polymerization
Summary of polymerization feed NCA-monomer/initiator, degree of polymerization by -^{1}H-NMR, molecular weight and polydispersity determined by DMF GPC with PMMA standards.

Six different amine moieties ranging in pKa (primary, secondary, and tertiary amines) and hydrophobicity (dimethylethanamine, dimethyl-propanamine, diethylamine, and diisopropylamine) were attached to four different molecular weight PPLG backbones and a PEG-b-PPLG diblock copolymer through the copper-mediated 1,3 cycloaddition between the alkynes on the PPLG backbone and the azide bearing amine groups, shown in Scheme 4.1. The labels under each side group are used to refer to each polymer bearing that side group. The PPLG was coupled with azido amines using CuBr/PMDETA as a catalyst in DMF with a molar ratio of alkyne/azide/CuBr/PMDETA

equal to 1/1.2/0.1/0.1. After the reaction was complete, the polymer was purified by dialysis against water acidified with HCl (pH ≤ 4) to remove any unreacted amino azides and the copper catalyst.

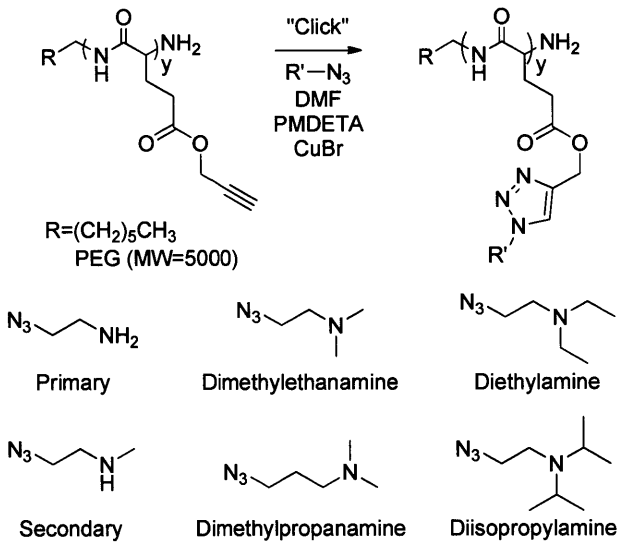

Scheme 4.1 Functionalization of PPLG by the alkyne-azide cycloaddition click reaction and the pH responsive side groups.

The polymer structures were confirmed using ^{1}H-NMR. Representative ^{1}H-NMR of the diethylamine and diisopropylamine substituted PPLG compared to the ^{1}H-NMR of PPLG are shown in Figure 4.1. For all amine groups, the coupling efficiency was near quantitative, as indicated by the disappearance of the PPLG alkyne peak (a, 3.4ppm) and ester peak (b, 4.7ppm) and the appearance of a new ester peak (k, 5.2ppm) and the triazole ring peak (m, 8.15ppm). Furthermore, the peak integration for all samples tested were as expected for near quantitative substitution without hydrolysis of the ester group on the polymer side chains.

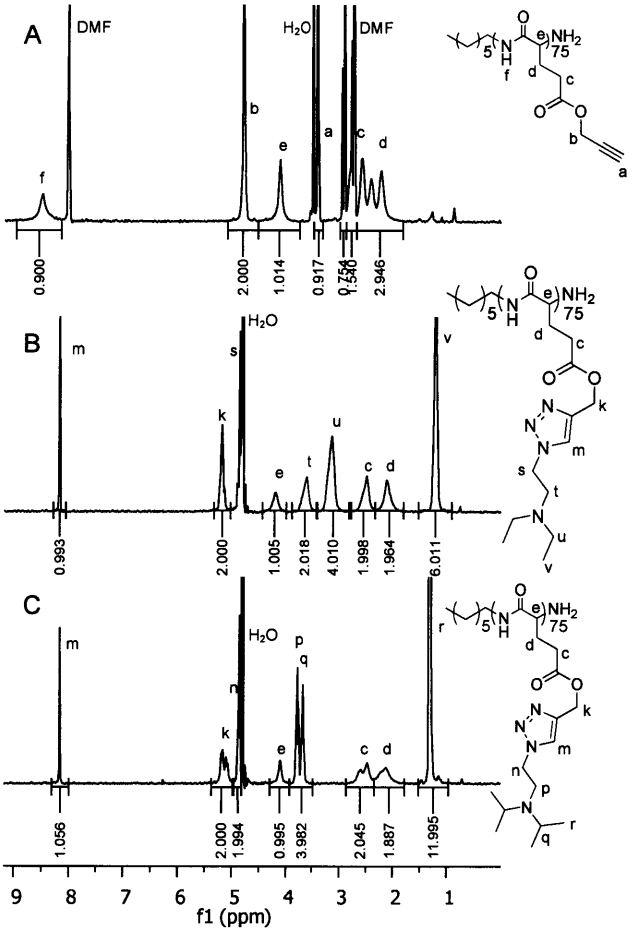

Figure 4.1 NMR Spectra of Functionalized PPLG
A) PPLG in d_7 DMF, B) PPLG functionalized with diethylamine in D_2O, and C) ^{1}H-NMR of PPLG functionalized with diethylamine in D_2O. The PPLG backbone has a degree of polymerization of 75.

4.4.2 Investigation of Polymer Buffering and Solubility

To investigate pH responsiveness and the buffering behavior of these polypeptide systems, titrations were performed on all polymers. Polymers were dissolved in 125 mM NaCl at 10 mM polypeptide-amine (molarity based on repeat unit), titrated with increasing pH to a pH of 10-10.5 using 0.1 M NaOH, and subsequently titrated with decreasing pH using 0.1 M HCl. After titrations were complete, representative samples were freeze dried, dissolved in D_2O, and analyzed using ^{1}H-NMR. From the ^{1}H-NMR, the spectra were nearly identical to those obtained before titrations, indicating that

hydrolysis did not occur during the 2-3 hour titration process. Representative titrations with increasing pH are shown in Figure 4.2, where Figure 4.2A consists of the dimethylethanamine polymers at varying degrees of polymerization, and Figure 4.2B consists of titrations of each polymer side functional group with a degree of polymerization of NCA backbone of 75. All polymers appear to have strong buffering capacity in the pH range of 5-7.4, which scales with the pH range of typical extracellular tissue to late endosomal pH [35, 36]. The diisopropylamine polypeptide exhibits the sharpest buffering transition at pH 5.25; the diethylamine polymer also buffers in this range, but with a broader transition that has a midpoint at the slightly higher pH of approximately 6.5. The primary and secondary amine functional polymers interestingly exhibit similar broad buffering behavior beginning at pH 5.5 with a midpoint at 7.25. One would typically expect buffering at higher pH for primary and secondary amines (pKa approximately 9-11) [48, 49], although some buffering is observed in these polymers from pH 8 to 10. Polyelectrolytes typically exhibit broad buffering behavior and shifted pKa values due to segmental charge repulsion. For the dimethyl substituted amines, the dimethylethanamine exhibits buffering behavior starting at the same pH as the primary and secondary amines with a midpoint falling between 6.5 and 7.0. These values are consistent with the series of polymers with ethylene linker groups to the tetrazole ring; whereas, the dimethylpropanamine polymer exhibits buffering at higher pHs. The additional carbon between the amine group and the triazole ring results in a higher pKa for the dimethylpropanamine. This shift in pKa could be the result of the amine group being further removed from the electron withdrawing triazole ring or from the decreased crowding experienced by the amine group. All of the polymers exhibit a

small amount of buffering at the start of the titration curve, at pH 3-4; the buffering in this region could be a result of the triazole ring generated during the click reaction; triazoles exhibit pKa's of less than 3.0 [48, 50]. The polymer buffering appears to have little dependence on polymer molecular weight, as indicated in Figure 4.2A.

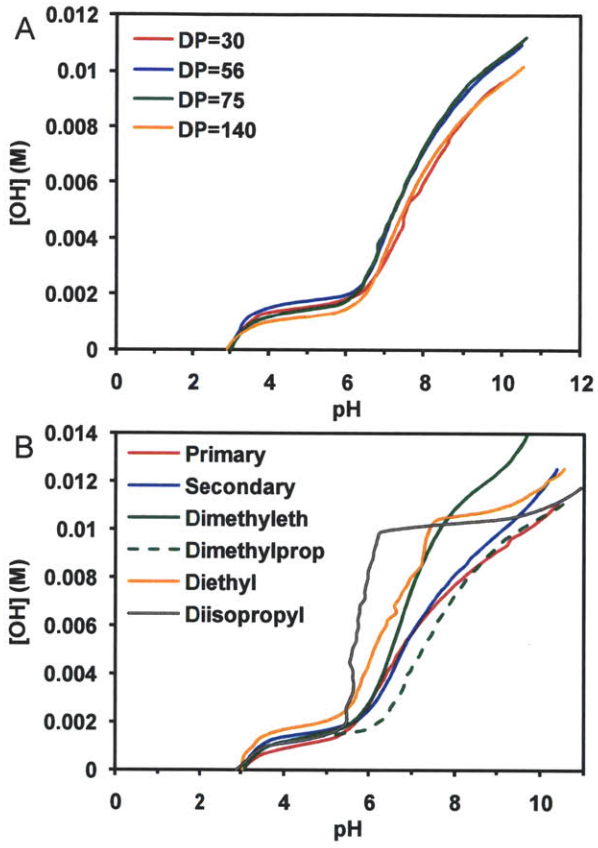

Figure 4.2 pH Buffering of PPLG Homopolymers
Titrations of polymers at a concentration of 10mM using 0.1M sodium hydroxide. A) PPLG polymers functionalized with dimethylethanamine with varying degrees of polymerization, and B) PPLG polymers with a degree of polymerization of 75.

The primary, secondary, and dimethyl polypeptides remain water soluble over the entire pH range; however, as the cationic diethylamine and diisopropylamine functionalized polypeptides are titrated from acidic to basic conditions, the amines become deprotonated. The resulting uncharged polypeptide is no longer soluble in water, leading to precipitation of the polypeptide from aqueous solution. For the diethylamine

and diisopropylamine functionalized PPLG, polymer precipitation was observed at various pH values depending on polymer molecular weight. To determine the pH where precipitation occurs, turbidity measurements were performed on the diethylamine and diisopropylamine functionalized PPLGs by monitoring polymer solution transmission at 550nm, shown in Figure 4.3. When the polymers begin to precipitate out of solution, there is a sharp drop in transmission. For the diethylamine functionalized PPLG (Figure 4.3, solid lines), precipitation occurred between 6.80 and 7.45 depending on the degree of polymerization and for the diisopropylamine functionalized PPLG (Figure 4.3, dashed lines), precipitation occurred between 5.23 and 5.59. These values are consistent with the titration data shown in Figure 4.2. In general we see the anticipated trend that increased molecular weight leads to precipitation at lower pH values and higher degrees of ionization of the polymer functional group. It is notable that the diethylamine series is more sensitive to molecular weight than the diisopropylamine series, which seems to approach a limiting minimum pH value for precipitation. This result may be due to the greater hydrophobicity of the diisopropylamine group as opposed to the diethylamine, which would lead to a lower degree of solubility of the amine side chain and a decreased dependence on molecular weight.

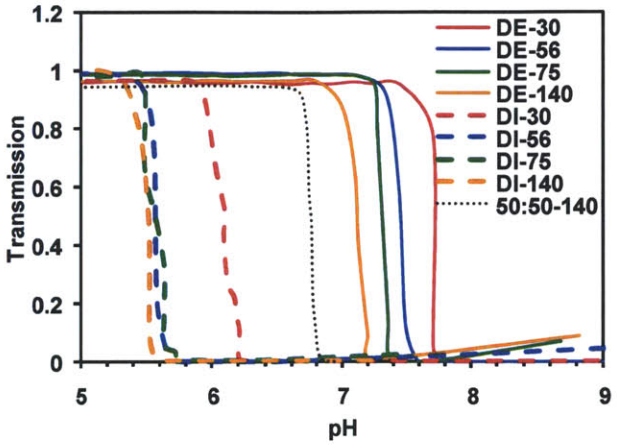

Figure 4.3 Solubility Variation with pH for Tertiary Amine Substituted PPLG
Transmission as a function of pH for all diethylamine and diisopropylamine functionalized polymers. Diethylamine is abbreviated DE and diisopropylamine is abbreviated DI.

The pH transition observed for both the diisopropylamine and diethylamine functionalized polymers can be utilized for the design of a pH responsive drug carrier in which the responsive PPLG block would be the interior, pH responsive block of a micellar system. To determine if the precipitation pH could be tuned, a 50:50 mixture of diethylamine and diisopropylamine side groups was attached to PPLG (DP=140) to generate a random copolymer. As shown in Figure 4.3 (dotted-gray line), the copolymer precipitation pH falls between the precipitation pH values observed for the diethylamine and diisopropylamine substituted PPLG (DP=140), indicating that the pH responsiveness of the amine substitute PPLG block can be fine tuned by changing the ratio of side groups. One could also envision using this strategy to incorporate side groups that will improve the loading of a specific drug or increase polymer-gene complexation efficiency. The buffering and the precipitation behavior were found to be fully reversible, as indicated by reverse titrations that were performed on all polymers. For the completely water soluble primary, secondary, and dimethyl polymers, the reverse titration curve has

the same shape as the original titration with no signs of hysteresis. For tertiary amine polymers that precipitated out of solution, hysteresis was often observed for the larger degrees of polymerization, such that the pH value for which the polymers re-dissolved was often lower than the value observed for precipitation. For the shortest degree of polymerization (DP=30), the polymers returned to solution at nearly the same pH as when the precipitation was initially observed (Figure 4.4).

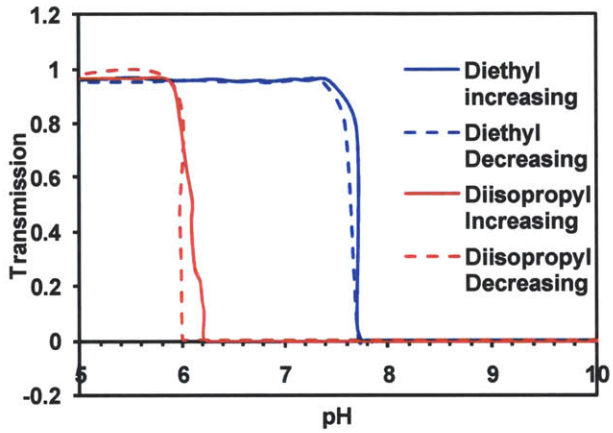

Figure 4.4 Solubility Hysteresis of Tertiary Amine PPLGs
Transmission as a function of increasing and decreasing pH for diethylamine and diisopropylamine with DP=30.

4.4.3 Secondary Structure

Circular dichroism (CD) was used to probe the secondary structure of the various polymers as a function of pH. Polymer dissolved at 1mg/mL was brought down to a pH of 3, titrated to a pH higher than 10, and then immediately titrated back to a pH of 3. A sample CD titration of a secondary amine polypeptide with DP=75 is shown in Figure 4.5. When initially brought down to a pH of 3, the sample adopts a mixture of α-helix and random coil conformations, as indicated by the minimum at 222nm, which is characteristic of an α-helix and the second, more negative minimum at 204nm, which is indicative of a combination of α-helix and random coil. As the sample pH is increased,

the sample adopts an all α-helical structure at high pH values (pH > 6.36), as indicated by the minimums at 208nm and 222nm [51]. When the pH is decreased stepwise back down to acidic pH, this α-helical structure transitions back to a mixture of α-helix and random coil. The α-helix to random coil transition correlates well with the pKa observed in the polymer titrations. In summary, the α-helix structure appears to correlate with the uncharged polymer backbone; as the backbone becomes charged, the helical structure becomes reversibly disrupted and exhibits some random coil structure.

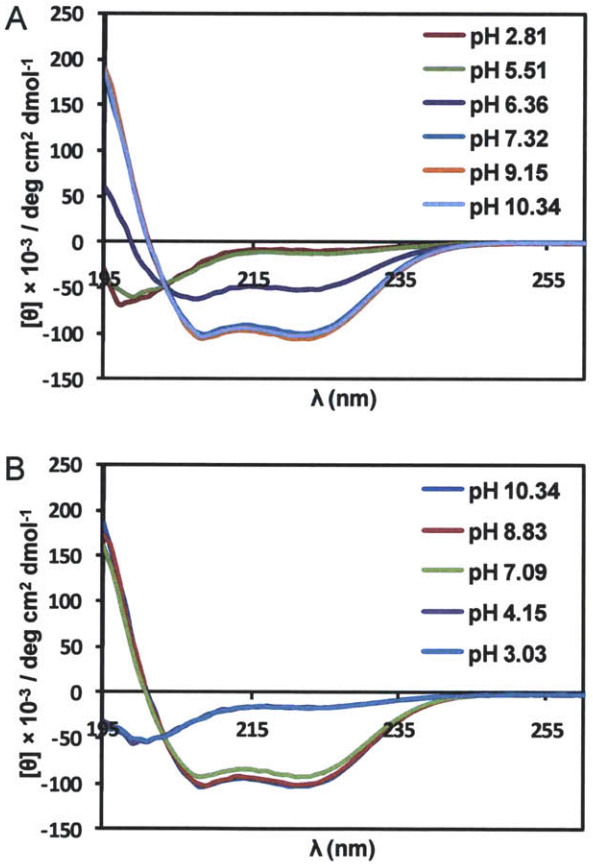

Figure 4.5 Circular Dichroism Spectra of PPLG with varying pH
A) Increasing pH CD titrations and B) decreasing pH CD titrations for secondary amine, DP=75

4.4.4 Functionalized PEG-b-PPLG Self-Assembly

The self assembly of PEG-b-PPLG functionalized with diethylamine and diisopropylamine was studied as a function of pH. The critical micelle concentration (CMC) was determined for PEG-b-PPLG in water and amine functionalized PEG-b-PPLG in buffer solutions at pH 9 and pH 5.5. The CMC was determined by fluorometry using a pyrene probe. A representative example of the diisopropylamine functionalized PEG-b-PPLG is show in Figure 4.6. As shown in Figure 4.6A, there is a clear break in the emission ratio indicating a CMC for the amine functionalized PEG-b-PPLG in pH 9 buffer. In pH 5.5 buffer, no break in emission ratio was observed for the functionalized polymer, indicating that these macromolecules do not self-assemble at all at this acidic pH, but remain completely soluble in water. The observed CMC values for all diblock polymers tested (Table 4.2), are of the same order of magnitude of PEG-b-PBLA [21] and are several orders of magnitude lower than Pluronic micelle CMC values [52]. To further verify that the self-assembled structures were micelles, AFM was performed on diethylamine and diisopropylamine substituted PEG-b-PPLG cast from a water solution adjusted with 0.1M NaOH to pH~9. Spherical micelles were observed for the amine substituted PEG-b-PPLG; Figure 4.6B shows an AFM image of the diisopropylamine functionalized diblock copolymer. The micelles are thus able to form at moderate to high pH, but become completely destabilized at low pH, making them of interest for drug release in which a pH triggered rapid disassembly of drug carrier can be designed to take place within acidic compartments to release a drug.

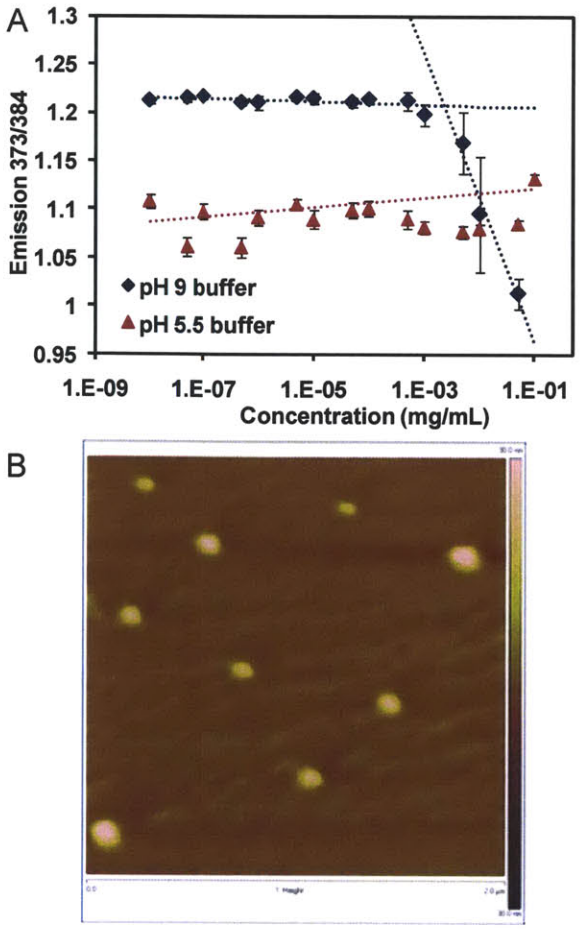

Figure 4.6 CMC Determination for PEG-b-PPLG
A) CMC determination by fluorometry using a pyrene probe for the diisopropylamine substituted PEG-b-PPLG in pH 5.5 and 9 buffer and B) AFM images of diisopropylamine substituted PEG-b-PPLG at pH 8.88. The AFM images are 2 by 2 μm with a height range from -30 μm to 30 μm.

	Solvent	CMC (mg/mL)	CMC (M)
PEG-b-PPLG	MQ water	3.75×10^{-4}	3.74×10^{-8}
Diethylamine	pH 9 buffer	1.11×10^{-2}	7.49×10^{-7}
	pH 5.5 buffer	--	--
Diisopropylamine	pH 9 buffer	1.05×10^{-3}	7.38×10^{-8}
	pH 5.5 buffer	--	--

Table 4.2 CMC values for PEG-b-PPLG
CMC values for PEG-b-PPLG in water and amine functionalized PEG-b-PPLG in pH 5 and pH 9 buffer

4.4.5 Impact of pH on Side Chain Hydrolysis

The functional groups introduced along the PPLG backbone are esters that can undergo hydrolysis under basic conditions, yielding the loss of the amino side group and the introduction of the carboxylate anion, thus introducing negative charge to the polyelectrolyte backbone. Slow or moderate changes in the polypeptide backbone may be of interest for drug delivery, gene delivery, tissue engineering, and coating applications [30, 42, 53, 54]. Specifically, for systemic use, positively charged polymers such as poly(L-lysine) and poly(ethylene imine) often exhibit significant cytotoxicity [41]. The introduction of a mechanism that eliminates the multivalent positive charge and transforms the polymer into the benign and naturally occurring negatively charged poly(γ-glutamic acid), which enhances the long-term biocompatibility of these polymers [40, 41].

To determine the side chain ester hydrolysis rate and the change in polymer secondary structure, ^{1}H-NMR and CD measurements were taken at various time points and pH conditions. Polymer samples (PPLG DP=75 with secondary amine and PEG-b-PPLG with diethylamine and diisopropylamine), were dissolved in various pH buffers to a concentration of 0.5-1 mg/mL and left to hydrolyze at room temperature. From ^{1}H-NMR, the amount of ester hydrolyzed was determined by comparing the peak integration of the triazole peak from the ester side chain (8.15 ppm) to the integration of a new triazole peak from the alcohol side chain byproduct (8.07 ppm). When the polyamide backbone, which maintains an α-helical structure when at equilibrium at all pH conditions investigated (pH 7.4, 9, and 11), undergoes hydrolysis, a glutamic acid residue

is generated. Poly(γ-glutamic acid), like poly(L-lysine), maintains an α-helix in the uncharged state, and is a random coil in the charged state [55]; thus as hydrolysis occurs at more basic conditions we observe the loss of the α-helical polymer structure. Circular dichroism at 222 nm was observed to determine the change in secondary structure as a function of time. At 222nm, a shift from a strong negative value towards a small positive value is indicative of a secondary structure shift, in this case, a shift from an α-helix to a random coil.

The results of the ester hydrolysis study are shown in Figure 4.7 and Figure 4.8. Representative ester hydrolysis plots for PPLG (DP = 75) functionalized with secondary amine and PEG-b-PPLG functionalized with diethyl and diisopropylamine are shown in Figure 4.7A, B, and C respectively. In Figure 4.8, the CD value observed at 222 nm is plotted at various pH values as a function of time for PPLG (DP = 75) functionalized with secondary amine. For all polymers, the rate of ester hydrolysis was highest at pH 11 and was increasingly slower as the pH was decreased. For example, in all cases complete hydrolysis was observed at pH 11 (at 2 days for the secondary amine and diethylamine and 11 days for the diisopropylamine), but at pH 5.5 after 15 days, all samples were less than 2% hydrolyzed. When comparing the ester side chain hydrolysis between polymers, the rate of hydrolysis at pH 7.4, 9, and 11 was fastest for PPLG functionalized with secondary amine and slowest for PEG-b-PPLG functionalized with diisopropylamine. For the diblock polymers, the polypeptide is encapsulated as the inner core of a micelle, and is partially protected from hydrolysis, thus greatly slowing the rate of hydrolysis.

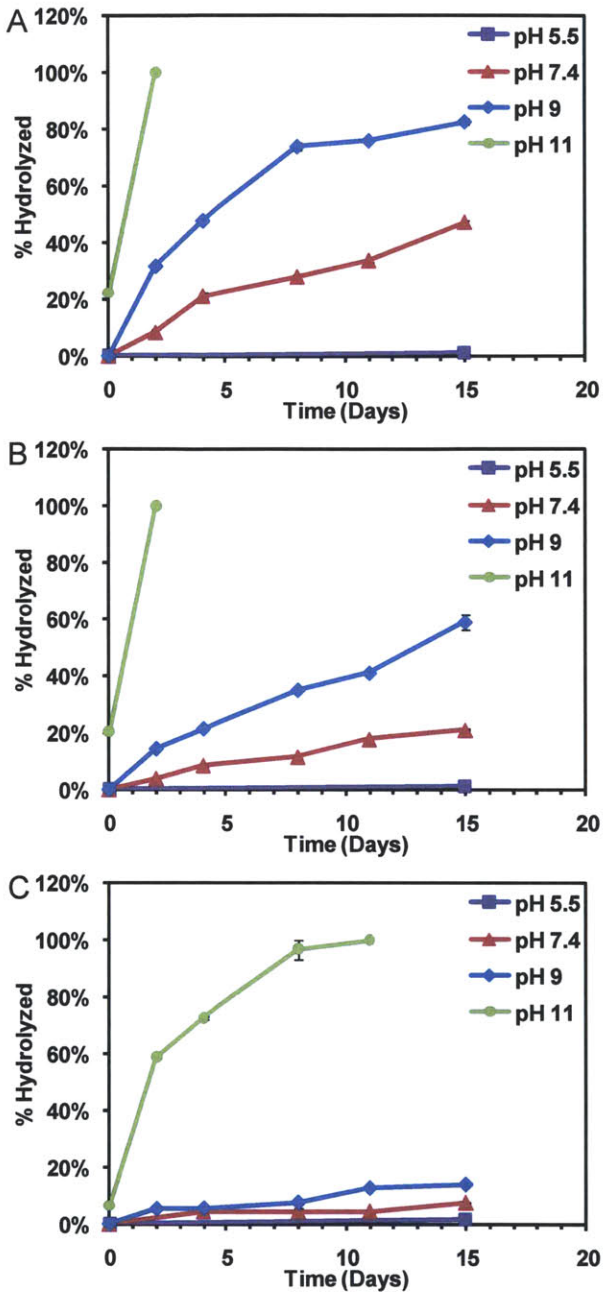

Figure 4.7 Ester Hydrolysis of Side Chains

A) Percentage of ester side chains hydrolyzed as a function of time for PPLG (DP=75) functionalized with secondary amine, B) PEG-b-PPLG functionalized with diethylamine, and C) PEG-b-PPLG functionalized with diisopropylamine.

When looking at the secondary structure of PPLG (DP=75) functionalized with secondary amine (Figure 4.8), the polymer adopts a random coil after 1 day (24 hours) in pH 11 buffer solution, at pH 9, the polymer gradually adopts a random coil over several

days, and at pH 7.4 the polymer primarily maintains an α-helical structure for multiple days. When compared to the ^{1}H-NMR data, at pH 11, the ester side chains have completely hydrolyzed in two days, leaving poly(γ-glutamic acid) which is in a random coil conformation. For pH 9, at day 4, the polymer is 50% hydrolyzed, and the polymer structure is nearly all random coil. This observation indicates that not all the ester side chains need to be hydrolyzed for the α-helix to be disrupted. Similar CD trends were observed for all PPLG (DP=75) and PEG-b-PPLG polymers tested. In summary, we can control the rate of ester degradation and the rate of α-helix disruption by changing the side chain functionality.

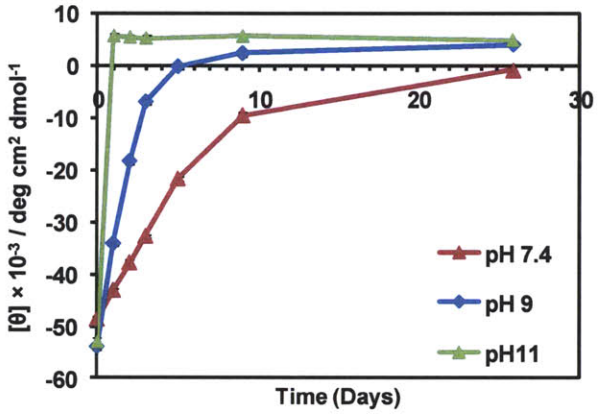

Figure 4.8 Secondary Structure of PPLG Mediated by Side Chain Hydrolysis
CD value observed at 222nm at various pH values as a function of time for PPLG (DP=75) functionalized with secondary amine.

4.4.6 siRNA Complexation

Studies have been performed to determine if the amine functionalized homopolymers could complex siRNA into protective polyplexes. Polymers were mixed with siRNA at various PPLG polymer to siRNA charge ratios (N/P) ranging from 1:1 to 50:1 in either sodium acetate buffer (pH 5.5) or PBS (pH 7.4). Ribogreen was used to determine the complexation efficiency of each polymer at the various ratios, shown in Figure 4.9. As

shown in Figure 4.9A and C, all amine functionalized PPLG homopolymers prevent dye access to more than 90% of siRNA at charge ratios above 4:1 in sodium acetate. Additionally PPLGs with primary amine substituents are able to completely complex siRNA at a charge ratio that is two-fold lower, indicating the strength of primary amines for complexation. At the higher pH of PBS (7.4), fewer amines are charged, particularly in the case of the dimethylethanamine, diethylamine, and diisopropylamine substituents, leading to looser complexes and greater dye access. This manifests itself both at low polymer:siRNA ratios for all of the polymers, and most notably for the dimethylethanamine, diethylamine, and diisopropylamine PPLGs (see Figure 4.9B and D). While these tertiary amine substituents may be useful for stimulating endosomal escape, copolymers with primary and tertiary amines are more likely to exhibit properties that enable full encapsulation of siRNA and buffering effects *in vivo*

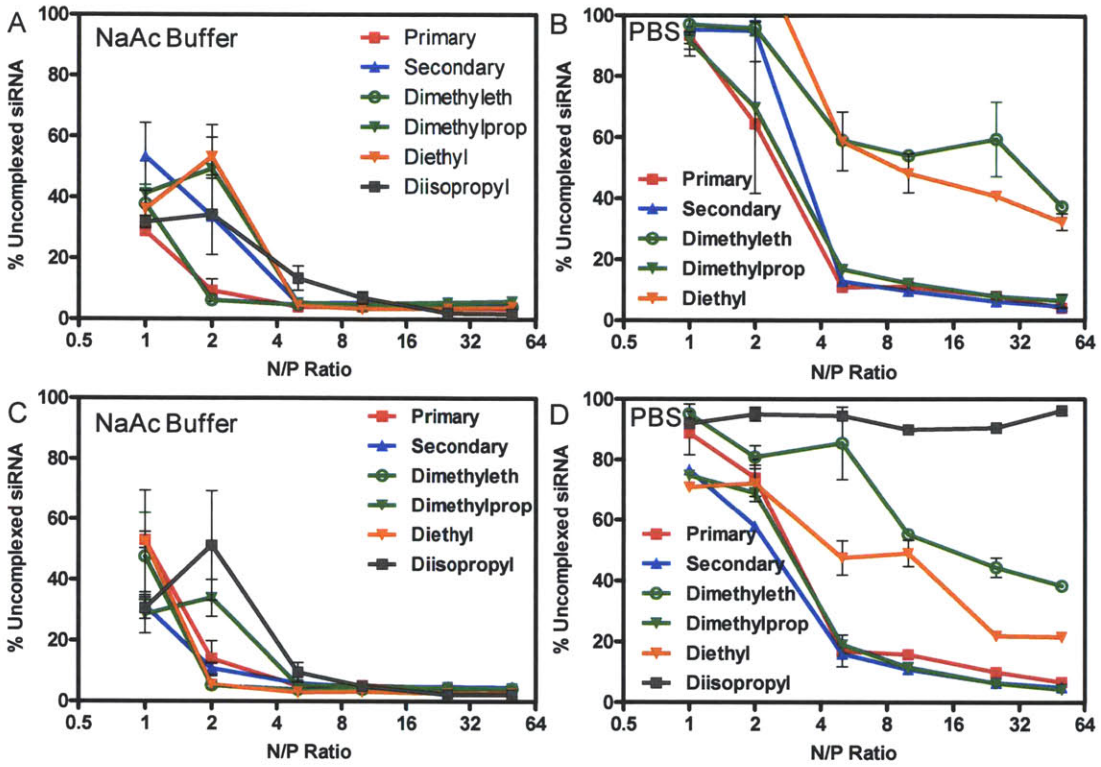

Figure 4.9 Complexation of siRNA by PPLG Homopolymers
Percentage of uncomplexed siRNA as a function of siRNA:Polymer (N/P) ratio for each amine substituted PPLG for degree of polymerization 140 (A,B) and 75 (C,D). Polyplexes were formed in either sodium acetate buffer (A,C) or PBS (B,D). The DP140 diisopropylamine sample was insoluble in PBS.

Polyplexes can be disrupted by the addition of a competing polyanion, such as heparin. In Figure 4.10A, PPLGs (DP = 140) with primary amine substituents were complexed at low (5:1) and high (25:1) N/P ratios in either sodium acetate or PBS, along with PEI and Lipofectamine 2000 as controls. As anticipated, relatively low levels of heparin were required to dissociate PPLG complexes formed at N/P 5:1 as compared with those complexes formed at the 25:1 N/P ratio. PPLG complexes formed in PBS were more easily disrupted than those formed at low pH, most likely because those formed at low pH contained more positively charged amines, and were thus more tightly

complexed. Figure 4.10B demonstrates this concept with different amine substituents. In the DP75 polymers (red), the tertiary amine in the dimethylpropanamine group forms a looser polyplex and is disrupted more readily than the secondary and primary amines. However, for DP140, the dimethylpropanamine polyplexes begin to dissociate with the same amount of added heparin as the primary and secondary polyplexes, indicating that molecular weight is also a factor in polyplex stability. Thus, the siRNA complexation behavior of these systems is tunable, and can be altered through the introduction of different buffering amine functionalities, molecular weight and pH conditions of complexation.

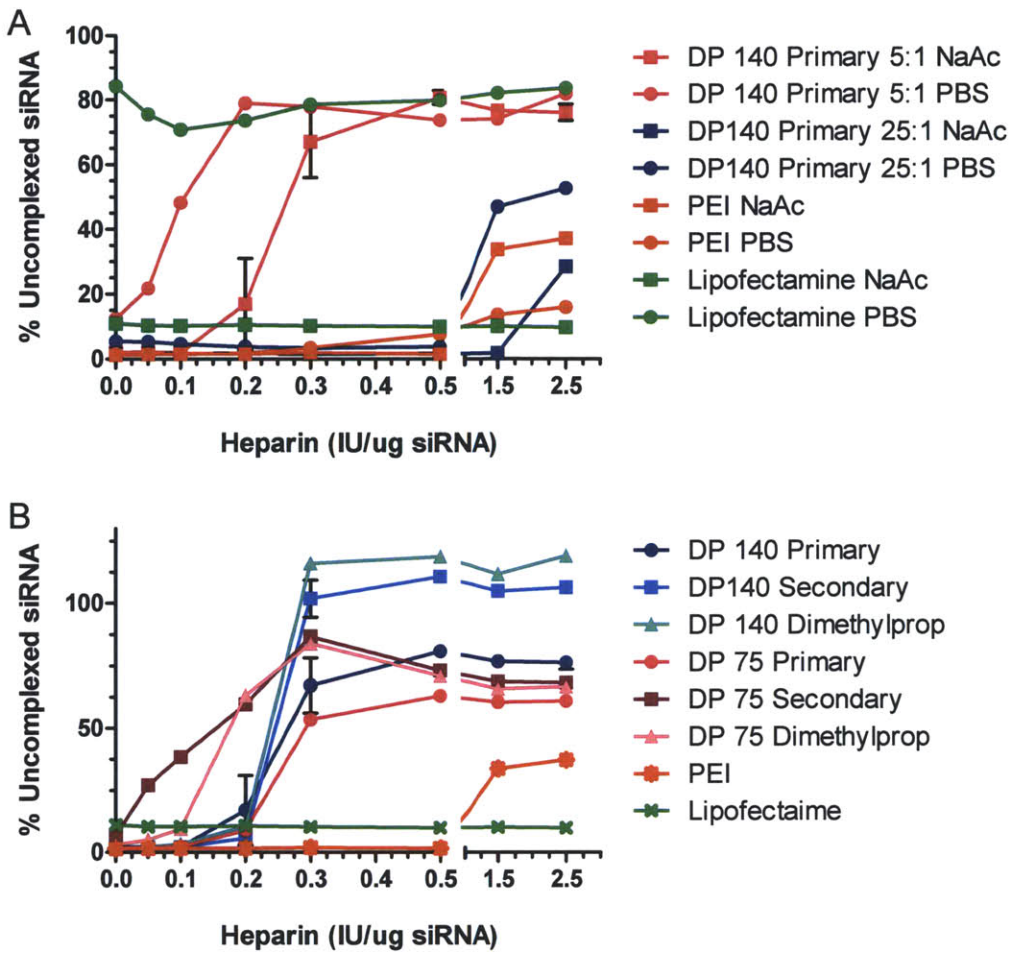

Figure 4.10 Heparin Dissociation of PPLG Polyplexes
A) Complexes were formed in pH 5.5 Sodium Acetate buffer (squares) or PBS (circles) at two different polymer:siRNA ratios (N/P). B) PPLGs with primary (circle), secondary (square), or dimethylpropanamine (triangle) substitutions were complexed in sodium acetate buffer prior to dissociation with heparin.

4.4.7 Cytotoxicity of PPLG

Given that PPLG polymers are able to efficiently encapsulate siRNA at relevant N/P ratios, evaluation of polyplex cytotoxicity and on-target knockdown followed. The MTT assay was used to evaluate the metabolic activity of cells treated with various PPLG/siRNA formulations. As shown in Figure 4.11, both homopolymers and block copolymers were generally well tolerated by HeLa cells, with viabilities generally at or

above 75% for all formulations tested. This is a first-pass screen for cytotoxicity, however, and future assays could examine membrane integrity, mitochondrial membrane potential, nuclear size, and other indicators of acute and delayed toxicity.

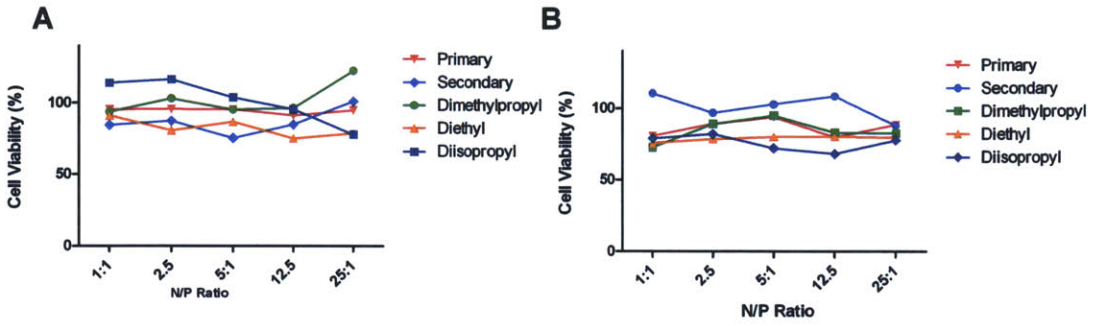

Figure 4.11 Cytotoxicity of PPLG Polymers
Relative Viability of cells treated with (A) PPLG homopolymers and (B) PEG-b-PPLG Block Copolymers as determined by the MTT assay

4.4.8 siRNA Knockdown of PPLG

Knockdown studies were carried out using a HeLa cell line stably expressing both firefly and *Renilla* luciferase such that on-target suppression of firefly luciferase could be normalized to any off-target effects on *Renilla* luciferase [43]. This knockdown assay can be performed in high-throughput and is amenable to screening many different polymers, formulations, and treatment conditions. Figure 4.12 demonstrates the lack of knockdown mediated by both PPLG homopolymers and PEG-b-PPLG block copolymers. The lack of knockdown by the pegylated block copolymers is not surprising, as pegylation has been shown to inhibit uptake of cationic polyplexes, which would therefore limit their capability for knockdown [56]. The homopolymers also demonstrated a lack of specific knockdown, regardless of amine substituent at both a moderate dose (50 ng/well) and high dose (150 ng/well) of siRNA. The latter dose was sufficient to suppress 75% of gene expression when delivered with Lipofectamine 2000, but not with any of the PPLGs.

Given that the efficient complexation of siRNA by PPLG has been established, uptake and endosomal escape were investigated further to determine the cause of the poor knockdown.

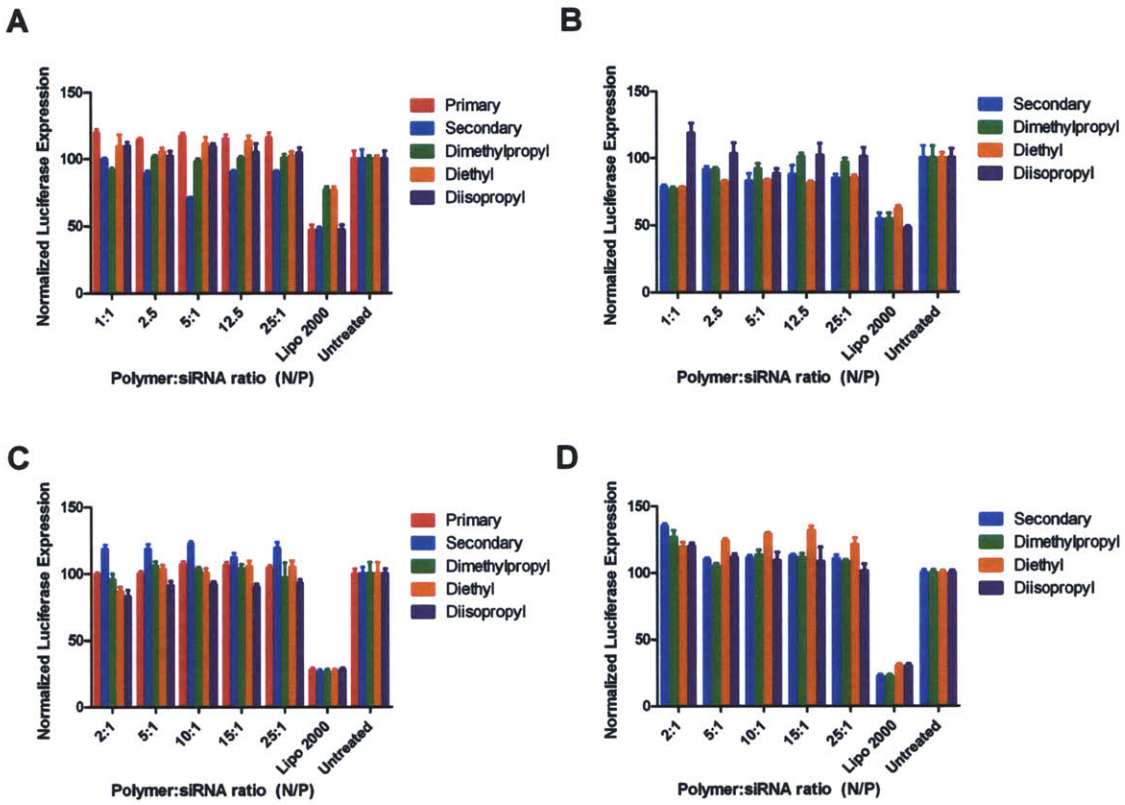

Figure 4.12 Knockdown of PPLG Homopolymers and PEG-b-PPLG Block Copolymers
Knockdown of firefly luciferase by polyplexes formed at the N/P ratios shown by PPLG Homopolymers (A,C) and PEG-b-PPLG Block Copolymers (B,D). HeLa cells were treated with 50 ng/well (A,B) or 150 ng/well (C,D).

4.4.9 Polyplex Uptake

Internalization of polyplexes was quantified by flow cytometry following incubation with polyplexes containing fluorescently labeled siRNA. As shown in Figure 4.13, all PPLGs with the exception of the highly hydrophobic diisopropylamine are internalized at least as well as Lipofectamine 2000, which is able to mediate efficient knockdown under the experimental conditions used. At N/P 5, internalization is inefficient as the complexes are

likely somewhat loose in the cell culture medium (pH 7.4). However at N/P 25, tighter complexes are formed, likely resulting in smaller sizes which are more easily internalized. As anticipated from the complexation results previously, the more charged primary and secondary amine polymers are able to generate the most uptake. Diblock copolymers showed very poor uptake (data not shown), likely as a result of the pegylation [56]. Figure 4.14 is a fluorescence microscopy image further demonstrating the effective internalization by PPLG, in this case the diethylamine substituent. Though tertiary amines such as diethylamine may have been expected to internalize poorly, they should be advantageous for escaping the endosom. Given that tertiary amine-based PPLG polyplexes formed at N/P of 25:1 are able to efficiently enter cells, the limiting barrier to effective knockdown must then either be endosomal escape or inefficient decomplexation.

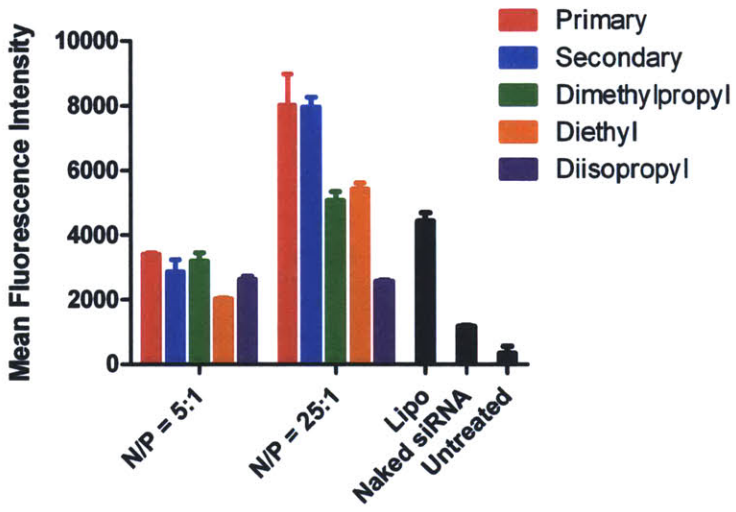

Figure 4.13 Uptake of PPLG Polyplexes
HeLa cells were treated with polyplexes formed using labeled siRNA and cell-associated fluorescence was subsequently measured by flow cytometry.

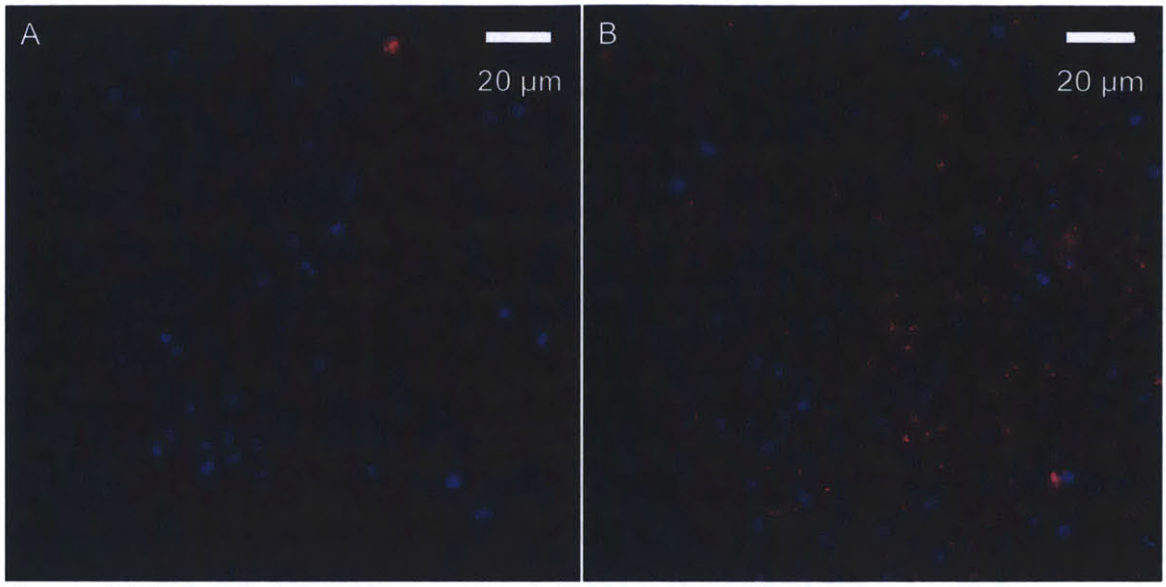

Figure 4.14 Fluorescent Micrograph of siRNA Internalization
Fluorescent microscope images showing cell uptake of fluorescently labeled siRNA with A) uncomplexed siRNA and B) complexed siRNA with diethylamine PPLG (DP = 75).

4.4.10 Endosomal Escape of PPLG

Endosomal escape was probed using methods described in detail in Chapter 2 of this thesis. Screening identified the diethyl-PPLG as the polymer most capable of causing endosomal escape. Figure 4.15 shows the escape caused by diethyl-PPLG as a function of total polymer concentration, as the majority of polymer is likely free in solution at an N/P ratio of 25:1. The free polymer stimulates escape at a lower concentration than that of the polyplex since the effective free polymer concentration is lower in the case of the polyplex due to the siRNA-bound polymer. Critically, the concentration at which escape is achieved with the best performing PPLG is greater than the concentration present in the high-dose siRNA knockdown treatment (dashed line). This implicates endosomal escape as the most relevant barrier to efficient knockdown, as there simply is not enough PPLG present in the endosomes to cause escape. One reason for this could be the lack of charge

density of the diethyl PPLG, which contains 6-7 fold more mass per tertiary amine than branched PEI.

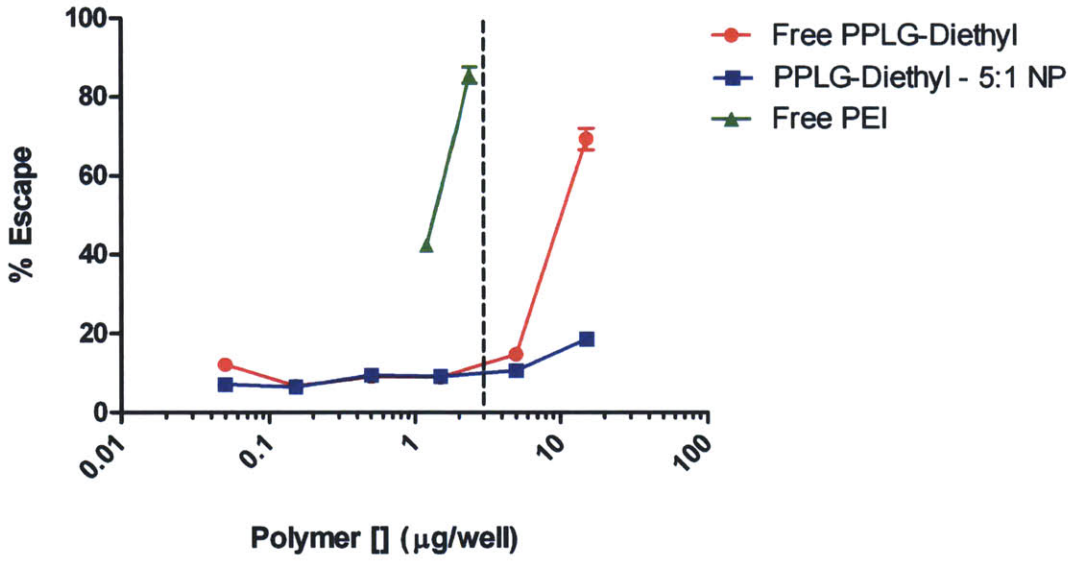

Figure 4.15 Endosomal Escape of PPLG-Diethyl Homopolymer and Polyplex
The endosomal escape caused by free diethyl-PPLG or diethyl-PPLG polyplexes was quantified using the calcein assay developed in Chapter 2. Free bPEI 25k is shown as a positive control. The dashed line indicates the polymer concentration used for the delivery of 150 ng/well siRNA.

4.5 Summary

We have developed a new library of pH responsive polypeptides based on the combination of NCA polymerization and alkyne-azide cycloaddition click chemistry. PPLG homopolymers and PEG-b-PPLG block copolymers were substituted with various amine moieties that range in pKa and hydrophobicity, and can be tuned for specific interactions and responsive behaviors. We have demonstrated that these new amine-functionalized polypeptides change solubility, or self assemble into micelles for the case of diblock polymers, with degree of ionization and adopt an α-helical structure at biologically relevant pHs. PPLG homopolymers and block copolymers were able to efficiently complex siRNA but were unable to achieve targeted knockdown. While

cellular internalization was sufficient, the amount of total polymer delivered to the cell was inadequate to cause endosomal escape.

4.6 References

1. Deming, T.J., *Synthetic polypeptides for biomedical applications.* Progress in Polymer Science, 2007. **32**(8-9): p. 858-875.
2. Deming, T.J., *Polypeptide and polypeptide hybrid copolymer synthesis via NCA polymerization*, in *Peptide Hybrid Polymers*. 2006, Springer. p. 1-18.
3. Osada, K. and K. Kataoka, *Drug and gene delivery based on supramolecular assembly of PEG-polypeptide hybrid block copolymers*, in *Peptide Hybrid Polymers*. 2006, Springer: Berlin. p. 113-153.
4. Daly, W.H., D. Poche, and I.I. Negulescu, *Poly(Gamma-Alkyl-Alpha, L-Glutamate)s Derived from Long-Chain Paraffinic Alcohols.* Progress in Polymer Science, 1994. **19**(1): p. 79-135.
5. Bromley, E.H.C., et al., *Peptide and Protein Building Blocks for Synthetic Biology: From Programming Biomolecules to Self-Organized Biomolecular Systems.* ACS Chemical Biology, 2008. **3**(1): p. 38-50.
6. Conn, P.M., ed. *Progress in Molecular Biology and Translational Science.* Molecular Biology of Protein Folding, Part A. Vol. 83, Part 1. 2008, Elsevier Inc.: London.
7. Harada, A., S. Cammas, and K. Kataoka, *Stabilized alpha-helix structure of poly(L-lysine)-block-poly(ethylene glycol) in aqueous medium through supramolecular assembly.* Macromolecules, 1996. **29**(19): p. 6183-6188.
8. Appel, P. and J.T. Yang, *Helix-Coil Transition of Poly-L-Glutamic Acid and Poly-L-Lysine in D_2O.* Biochemistry, 1965. **4**(7): p. 1244-1249.
9. Ciferri, A., D. Puett, and L. Rajagh, *Potentiometric Titrations and Helix-Coil Transition of Poly(L-Glutamic Acid) and Poly-L-Lysine in Aqueous Salt Solutions.* Biopolymers, 1968. **6**(8): p. 1019-1036.
10. Zimm, B.H. and J.K. Bragg, *Theory of the Phase Transition between Helix and Random Coil in Polypeptide Chains.* Journal of Chemical Physics, 1959. **31**(2): p. 526-535.
11. Engler, A.C., H.I. Lee, and P.T. Hammond, *Highly Efficient "Grafting onto" a Polypeptide Backbone Using Click Chemistry.* Angewandte Chemie-International Edition, 2009. **48**(49): p. 9334-9338.
12. Kolb, H.C., M.G. Finn, and K.B. Sharpless, *Click chemistry: Diverse chemical function from a few good reactions.* Angewandte Chemie-International Edition, 2001. **40**(11): p. 2004-2021.
13. Xiao, C., et al., *Facile Synthesis of Glycopolypeptides by Combination of Ring-Opening Polymerization of an Alkyne-Substituted N-carboxyanhydride and Click "Glycosylation".* Macromolecular Rapid Communications, 2010. **31**(11): p. 991-997.
14. Tang, H.Y. and D.H. Zhang, *General Route toward Side-Chain-Functionalized alpha-Helical Polypeptides.* Biomacromolecules, 2010. **11**(6): p. 1585-1592.

15. Sun, J. and H. Schlaad, *Thiol-Ene Clickable Polypeptides.* Macromolecules, 2010. **43**(10): p. 4445-4448.
16. Huang, J., et al., *Hydrolytically Stable Bioactive Synthetic Glycopeptide Homo- and Copolymers by Combination of NCA Polymerization and Click Reaction.* Macromolecules, 2010. **43**(14): p. 6050-6057.
17. Reshetnyak, Y.K., et al., *Energetics of peptide (pHLIP) binding to and folding across a lipid bilayer membrane.* Proceedings of the National Academy of Sciences of the United States of America, 2008. **105**(40): p. 15340-15345.
18. Zoonens, M., Y.K. Reshetnyak, and D.M. Engelman, *Bilayer interactions of pHLIP, a peptide that can deliver drugs and target tumors.* Biophysical Journal, 2008. **95**(1): p. 225-235.
19. Reshetnyak, Y.K., et al., *Translocation of molecules into cells by pH-dependent insertion of a transmembrane helix.* Proceedings of the National Academy of Sciences of the United States of America, 2006. **103**(17): p. 6460-6465.
20. Yokoyama, M., et al., *Preparation of micelle-forming polymer-drug conjugates.* Bioconjugate Chemistry, 1992. **3**(4): p. 295-301.
21. Kwon, G., et al., *Micelles Based on Ab Block Copolymers of Poly(Ethylene Oxide) and Poly(Beta-Benzyl L-Aspartate).* Langmuir, 1993. **9**(4): p. 945-949.
22. Katayose, S. and K. Kataoka, *PEG-poly(lysine) block copolymer as a novel type of synthetic gene vector with supramolecular structure.* Advanced Biomaterials in Biomedical Engineering and Drug Delivery Systems, 1996: p. 319-320.
23. Takae, S., et al., *PEG-detachable polyplex micelles based on disulfide-linked block catiomers as bioresponsive nonviral gene vectors.* Journal of the American Chemical Society, 2008. **130**(18): p. 6001-6009.
24. Miyata, K., et al., *PEG-based block catiomers possessing DNA anchoring and endosomal escaping functions to form polyplex micelles with improved stability and high transfection efficacy.* Journal of Controlled Release, 2007. **122**(3): p. 252-260.
25. Masago, K., et al., *Gene delivery with biocompatible cationic polymer: Pharmacogenomic analysis on cell bioactivity.* Biomaterials, 2007. **28**(34): p. 5169-5175.
26. Opanasopit, P., et al., *Block copolymer design for camptothecin incorporation into polymeric micelles for passive tumor targeting.* Pharmaceutical Research, 2004. **21**(11): p. 2001-2008.
27. Itaka, K., et al., *Biodegradable polyamino acid-based polycations as safe and effective gene carrier minimizing cumulative toxicity.* Biomaterials, 2010. **31**(13): p. 3707-3714.
28. Dekie, L., et al., *Poly-L-glutamic acid derivatives as vectors for gene therapy.* Journal of Controlled Release, 2000. **65**(1-2): p. 187-202.
29. Dubruel, P., L. Dekie, and E. Schacht, *Poly-L-glutamic acid derivatives as multifunctional vectors for gene delivery. Part A. Synthesis and physicochemical evaluation.* Biomacromolecules, 2003. **4**(5): p. 1168-1176.
30. Chen, S.F., Z.Q. Cao, and S.Y. Jiang, *Ultra-low fouling peptide surfaces derived from natural amino acids.* Biomaterials, 2009. **30**(29): p. 5892-5896.

31. Wan, Q., et al., *A Potentially Valuable Advance in the Synthesis of Carbohydrate-Based Anticancer Vaccines through Extended Cycloaddition Chemistry.* The Journal of Organic Chemistry, 2006. **71**(21): p. 8244-8249.
32. Yang, C.Y., et al., *Biocompatibility of amphiphilic diblock copolypeptide hydrogels in the central nervous system.* Biomaterials, 2009. **30**(15): p. 2881-2898.
33. Pochan, D.J., et al., *SANS and Cryo-TEM study of self-assembled diblock copolypeptide hydrogels with rich nano- through microscale morphology.* Macromolecules, 2002. **35**(14): p. 5358-5360.
34. Nowak, A.P., et al., *Rapidly recovering hydrogel scaffolds from self-assembling diblock copolypeptide amphiphiles.* Nature, 2002. **417**(6887): p. 424-428.
35. Vaupel, P., F. Kallinowski, and P. Okunieff, *Blood-Flow, Oxygen and Nutrient Supply, and Metabolic Microenvironment of Human-Tumors - a Review.* Cancer Research, 1989. **49**(23): p. 6449-6465.
36. Mellman, I., *The Importance of Being Acid-The Role of Acidification in Intracellular Membrane Traffic.* Journal of Experimental Biology, 1992. **172**: p. 39-45.
37. Sonawane, N.D., F.C. Szoka, and A.S. Verkman, *Chloride accumulation and swelling in endosomes enhances DNA transfer by polyamine-DNA polyplexes.* Journal of Biological Chemistry, 2003. **278**(45): p. 44826-44831.
38. Whitehead, K.A., R. Langer, and D.G. Anderson, *Knocking down barriers: advances in siRNA delivery.* Nat Rev Drug Discov, 2009. **8**(2): p. 129-138.
39. Boeckle, S., et al., *Purification of polyethylenimine polyplexes highlights the role of free polycations in gene transfer.* Journal of Gene Medicine, 2004. **6**(10): p. 1102-1111.
40. Adams, M.L., A. Lavasanifar, and G.S. Kwon, *Amphiphilic block copolymers for drug delivery.* Journal of Pharmaceutical Sciences, 2003. **92**(7): p. 1343-1355.
41. Lynn, D.M. and R. Langer, *Degradable poly(beta-amino esters): Synthesis, characterization, and self-assembly with plasmid DNA.* Journal of the American Chemical Society, 2000. **122**(44): p. 10761-10768.
42. Veron, L., et al., *New hydrolyzable pH-responsive cationic polymers for gene delivery: A preliminary study.* Macromolecular Bioscience, 2004. **4**(4): p. 431-444.
43. Akinc, A., et al., *A combinatorial library of lipid-like materials for delivery of RNAi therapeutics.* Nat Biotech, 2008. **26**(5): p. 561-569.
44. Schutte, E., T.J.R. Weakley, and D.R. Tyler, *Radical cage effects in the photochemical degradation of polymers: Effect of radical size and mass on the cage recombination efficiency of radical cage pairs generated photochemically from the (CpCH2CH2N(CH3)C(O)(CH2)(n)CH3)(2)MO2(CO)(6) (n = 3, 8, 18) complexes.* Journal of the American Chemical Society, 2003. **125**(34): p. 10319-10326.
45. Carboni, B., A. Benalil, and M. Vaultier, *Aliphatic Amino Azides as Key Building-Blocks for Efficient Polyamine Syntheses.* Journal of Organic Chemistry, 1993. **58**(14): p. 3736-3741.
46. Kalyanasundaram, K. and J.K. Thomas, *Environmental Effects on Vibronic Band Intensities in Pyrene Monomer Fluorescence and Their Application in Studies of*

Micellar Systems. Journal of the American Chemical Society, 1977. **99**(7): p. 2039-2044.
47. Poche, D.S., M.J. Moore, and J.L. Bowles, *An unconventional method for purifying the N-carboxyanhydride derivatives of gamma-alkyl-L-glutamates.* Synthetic Communications, 1999. **29**(5): p. 843-854.
48. Clayden, J., et al., *Organic Chemistry*, ed. J. Clayden. 2001, Oxford: Oxford University Press. 1508.
49. Bhatia, S.R., S.F. Khattak, and S.C. Roberts, *Polyelectrolytes for cell encapsulation.* Current Opinion in Colloid & Interface Science, 2005. **10**(1-2): p. 45-51.
50. Eicher, T., S. Hauptmann, and A. Speicher, *The Chemistry of Heterocycles*. 2nd ed. 2003, Weinheim: Wiley-VCH. 221.
51. Johnson, W.C., *Protein Secondary Structure and Circular-Dichroism - a Practical Guide.* Proteins-Structure Function and Genetics, 1990. **7**(3): p. 205-214.
52. Alexandridis, P., J.F. Holzwarth, and T.A. Hatton, *Micellization of Poly(Ethylene Oxide)-Poly(Propylene Oxide)-Poly(Ethylene Oxide) Triblock Copolymers in Aqueous-Solutions - Thermodynamics of Copolymer Association.* Macromolecules, 1994. **27**(9): p. 2414-2425.
53. Liu, X.H., J.T. Zhang, and D.M. Lynn, *Ultrathin Multilayered Films that Promote the Release of Two DNA Constructs with Separate and Distinct Release Profiles.* Advanced Materials, 2008. **20**(21): p. 4148-4153.
54. Zhang, J.T. and D.M. Lynn, *Ultrathin multilayered films assembled from "Charge-Shifting" cationic polymers: Extended, long-term release of plasmid DNA from surfaces.* Advanced Materials, 2007. **19**(23): p. 4218-4223.
55. Myer, Y.P., *The pH-Induced Helix-Coil Transition of Poly-L-lysine and Poly-L-glutamic Acid and the 238-mu Dichroic Band.* Macromolecules, 1969. **2**(6): p. 624-628.
56. Sung, S.-J., et al., *Effect of Polyethylene Glycol on Gene Delivery of Polyethylenimine.* Biological & Pharmaceutical Bulletin, 2003. **26**(4): p. 492-500.

Chapter 5. Summary and Future Work

5.1 Summary

Nucleic acid delivery has the potential to treat a wide array of medical conditions more effectively than the current standard of care, but vectors of suitable efficiency have not yet been established. This thesis sought to examine the efficacy and toxicity of nonviral nucleic acid delivery vehicles with respect to the sequential cellular processes needed for transfection. In order to facilitate the design of such vehicles, emphasis was placed on understanding the relationship between polymer structure and the efficiency of the polymer in overcoming the various cellular barriers to transfection.

In the first portion of the thesis, tools were developed to analyze the intracellular fate of a targeted block copolymer previously developed in the Hammond and Langer labs [1]. This PAMAM-PEG-peptide triblock copolymer system was shown the be eight-fold more efficient than the standard commercially available branched PEI (bPEI) in the presence of serum. Cell uptake was efficient and ligand-mediated, however endosomal escape was only achieved in one-third of cells under optimized conditions. This quantification of endosomal escape was made possible by a novel image-based high-throughput assay developed as a part of this thesis, which can be applied to any material system in which endosomal escape is an important parameter. Finally nuclear localization and intracellular disassembly were both shown to be important obstacles that the PAMAM-PEG system was inadequately addressing [2].

The second portion of this thesis sought to address these shortcomings by developing a hyperbranched polyamine capable of controlled disassembly and enhanced

endosomal escape. A modular synthesis conducive to the crosslinking of any polyamine with any diacid was employed to generate a small library of crosslinked linear polyethylenimines (xLPEIs). These polymers contained either a disulfide linkage, in order to degrade in response to intracellular reducing conditions, or a non-degradable linkage as a control. The xLPEIs showed excellent transfection efficiency compared to Lipofectamine and bPEI 25k as well as reduced toxicity, agreeing well with literature reports of similar polymers. These excellent properties are conventionally ascribed to the intracellular degradation of the polyplex via the bioresponsive disulfide crosslinker, however this work demonstrates the reduction to be inconsequential for this particular system. Instead, the excess free polymer not incorporated in the polyplex is shown to promote highly efficient endosomal escape with remarkably low membrane toxicity, leading to the improved properties over bPEI. Taken together, this emphasizes that further development of electrostatically assembled polyplexes must be analyzed for the impact on the excess polymer.

Finally, the tools developed for the study of plasmid DNA delivery were applied to the delivery of siRNA by a class of amine-functionalized synthetic polypeptides. A library of PPLG and PEG-b-PPLG synthetic polypeptides were functionalized with various amine functionalities to generate polymers capable of siRNA binding, cell uptake, and endosomal escape. As anticipated, polymers containing amines with higher pK_a values formed tighter complexes and were taken up by cells more efficiently. However, high-throughput endosomal escape studies demonstrated that the minimum concentration of polymer needed to achieve efficient escape was well above that present in high-dose siRNA transfection studies, resulting a lack of knockdown. This systematic

analysis suggests that the low charge density of this library, which arises as a result of its excellent molecular weight control and ease of functionalization, is likely responsible for the poor siRNA delivery.

5.2 *Future Work*

The thesis developed assays, mechanistic insights, and several classes of bioresponsive materials in which the influence of material structure on the various steps in nucleic acid delivery was studied. While the PAMAM and polypeptide based systems have shown limitations that have been discussed thoroughly in this thesis, several important questions and directions for materials development involving the xLPEI will be discussed here.

5.2.1 Hybrid Branched-Linear xLPEI systems

The xLPEI polymers investigated were shown to be remarkably efficient in promoting endosomal escape with low membrane toxicity. However, xLPEIs form large, loosely compacted polyplexes, which would likely aggregate in serum, allow degradation of the plasmid DNA, and be ineffective *in vivo.* Therefore the development of a system in which smaller, more stable polyplexes are formed would be desirable. To that end, the development of crosslinked branched PEI (xBPEI), which contains primary amines, could lead to a polyplex with better biophysical properties. A hybrid system which uses xBPEI at low N/P ratios to form the polyplex and is then supplemented with xLPEI at a high N/P ratio may be effective. In such a system, the majority of the xLPEI would remain free in solution as its secondary and tertiary amines would not confer enough charge density to displace the xBPEI. The more stable polyplex would still be able to efficiently escape the endosome as the free xLPEI would provide endosome

destabilization. Intracellular destabilization of the polyplex could be achieved using a degradable crosslinker (disulfide, hydrolytic, enzymatic, etc.). Figure 5.1 shows preliminary data on xBPEI polyplexes, demonstrating their ability to disassemble in response to intracellular reducing conditions.

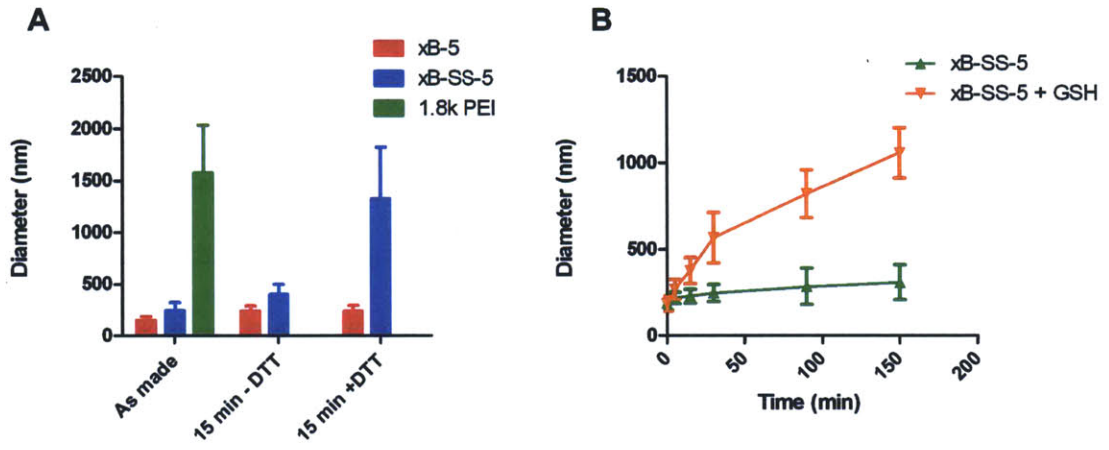

Figure 5.1 Disulfide-Mediated Dissociation of xBPEI Polyplexes
(A) Polyplexes were formed at N/P 3 in PBS and subsequently treated with 100 mM DTT, causing destabilization of disulfide linked polyplexes but not control polyplexes. (B) Disulfide-linked xBPEI polyplexes were formed as in (A) and subjected to 10 mM glutathione (GSH), mimicking intracellular reducing conditions.

Though the idea of a 2-component, polyplex/free polymer hybrid system may seem unnecessarily complex, it is the reality in any electrostatically assembled polymer gene carrier. In fact, Wagner, et. al. have shown that the free polymer is essential for transfection *in vivo*, demonstrating that free polymer is in fact able to reach the same cellular compartments as polyplexes *in vivo* [3], indicating that this hybrid approach could be successful.

5.2.2 Ligand-targeted xLPEI systems

The initial rationale for developing the crosslinked PEI system was to develop a material which would be a substitute for the PAMAM block of the PAMAM-PEG-ligand block copolymer delivery system. To that end, xLPEI (as well as xBPEI as discussed in 5.2.1) should be functionalized with PEG and targeting ligands to create block copolymers similar to those investigated in Chapter 2. These block copolymers would have the benefit of serum stability conferred by the PEG as well as tissue specificity as a result of the ligand. Such a system would be ideal to explore the impact of targeting ligand on the free polymer versus the polyplex, determining the optimal efficiency of these systems in the presence of serum, and quantifying the effect of the PEGylation on endosomal escape and toxicity. While PEGylation may abrogate some of the nonspecific uptake of the xLPEI, specific uptake via receptor-ligand interactions may effectively compensate. Optimization of this system would be an ideal intermediate step prior to *in vivo* experiments for a specific application.

5.2.3 *In vivo* Evaluation of xLPEI toxicity and efficacy

Of greatest interest with any gene carrier is its ability to transfect tissues of interest *in vivo*. As presently designed, preliminary biocompatibility studies could be quite useful, though as mentioned in 5.2.2, PEGylation and tissue targeting with a homing peptide may yield the most effective *in vivo* vector. Preliminary studies with xLPEI/xBPEI will be quite useful, as commercial bPEI has several important toxicities, though it is nonetheless used frequently in animal studies [4]. xLPEI has been shown to be less cytotoxic than commercial bPEI *in vitro* as a result of causing less membrane damage, however it remains to be seen whether this means *in vivo* toxicities such as red blood cell

aggregation can be avoided. As a substantial fraction of xLPEI would have to be present free in solution, dose-limiting toxicities for this free polymer could be established prior to the development of more sophisticated targeted block copolymers.

5.2.4 Nuclear targeting

Chapter 2 demonstrated that a limiting factor in the PAMAM-PEG-ligand gene carrier system was nuclear import. While *in vitro* transfection can still occur in systems with poor nuclear import since immortalized cell lines are continuously dividing, *in vivo* transfection cannot rely on the cell cycle for nuclear import. As a result, polymers which can specifically transport to the nucleus and then subsequently disassemble would be of great interest to the field. Nuclear translocation is frequently improved by the addition of a short peptide which is recognized and bound by the importin protein family and then transported into the nucleus [5]. This nuclear localization sequence (NLS) has been shown to increase transfection efficiency when appended to DNA in various configurations [6]. While the entire polyplex would be unable to cross the nuclear pore complex (NPC), attaching NLS to the polymer may allow for the polyplexes to be trafficking near the nucleus, or for partially disassembled polyplexes (e.g. plasmid DNA with some polymer still bound) to be internalized.

5.2.5 High-Throughput Synthesis of Crosslinked Polyamines

Many structure-function relationships in gene delivery have been derived through the high-throughput screening of combinatorial libraries of different polymeric materials [7, 8]. These approaches have also led to the identification of some of the most efficient materials to date. One of the strengths of the xLPEI synthesis shown is that it can in

principle be applied to the crosslinking of any polyamine with any diacid, allowing the generation of a library of crosslinked polyamines. Synthetically, this can be accomplished either with a robotics system or simply in a 96-well format on the benchtop. Purification can be handled by 96-well ultrafiltration membranes and the remaining product can be stored in aqueous solution or lyophilized. The advantage to such a strategy is that not only could materials be generated in high-throughput, but analysis of the DNA binding, cell uptake, endosomal escape, and overall transfection efficiency could be accomplished in a 96-well plate format as well. Bringing high-throughput combinatorial approaches to this system could identify the most ideal crosslinking conditions and crosslinking components, as well as revealing new structure-function relationships.

5.3 Conclusions

This thesis described the rational design and systematic study of bioresponsive polymers for nucleic acid delivery. A central theme of the study was understanding how the structure of the polymers impacted each of the intracellular steps of delivery, rather than solely the end result. A powerful tool for efficiently quantifying endosomal escape was developed and applied to each of the material systems described. This assay was used to demonstrate that free polymer in solution, not the presence of a functional bioresponsive domain (as previously thought), was responsible for the highly efficient and relatively nontoxic DNA delivery of a promising class of crosslinked polyamines. The development of efficient gene carriers has been underway for decades, and yet no FDA-approved therapies exist. It is hoped that the tools, materials, and systemic analysis of structure-function relationships in this thesis will enhance the process of discovery and development of clinically relevant gene carriers.

5.4 References

1. Wood, K.C., et al., *Tumor-targeted gene delivery using molecularly engineered hybrid polymers functionalized with a tumor-homing peptide.* Bioconjugate chemistry, 2008. **19**: p. 403-5.
2. Bonner, D.K., et al., *Intracellular Trafficking of Polyamidoamine - Poly(ethylene glycol) Block Copolymers in DNA Delivery.* Bioconjugate Chemistry, 2011. **22**(8): p. 1519-1525.
3. Boeckle, S., et al., *Purification of polyethylenimine polyplexes highlights the role of free polycations in gene transfer.* The journal of gene medicine, 2004. **6**: p. 1102-11.
4. Lai, W.F., *In vivo nucleic acid delivery with PEI and its derivatives: current status and perspectives.* Expert Rev Med Devices, 2011. **8**(2): p. 173-85.
5. Pouton, C.W., et al., *Targeted delivery to the nucleus.* Advanced drug delivery reviews, 2007. **59**: p. 698-717.
6. Lam, a.P. and D.A. Dean, *Progress and prospects: nuclear import of nonviral vectors.* Gene therapy, 2010: p. 1-9.
7. Green, J.J., R. Langer, and D.G. Anderson, *A Combinatorial Polymer Library Approach Yields Insight into Nonviral Gene Delivery.* Accounts of chemical research, 2008. **41**.
8. Akinc, A., et al., *A combinatorial library of lipid-like materials for delivery of RNAi therapeutics.* Nat Biotech, 2008. **26**(5): p. 561-569.